Fast Analysis of Short Chain Fluorinated Organics in River Water by Online Solid-Phase Extraction and Liquid Chromatography High-Resolution Mass Spectrometry

Yu Wang
Department of Civil Engineering
McGill University, Montreal, Quebec, Canada
August 2023

A thesis submitted to McGill University in partial fulfillment of the requirements of the degree of Master of Science

Abstract

A fast and sensitive analytical method was developed for the determination of 11 ultra-short and short-chain PFAS in surface water. For the first time, online solid-phase extraction coupled with liquid chromatography high-resolution mass spectrometry (on-line SPE-LC-HRMS) was used to analyze these emerging PFAS. Screening of 7 chromatographic columns and 5 on-line SPE columns was performed, and experimental designs were applied to optimize SPE loading conditions. Other method parameters were tested, leading to the choice of filter (glass fiber), sample acidification, chromatographic mobile phases (25mM ammonia acetate in water/acetonitrile), and SPE loading mobile phase (0.0125% formic acid in mQ-water). The method was validated in surface water matrix with suitable determination coefficients, detection limits (LOD range: 0.006-3.3 ng/L), accuracy (71%-130%), intraday precision (0.48%-20%), and inter-day precision (0.92%-19%). The method was applied to 44 river water samples collected in Eastern Canada, including airport sites with fire-training areas. Of the 11 ultra-short and short-chain PFAS targeted for screening, the most frequent were trifluoroacetic acid (TFA, 4.6–220 ng/L), perfluorobutanoic acid (PFBA, 0.85–33 ng/L), perfluoropentanoic acid (PFPeA, 1.2–2100 ng/L), trifluoromethane sulfonic acid (TMS, 0.01–4.3 ng/L), and perfluorobutane sulfonic acid (PFBS, 0.07–450 ng/L). Levels of PFBS, PFBA, and PFPeA were orders of magnitude higher in rivers near fire-training area sites compared with other rivers, while TFA and TMS were not, likely reflecting atmospheric deposition sources for these two compounds. Ultrashort 1:3, 2:3 and 3:3 polyfluoroalkyl acids were also detected in environmental waters for the first time.

Résumé

Une méthode d'analyse rapide et sensible a été mise au point pour la détermination de 11 PFAS à chaîne courte et ultra-courte dans les eaux de surface. Pour la première fois, l'extraction en phase solide en ligne couplée à la chromatographie liquide avec spectrométrie de masse à haute résolution (SPE-LC-HRMS en ligne) a été utilisée pour analyser ces PFAS émergents. Une sélection de 7 colonnes chromatographiques et de 5 colonnes SPE en ligne a été réalisée, et les conditions de chargement de la SPE ont été optimisées. D'autres paramètres de la méthode ont été testés, ce qui a conduit au choix suivants : le filtre (fibre de verre), l'acidification de l'échantillon, les phases mobiles chromatographiques (acétate d'ammoniaque 25mM dans l'eau/acétonitrile) et la phase mobile de chargement de la SPE (0,0125% d'acide formique dans l'eau mQ). La méthode a été validée dans une matrice d'eau de surface et la méthode établie a satisfait à plusieurs critères de qualités, notamment, les coefficients de détermination, les limites de détection (gamme LOD : 0,006-3,3 ng/L), une exactitude (71%-130%), une précision intra-journalière (0,48%-20%) et une précision inter-journalière (0,92%-19%). La méthode a été appliquée à un ensemble de 44 échantillons d'eau de rivière prélevés dans l'est du Canada, y compris des aéroports comportant des zones d'entraînement à la lutte contre les incendies. Parmi les 11 PFAS à chaîne courte et ultra-courte ciblés pour le dépistage, les plus fréquents étaient l'acide trifluoroacétique (TFA, 4,6-220 ng/L), l'acide perfluorobutanoïque (PFBA, 0. 85-33 ng/L), l'acide perfluoropentanoïque (PFPeA, 1,2-2100 ng/L), l'acide trifluorométhane sulfonique (TMS, 0,01-4,3 ng/L) et l'acide perfluorobutane sulfonique (PFBS, 0,07-450 ng/L). Les niveaux de PFBS, PFBA et PFPeA étaient de plusieurs ordres de grandeur plus élevés dans les rivières proches des sites d'entraînement à la lutte contre les incendies que dans les autres rivières, ce qui n'était pas le cas du TFA et du TMS (ce qui reflète probablement les sources de dépôt atmosphérique pour ces deux composés). Des acides polyfluoroalkylés ultra-courts (1 :3 2 :3 et 3 :3) ont également été détectés dans les eaux environnementales, pour la première fois.

Contents

List of Tables

List of Figures

List of Abbreviations

ACN	Acetonitrile
AFFFs	Aqueous film-forming foams
AmAc	Ammonium acetate
AOF	Adsorbable organic fluorine
BBD	Box-bBehnken design
CIC	Combustion ion chromatography
DOE	Design of experiments
ECF	Electrochemical fluorination
EtFOSAA	Ethyl-perfluorooctane sulfonamido acetic acid
FA	Formic acid
FAB-MS	Fast atom bombardment mass spectrometry
FT	Fluorotelomerization
FTCA	Fluorotelomer carboxylic acid
GC	Gas chromatography
HCFCs	Hydrochlorofluorocarbons
HFCs	Hydrofluorocarbons
HILIC	Hydrophilic interaction liquid chromatography
HPLC	High-performance liquid chromatography
HRMS	High-resolution mass spectrometry
IC	Ion chromatography
ISs	Internal standards
LC	Liquid chromatography
LOD	Limit of detection
LOQ	Limit of quantification
MeOH	Methanol
MeFOSAA	Methyl-perfluorooctane sulfonamido acetic acid
MMLC	Mixed-mode liquid chromatography
MS	Mass spectrometry
NPLC	Normal phase liquid chromatography
PFAAs	Perfluoroalkyl acids
PFAS	Per- and polyfluoroalkyl substances
PFBS	Perfluorobutane sulfonic acid
PFCA	Perfluoroalkyl carboxylic acid
PFEtS	Perfluoroethane sulfonic acid
PFPeA	Perfluoropentanoic acid
PFPrA	Perfluoropropanoic acid
PFPrS	Perfluoropropanesulfonic acid
PFOA	Perfluorooctanoic acid

PFOS	Perfluorooctane sulfonate
QC	Quality control
QToF-MS	Quadrupole-time-of-flight mass spectrometry
RPLC	Reversed-phase liquid chromatography
RSD	Relative standard deviation
SFC	Supercritical fluid chromatography
SPE	Solid-phase extraction
TFA	Trifluoroacetic acid
TMS	Trifluoromethane sulfonic acid
UPC^2	Ultra-performance convergence chromatography

Thesis Structure and Contribution of Authors

This thesis adheres to the traditional format dictated by the Graduate and Postdoctoral Studies office of McGill University. The first two chapters of the thesis serve as an introduction to the study and a comprehensive review of the existing literature. Chapter 3 details the materials and methods employed, providing an understanding of the experiment's design and implementation. In Chapter 4, the results of the investigation and discussion are presented. Chapter 5 draws together the key findings of the study and highlights the broader implications for the field. The last section is followed by supplementary information.

The candidate Yu Wang, under the co-supervision of Profs. Jinxia Liu (McGill University) and Sébastien Sauvé (University of Montreal), was responsible for conducting the experiment, analyzing the data, and writing the thesis. Drs. Gabriel Munoz and Sung Vo Duy (University of Montreal; currently with Ministère de l'Environnement, de la Lutte contre les changements climatiques, de la Faune et des Parcs) contributed to the experimental design and assisted with instrumental analysis.

Acknowledgements

I am deeply grateful to Prof. Jinxia Liu for her unwavering support and guidance. She offers her expertise and knowledge to help me navigate the academic world. It was her unwavering faith in my abilities and her encouragement that helped me persevere. Prof. Liu has not only provided me with academic support but also inspired and motivated me to excel in my research and encourage critical thinking. The opportunity to work with such an exceptional supervisor has been invaluable.

It would not have been possible for this research project to be completed without the valuable contributions of Dr. Gabriel Munoz and Dr. Sung Vo Duy. The direction and results of this study were shaped by their expertise in analytical chemistry. Their commitment and enthusiasm were greatly appreciated. As a result of their guidance, I was able to develop the analytical chemistry methods that were crucial to the success of this project. Due to their invaluable insights and technical expertise, every step of the experiment was carried out with precision and accuracy.
I would also like to thank the Lampsilis research vessel crew and all those who participated in the sampling campaigns. I also thank Transport Canada and Transport Québec for providing field samples and site access. This work was possible thanks to a grant from the Fonds de Recherche du Québec Nature et Technologies (FRQNT), the Réseau Québec Maritime (RQM), and the Canada Foundation for Innovation (CFI). This project was also supported by the Natural Sciences and Engineering Research Council of Canada Strategic Project Grant (NSERC STPGP478774-15) and the Strategic Environmental Research and Development Program (SERDP ER19-1157).

Finally, I would like to thank my family. My parents' support and belief in me have given me the strength and courage to navigate life and academia. I am forever grateful for their sacrifices, unwavering love, and endless encouragement. I am also fortunate to have met some incredible friends here, especially my lab members. Their friendship has been a source of joy and inspiration throughout my journey, and I am forever grateful for the memories we have shared.

1. Introduction

1.1. Background

Per- and polyfluoroalkyl substances (PFAS) are a group of manufactured chemicals that include thousands of compounds used in various industrial and commercial products due to their water- and oil-repellent properties, surfactant properties, and thermal and chemical stability. [1] As a result of the extensive use of PFAS and their persistence, these compounds have been released into the environment on a global scale. [2] PFAS can enter the environment through manufacturing activities, [3] domestic or industrial wastewater discharge, [3,4] land application of biosolids, [5] landfill leachates, [6] aqueous film-forming foams (AFFFs), [7] oil recovery and drilling/mining processes, [8] and many other routes. Concerns over the persistent, bioaccumulative, and toxic properties of PFAS have led to the phase-out of certain long-chain perfluoroalkyl acids (PFAAs), such as perfluorooctanoic acid (PFOA), perfluorooctane sulfonate (PFOS), and related salts and precursors. Current-use alternatives include not only PFAS of different chemistries, such as fluorotelomers and fluoroalkyl ethers but also short-chain and ultra-short-chain analogues of PFOS and PFOA.[9]

Short-chain and ultra-short-chain PFAS are classified according to the number of CF_2 molecules when they have 3-6 and 1-2 fully fluorinated carbon atoms, respectively. [10] Though they are considered less bioaccumulative than their long-chain homologues, [11] they are highly persistent and mobile in the environment. This high mobility is attributed to their high solubility in water and poor adsorption to solids and organic matter, which also explains why they can escape conventional water treatment processes. [9, 12] Besides, as the technical performance (e.g., surface tension lowering properties) of short-chain alternatives may be lower than that of long-chain PFAS, achieving similar performance may require the use of more significant amounts of short-chain PFAS in formulations. [13] Sustained releases from point sources, such as from firefighting training sites where AFFFs were used, can cause groundwater contamination and increase levels of short-

chain PFAS in drinking water over time, thus potentially increasing human exposure. [12, 13] Ultrashort-chain trifluoroacetic acid (TFA), a C2 perfluorocarboxylic acid (PFCA), has been detected at higher concentrations in the atmosphere, precipitation, surface river water, soil and sediments than its long-chain PFCA homologues. [14-16] Although it was suspected TFA has natural sources of TFA, such as hydrothermal vents,[17] widespread presence of TFA can mainly be attributed to the direct anthropogenic emission of TFA and the degradation of anthropogenic chemicals, including fluoropolymers, [18] fluorotelomer alcohols, [19] hydrochlorofluorocarbons (HCFCs), hydrofluorocarbons (HFCs), [20] and certain pesticides and pharmaceuticals containing the trifluoromethyl group (-CF_3). [21] Several studies have reported the presence of TFA in surface waters. The concentrations of TFA in Swiss rivers ranged from 0.01 to 0.33 μg/L, [22] and the average concentration observed in the main rivers of Germany was 0.14 μg/L. [23] Moreover, TFA has been detected in rain and snow samples from Switzerland, [22] China, [14 24] the United States, [25] Sweden, Canada, Ireland, and Poland [26] in the μg/L range. Studies about the sources of other short-chain and ultra-short-chain PFAS, for example, perfluoropropanoic acid (PFPrA), trifluoromethane sulfonic acid (TMS), and perfluoroethane sulfonic acid (PFEtS) in the environment is limited, and the environmental distribution of these PFAS remains unclear, [9] although some of them have also been detected in bottled water, [27] surface snow, [28] and groundwater. [29] Recently, PFPrA and PFBA, as well as TFA, were found in ice caps in remote areas, suggesting that they are globally distributed, even in polar regions. [30] Additionally, TFA and PFPrA were investigated in human serum samples from Tianjin, China; the concentration of TFA was higher than most PFAS except for perfluorooctanoic acid (PFOA) and perfluorooctanesulfonic acid (PFOS). [31]

However, short-chain and ultra-short-chain PFAS pose challenges in chemical detection and measurement. Current analytical techniques of ultra-short-chain and short-chain PFAS are summarized in Table S1. Earlier studies mainly utilized gas chromatography (GC) to measure ultra-short-chain PFAS (e.g., TFA) in the water matrix after chemical derivatization. [32-36] For instance, Scott et al. developed a method for determining (C_2-C_9) PFCAs by adding 2,4-

difluoroaniline and N,N-dicyclohexylcarbodiimide to produce 2,4-difluoroanilides analogues of the acids prior GC-MS analysis. [36] However, derivatization is time-consuming and can suffer other pitfalls, such as the difficulty of controlling derivatization yields across samples. Alternatively, developing analytical methods for underivatized TFA and other ultra-short-chain PFAS will be advantageous, particularly the ones based on high-performance liquid chromatography-mass spectrometry techniques (HPLC-MS). [37] There are several analytical challenges associated with the use of conventional reversed-phase liquid chromatography (RPLC) systems for ultra-short and short-chain PFAS analysis. The high polarity of these PFAS typically results in poor chromatographic retention and separation and poor peak resolutions. [38] Poor retention on the RPLC column implies early elution with other highly polar matrix components of an aqueous sample in the inter-particle volume (void volume) of the column, which also results in poor electrospray ionization efficiency under the highly aqueous conditions at the start of the RPLC gradient. [39-41] Besides, these polar and water-soluble PFAS are difficult to concentrate using procedures previously developed for conventional long-chain PFAS. Ultra-performance convergence chromatography (UPC^2), [38] mixed-mode liquid chromatography (MMLC), [41, 42] and supercritical fluid chromatography (SFC) [28, 43] are emerging as alternative techniques to analyze ultra-short-chain and short-chain PFAS. Among these techniques, SFC achieved the lowest instrument detection limits for C_1-C_4 PFAS, all at 0.009 ng/L, [28] but it has not yet gained wide popularity due to the need for specific instrumentation and pressure conditions. Despite significant advances in recent years, the analytical separation and detection of ultra-short-chain and short-chain PFAS remains challenging. Therefore, developing reproducible and accurate analysis techniques to determine short-chain and ultra-short-chain PFAS is essential to support environmental fate and source tracking.

Among the alternatives to RPLC, hydrophilic interaction liquid chromatography (HILIC) is a liquid chromatography mode for the efficient retention and separation of moderately to highly hydrophilic and polar compounds. It is based on a hydrophilic stationary phase routinely used in

normal phase liquid chromatography (NPLC) but combined with a mobile phase (water/polar organic solvent mixture) typically used in RPLC. [44] In contrast to NPLC that uses apolar solvents (hexane or dichloromethane), HILIC has a distinct advantage that makes it very attractive: its good compatibility with mass spectrometry (MS), especially with electrospray ionization (ESI) interfaces, because the solvents used as mobile phases in HILIC are similar to those used in RPLC, and acetonitrile-rich eluents can enhance ionization efficiency resulting in increased detection sensitivity. [44 45] However, one main challenge in using HILIC is the difficulty in selecting proper columns for method development, given the large number of materials used as stationary phases in HILIC and a lack of guidance in developing new HILIC methods. [45] Over the past few years, HILIC has become one of the preferred analytical techniques to analyze many highly polar compounds, [46] such as biological toxins, [47] nucleosides, [48] carbohydrates, [49 50] amino acids, and [51] peptides. [52] A few studies have focused on using HILIC for PFAS analysis. [53-55] For instance, Zahn et al. developed a HILIC-HRMS non-target screening method utilizing a Nucleodur HILIC column for analyzing halogenated methanesulfonic acids in the water cycle, including TMS. [55] To date, however, no study has investigated sample pre-concentration coupled on-line to HRMS for faster turnaround times and improved sensitivity of ultra-short-chain PFAS.

1.2. Thesis Objectives

The objective of this thesis was to develop a fast and sensitive analytical method for the determination of environmentally important ultra-short-chain and short-chain PFAS in river water. Target compounds included TFA, perfluoropropanoic acid (PFPrA), perfluorobutanoic acid (PFBA), trifluoromethane sulfonic acid (TMS), perfluoroethane sulfonic acid (PFEtS), and ultra-short/short-chain n:3 acids (n = 1-3). The specific objectives were to:

(1) Optimize HPLC column selection and sensitivity/retention factors by screening 7 columns in HILIC, anion-exchange, and RPLC modes, including changes in mobile phase composition, flow rate, and acid amendment;

(2) Optimize the SPE parameters by testing the selected separation column with several online preconcentration columns;

(3) Validate the method on blank surface water, assessing linearity, limits of detection and quantification, recovery, accuracy, and precision;

(4) Apply the developed method to a collection of river water samples obtained from background and AFFF-impacted areas in Eastern Canada.

2. Literature Review

2.1. PFAS Chemistry and Applications

Per- and polyfluoroalkyl substances (PFAS) are anthropogenic chemicals used for decades in various consumer and industrial products.[56] These chemicals are categorized as organofluorine compounds, in which fluorine atoms partially or wholly replace hydrogen atoms. This chemical alteration makes PFAS possess many unique properties besides being highly chemically, biologically and thermally stable. Perfluoroalkyl substances are compounds in which fluorine atoms replace all hydrogen atoms in the molecule except those in the hydrophilic functional groups. Polyfluoroalkyl substances, on the other hand, contain a mixture of carbon-fluorine and carbon-hydrogen bonds. These bonds can impact the chemical and physical properties of the substance, affecting its solubility, volatility, and stability.

The manufacturing of PFAS has historically relied on two primary synthesis routes: electrochemical fluorination (ECF) and fluorotelomerization (FT). The electrochemical fluorination process produces a mixture of branched and linear isomers, while fluorotelomerization primarily yields linear PFAS. Branching of the main C backbone results in numerous PFAS isomers. [57] For example, perfluorooctane sulfonic acid (PFOS), a well-known PFAS, can exist in a mixture of the linear isomer and 10 branched isomers, with 89 congeners theoretically possible. [58, 59] Figure 1 shows the structures of several most common PFAS classes.

Since the 1950s, PFAS have been widely used in various consumer and industrial products, owing to their versatility and durability. They have been a popular choice in cookware, bakeware, food packaging, outdoor clothing, tents, car interiors, etc. The electronics industry extensively utilizes PFAS to manufacture computer chips, semiconductors, and other electronic components. Furthermore, PFAS have found applications in industrial processes such as carpet manufacturing,

paint production, and adhesive formulations. [60] Personal care products, including cosmetics and lotions, often contain PFAS to enhance their texture and consistency. [61] Firefighting foams, widely employed to extinguish fires and prevent their spread, also incorporate PFAS for their firefighting capabilities. [62-64]

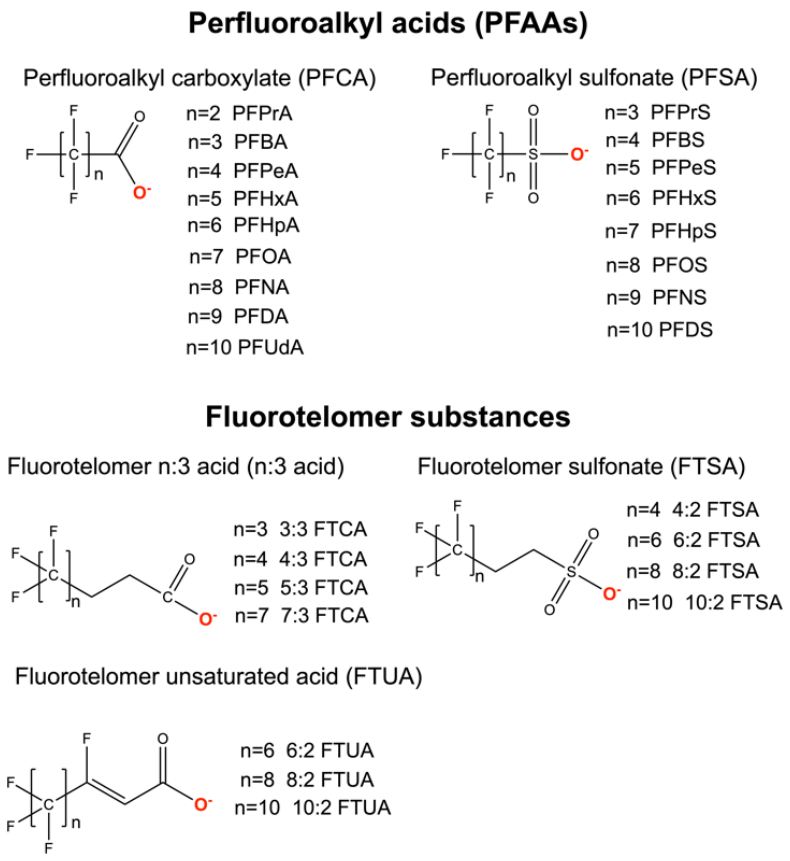

Figure 1 Structures of some common PFAS classes

2.2. Environmental and Health Concerns

PFAS can enter the environment through manufacturing operations discharge,[3] domestic or industrial wastewater discharge,[3 4] biosolids application,[5] landfill leachate,[65] AFFF use,[7] or other waste streams. Widespread use and extremely high resistance to degradation have caused these compounds to be omnipresent in the environment. Kim et al. [66] examined the presence of PFAS in wastewater from 77 industrial plants in Korea. A total of 28 novel and legacy PFAS were detected,

with 19 found in untreated industrial wastewater and 9 in river water. The mean PFAS concentration in industrial wastewater treatment plant effluent was 5.18 μg/L. Perfluorohexanesulfonate is the predominant PFAS found in all effluents and contributes to 96% of the total PFAS discharged. Masoner et al. [67] investigated the prevalence and concentration of PFAS in landfill leachates and wastewater influent/effluent from three landfill-WWTP systems in Florida. This finding revealed that PFAS were detected more often in leachates (92%) and at higher levels than in wastewater influents. Total PFAS concentrations in leachate (93100 ng/L) were more than 10 times higher than in influent (6950 ng/L) and effluent samples (3730 ng/L). McCord et al. [68] identified new chloro-perfluoro-polyether carboxylates and related compounds in water samples from southwestern New Jersey using nontarget LC-HRMS analysis.

Exposure to contaminated drinking water has become the most significant source of PFAS exposure for impacted communities. [69] It was estimated that more than 6 million U.S. residents are affected by this issue, with drinking water supplies exceeding the former U.S. EPA lifetime health advisory levels of 70 ng/L for PFOA and PFOS. [69] This exposure is often linked to aqueous film-forming foam (AFFF) use in fire training areas at military sites and civilian airports and industries that manufacture or use PFAS and wastewater treatment plants. These sources have been shown to contribute significantly to the levels of PFAS in drinking water. [70] In addition to exposure to drinking water, other important pathways of exposure to PFAS have been identified. For instance, the consumption of certain foods, particularly fish, shellfish, and meat, has been identified as a significant source of exposure to PFAS. [71] This is because these compounds can bioaccumulate in the food chain. Moreover, studies have shown that neutral PFAS compounds are typically more prevalent in indoor air and dust and may contribute to overall exposure in household settings. For young children, breastmilk ingestion was identified as a significant exposure pathway for PFAS, [72] along with exposure to house dust. [73]

Human exposure to PFOA, among the most often detected PFAS, has been associated with cancer, elevated cholesterol, obesity, immune suppression, and endocrine disruption.[74] [75] [76] Toxicity of

most PFAS used in commerce has not been studied, but the persistence alone leads some researchers to call for completely banning these substances.[77] [78] Also, wide variability in PFAS structures results in varying properties. Some are bioaccumulative and pose mammalian toxicity, while many are not bioaccumulative but highly mobile in the environment,[79] [80] such as certain short-chain PFAS.[81] [82]

2.3. PFAS Analytical Methods

The global concern regarding the health and environmental impacts associated with PFAS exposure has been mounting, triggering an urgent need for research to understand the occurrence, fate, and transport of these compounds in the environment and living organisms. To address this challenge, a range of analytical methods and instruments have been developed to detect and quantify PFAS. These include targeted analysis, non-standardized analysis, isomers/enantiomers analysis, and total PFAS analysis, among others. Although each method has unique strengths, they also have inherent limitations, which require careful evaluation when selecting the most appropriate method for a particular sample or matrix. Often, it is necessary to use complementary tools in tandem to provide a more comprehensive understanding of the PFAS present in a given sample or matrix.

2.3.1. Targeted Analysis

Target analysis is a well-established and reliable approach for the detection of PFAS. This approach relies on reference standards and isotope-labeled internal standards to detect and quantify known PFAS. The high precision and sensitivity offered by liquid chromatography-tandem mass spectrometry (LC-MS/MS) make it the preferred method for this type of analysis. EPA methods such as EPA-537, EPA-537.1, EPA-533, and EPA-1633 have been developed to standardize the target analysis process, and each method targets a different set of PFAS compounds, with EPA-537 containing 14 analytes, EPA-537.1 containing 18, EPA-533 containing 25, and EPA-1633 containing 40. [83] The first three methods are only for drinking water, while the last method covers

a diverse range of environmental matrices, including surface water, groundwater, wastewater, soil, biosolids, sediment, landfill leachate, and fish tissue.

Although target analysis is a reliable method for PFAS detection and quantification, the approach alone often cannot fully encompass the type of PFAS present in environmental samples. There are approximately 5000 PFAS on the global market, and most of these compounds are polyfluoroalkyl compounds and have the potential to transform into other persistent types of PFAS, including perfluoroalkyl acids. [84] Therefore, the analyte lists of these standardized methods are far from being comprehensive enough and leave out some potentially important compounds. For instance, 5:3 fluorotelomer carboxylic acid (5:3 FTCA), a unique metabolite of biotransformation of 6:2 fluorotelomer, is not covered by any of these EPA Methods. A study has shown that 5:3 FTCA was the largest contributor to overall PFAS release in landfill leachate and, therefore, could be used as a marker compound to indicate contamination from landfill leachate.[65] Many other examples of important PFAS being left out of analyte lists for PFAS risk assessment, source tracking and remediation efforts. [84] In addition, these standard methods are generally limited to anionic and non-volatile compounds in aqueous or solid matrices, while no standard method has specifically focused on volatile PFAS.

2.3.2. Non-standardized Analysis

In recent years, the limitations of commercial PFAS analysis methods have become increasingly apparent, prompting a search for more advanced technologies that can provide more comprehensive PFAS characterization. High-resolution mass spectrometry (HRMS) has emerged as a promising technique. HRMS provides higher resolution and mass accuracy, enabling the identification of unknown and non-targeted PFAS compounds. Due to its high resolution and high full-scan sensitivity, HRMS can be applied to identify multiple PFAS simultaneously. [85] LC and GC combined with various HRMS-based techniques, such as quadrupole-time-of-flight mass spectrometry (QToF-MS), Fourier transform infrared mass spectrometry (FTIR-MS), and Orbitrap, have been widely used to identify and semi-quantify many PFAS that lack analytical standards. [85]

[86] [87] D'Agostino et al. [7] identified 103 new PFAS compounds from 10 different PFAS classes in 10 AFFF formulations using LC-QToF-MS. QToF-MS was also utilized by Barzen-Hanson et al. [88] to identify 40 new classes of PFAS in AFFF products and AFFF-impacted groundwater. They further reported that 34 of those classes originated from the electrochemical fluorination (ECF) process. Using fast atom bombardment mass spectrometry (FAB-MS) with UPLC-QTOF-MS, Place et al. [89] identified 27 PFAS in AFFFs. Liu et al. [90] employed LC-Orbitrap-HRMS to identify over 330 fluorinated analytes from 10 classes of PFAS in pooled fish livers, including six sulfonate classes, two amine classes, one carboxylate class, and one N-heterocycle class. Xiao et al. [91] created a non-targeted identification method to detect emerging PFAS based on parent ion search (PIS) using a ToF-MS system with continuously interleaved scans at low and high collision energies (TOF-MS^E HRPIS). The approach resulted in the identification of 47 novel and 43 never-reported PFAS in commercial surfactant products, including 40 non-ionic, 30 cationic, 15 zwitterionic, and 5 anionic compounds.

Although different identification methods and strategies have been developed, non-target analysis based on HRMS possesses roughly the same workflow steps as illustrated in Figure S1.[92] The five steps are: (1) generate high-resolution full-scan spectra to discover all detectable ions in a sample, (2) select the expected PFAS characteristics from the full-scan data, (3) assign reasonable molecular formulas, (4) perform MS^n ($n \geq 2$) fragmentation experiments to confirm the molecular formula and reveal structural information, and (5) structure proposal and confirmation. However, HRMS instrumentation is expensive, and the data interpretation is complex, time-consuming, and requires high technical skills. Moreover, since quality assurance protocols for HRMS are not standardized, this technology is prone to false-positive and false-negative PFAS identification. [93].

2.3.3. Isomers/Enantiomers Analysis

Historically, PFAS were manufactured through two main synthesis routes: electrochemical fluorination (ECF) and fluorotelomerization (FT). The compounds produced by ECF and FT differ in the distribution of perfluoroalkyl chain length, isomer composition, and terminal functional

groups. During ECF manufacturing, long-chain or higher molecular weight PFCAs, including PFOA, are formed. [94] These structures provide multiple positions for methyl- or ethyl- substitution, leading to several isomers for each corresponding linear isomer. LC can separate these PFAS structural isomers from their linear counterparts. Benskin et al. built a comprehensive method to simultaneously separate and detect PFAS and PFAS precursor isomers using LC-MS/MS. [95] An analytical column with a perfluorooctyl stationary phase combined with acidified mobile phase further enhanced the separation efficiency for many PFCA, perfluoroalkyl sulfonates (PFSAs), and perfluorooctane sulfonamide (FOSA) isomers. In 2012, Benskin et al. further reduced the elution time by developing a rapid (<23 min) HPLC-MS/MS method to simultaneously characterize 24 PFAS. [96] Not only the isomer-specific analysis of perfluorooctane sulfonate and perfluorooctanoate was performed, but also branched from linear isomer separation was completed for C6 and C10 perfluoroalkyl sulfonates, C6, C7 and C9-C11 PFCAs, perfluorooctane sulfonamide and, for the first time, 3 perfluorooctane sulfonamidoacetates.

The existence of branched isomers indicates that they come from ECF manufacture, while FT-based products are linear. The ratio of branched to linear isomers in the original ECF product is roughly 22-35% branched and 65-78% linear [97]. For example, the technical PFOA mixture produced by the ECF manufacture of 3M contained 78% linear and 22% branched-chain isomers.[98] PFOS was only produced by ECF manufacturers. The percentage of linear PFOS (L-PFOS) in commercial products is mostly in the 67% - 82% range. Theoretically, there may be hundreds of PFOS isomers whose elemental composition is $C_8F_{17}SO_3^-$.[99] However, fluorine-19 nuclear magnetic resonance (19F-NMR) analysis showed that perfluoromonomethyl and perfluoroisopropyl isomers are the most abundant, and most of the rest are tert-perfluorobutyl and germinal- substituted perfluoreodimethyl compounds. The structures of some common PFOS isomers are displayed in Figure S2. However, little information is available on the isomer composition of many ECF-based PFAS.

Some branched PFAS isomers contain a chiral carbon center, and therefore, each may exist as two non-superimposable mirror-image molecules, as we call enantiomers. [94] Most manufactured or non-biologically produced enantiomers are racemic, and the ratio of enantiomers is 1:1. [100] Enantiomers have the same physical and chemical properties, so abiotic transformations such as leaching, volatilization, and hydrolysis do not change the enantiomer ratio. However, metabolism (by enzymes and microorganisms) is enantioselective, producing nonracemic mixtures of enantiomers and the change of enantiomer ratio. [101] This change can provide valuable information about enantiomers' environmental transport, degradation, and bioaccumulation. In addition, different enantiomers may have different biotransformation rates when interacting with molecules such as proteins, which means that different enantiomers usually have different toxicities.[98] [102] Wang et al. proved the enantioselective biotransformation of PFOS precursors by monitoring the biodegradation rates of the enantiomers in human liver microsomes. [103] The metabolic rate of one enantiomer was $k = 6.5 \times 10^{-2}$ min^{-1} and for the other one $k = 5.2 \times 10^{-2}$ min^{-1}. This is the first demonstration that biotransformation of PFOS precursors may be enantioselective, making the application of PFOS enantiomer profiles a promising source tracking tool for PFOS in biological samples. Consequently, establishing a sensitive and accurate analytical method is crucial for the enantioseparation of PFAS in environmental samples.

Enantioseparation of chiral PFAS in environmental matrices is usually performed using LC, especially for PFOS. Previously reported studies focused on the separation of 1m-PFOS and its precursors using an anion exchange chiral column based on cellulose tris (3,5-dichlorophenyl) carbamate [103] [104] or a quinine derivate (Chiralpak QN-AX) [105-107] with LC. Recently, chiralpak QN-AX has been successfully used in separating the enantiomers of 1m-PFOS using supercritical fluid chromatography (SFC) in the human placenta. [107] SFC shows shorter elution time and better enantioresolution compared to LC. In another study, it was found that the enantiomers of 3m, 4m-, 5m-, and 4, $5m_2$-PFOS can not be separated by SFC on a Chiralpak QN-AX column. Thus only 1m-PFOS has achieved enantioseparation on a Chiralpak QN-AX column so far. [106]

2.3.4. Total PFAS Analysis

The identification and quantification of all PFAS in a given environmental or biota sample are challenging owing to the complexity of PFAS and the lack of reference standards and analytical methods. In response to this challenge, total PFAS analysis can be used as an alternative to assessing PFAS contamination comprehensively.

Adsorbable organic fluorine (AOF) is one method for capturing most PFAS (known and unknown) in environmental waters.[108] Combustion-ion chromatography (CIC) is the most common technique to determine the fluorine content of PFAS concentrated by a sorbent such as activated carbon. The specific procedures are illustrated in Figure S3. Firstly, the sample is passed through cartridges containing activated carbon, organofluorine chemicals are adsorbed, and residual inorganic fluoride is removed with a sodium nitrate washing solution. Then the adsorbent is combusted at 900-1000 °C to convert organic fluorine to hydrofluoric acid, which is absorbed into a solution of sodium hydroxide. Finally, the total concentration of fluoride ions is determined by ion chromatography (IC). Willach et al. [109] investigated the contribution of PFAS to the total adsorbable organic fluorine in German rivers and contaminated groundwater by exploiting a simplified AOF method. A portion of the AOF (32-51%) could be explained by the 17 individual PFAS measured for the groundwater. Recently, Han et al. [110] further improved the AOF method by lowering the limits of detection and quantification to 300 and 400 ng/L, respectively. Abercron et al. [111] conducted the AOF analysis on 22 samples from an industrial wastewater treatment plant and identified 14 individual PFAS via LC-MS/MS. In these samples, the AOF values reached 555 μg/L, but the summed individual PFAS (calculated as fluorine) was 8.8 μg/L. AOF encompasses many organofluorine chemicals that cannot currently be detected by LC-MS/MS, which demonstrates that the AOF can be used as a powerful screening test to support LC-MS/MS methods. However, the AOF method is only applicable to water matrix,[112] which greatly limits the measurement of PFAS in environmental samples.

The total oxidizable precursor (TOP) assay is another approach that has gained popularity. It works by oxidizing and converting multiple polyfluoroalkyl compounds with hydroxyl radicals into several common PFCA products, which simplifies the complexity of a PFAS mixture and allows the estimation of PFAS that otherwise cannot be quantified. [113] The assay relies on sodium or potassium persulfate as the oxidant, and the activation can be achieved by heating or UV irradiation. The TOP assay is the most sensitive among surrogate methods because it is based on LC-MS/MS analysis of perfluoroalkyl acids (PFAAs), which have very low detection limits. Furthermore, the TOP assay can distinguish between FT and ECF-based precursors by analyzing the ratio of oxidation products and examining branched and linear isomers. Ruyle et al. [114] combined TOP assay results with other statistical methods, such as Bayesian inference, to reconstruct the concentrations of oxidizable precursors and their perfluorinated carbon chain length and manufacturing origin. Robel et al. [115] compared the molar sums of PFAS used to treat paper and textiles acquired by GC-MS, LC-MS/MS, and the TOP assay with the total fluorine content measured by particle-induced gamma-ray emission (PIGE) spectroscopy. Volatile, ionic, and unknown PFAS accounted for 0-2.2% (GC-MS), 0-0.41% (LC-MS/MS), and 0.021-14% (TOP assay) of the total fluorine measured by PIGE, respectively. Although the TOP assay cannot capture all PFAS in a sample, it can reveal the presence of many PFAS that are not yet captured as individual PFAS by GC-MS or LC-MS/MS. Consequently, the TOP assay can be considered an effective screening tool to evaluate the presence or absence of the precursors to PFAAs.

However, the TOP assay is less inclusive, limited to compounds that can be oxidized by hydroxyl radicals to form LC-amenable PFAAs, leading to the omission of some PFAS. Moreover, the TOP assay is subject to the selectivity issues inherent in reversed-phase LC, meaning that short-chain compounds that are not retained by LC analytical columns will be lost. Zhang et al. [116] investigated the fate of 15 per- and polyfluoroalkyl ether acids (PFEAs) in the TOP assay. It was found that NVHOS and HydroEVE, 2 PFAS compounds identified from the Nafion® production process, were easily oxidized in the TOP assay. However, their oxidation products were probably low-

molecular-weight organofluorine species, volatile organofluorine species, and fluoride, which are not captured by LC-HRMS. Zhang et al. [116] also found that the remaining 11 of the 15 PFEAs were stable in the TOP assay, suggesting that these compounds can be considered new terminal products that are persistent in the environment. Therefore, adding these PFEAs to the conventional target analyte list of TOP assay can improve the inclusivity of the TOP assay. Besides, the TOP assay combined with LC-HRMS and GC-HRMS to detect a broader range of oxidation products can further enhance inclusivity. [112]

2.4. Short-chain and ultra-short-chain PFAS Analysis

Certain PFAS chemicals, known for their persistence and bioaccumulation, have gained regulatory attention in the EU and were included in the candidate list of substances. Besides, PFOS has been added to the persistent organic pollutants (POPs) list at the Stockholm Convention in 2009. [117] These regulatory measures have prompted manufacturers to seek alternative solutions for commercial production, leading to the adoption of short-chain and ultra-short-chain PFAS, as well as other fluorinated alternatives like perfluoropolyethers. [29 118-120] However, challenges arise with the use of short-chain PFAS. As documented by Lindstrom et al., [121] the technical performance of short-chain alternatives paled in comparison to their long-chain counterparts. Consequently, significantly larger quantities of these short-chain PFAS compounds had to be employed to attain comparable levels of performance. These alternatives also form persistent transformation products, as evidenced by studies conducted by Hurley et al., [122] Lee et al., [123] Liou et al., [124] and Butt et al.. [125] Adding to the complexity, many short-chain PFAS structures and compositions remain unknown, either due to proprietary formulas or undisclosed byproducts resulting from the manufacturing process. [10] The continuous release of these compounds suggests potential adverse effects. Understanding the risks associated with short-chain and ultra-short-chain PFAS is crucial.

2.4.1. Short-chain and ultra-short-chain PFAS

PFAS are classified into ultra-short-chain and short-chain categories based on the number of CF_2 moieties, namely 2–3 and 4–7 fully fluorinated C-atoms. As the perfluorinated alkyl chains become shorter, these compounds exhibit enhanced solubility and weaker sorption to environmental media. [126] For example, studies from Li et al. [127] revealed that PFBS exhibits a substantially lower fraction (approximately 30%) partitioned to soil compared to the more persistent PFOS, which exhibits a higher partitioning fraction of around 70%.

Short-chain and ultra-short-chain PFAS compounds align with the proposed criteria for persistent, mobile, and toxic (PMT) or very persistent and very mobile (vPvM) substances, as established by the German Environment Agency (UBA). [128] The high persistence and continued emissions can result in environmental accumulation, leading to increased human external exposure as described by Cousins et al.. [12] The high mobility in the environment because of high solubility in water and poor adsorption to organic matter, enabling them to traverse natural barriers and human-made structures. [12] Point source releases, for example, from firefighting training sites where AFFFs are used, result in groundwater contamination, ultimately finding their way into drinking water sources. Also, conventional remediation techniques prove ineffective in adequately addressing the presence of short-chain and ultra-short-chain PFAS compounds, leaving behind remnants of these persistent contaminants. [129] [9] As a result, wastewater treatment plants (WWTPs) become the point sources of PFAS contamination in the aquatic environment. [130-132] The inability to completely eliminate these compounds during the treatment process exacerbates their prevalence in the environment.

2.4.2. Analytical methods for short-chain and ultra-short-chain PFAS

The current state of research in the PFAS analysis field has predominantly focused on a restricted subset of PFAS compounds, neglecting the extensive array of variants that exist, including the often overlooked ultra-short-chain and short-chain PFAS. This disparity in attention may be attributed, at least in part, to the analytical challenges encountered when employing conventional

reversed-phase liquid chromatography (RPLC) systems. [37] The highly polar ultra-short-chain PFAS pose poor chromatographic retention, thereby impeding their accurate identification and quantification.

Gas chromatography (GC): The advent of PFAS analysis began with the utilization of gas chromatography (GC) coupled with flame ionization detector (FID) and electron capture detector (ECD). [133]. Studies focusing on the GC analysis of short-chain PFAS compounds have employed chemical derivatization techniques using 2,4-difluoroaniline in the presence of N,N-dicyclohexylcarboimide to produce 2,4-difluoroanilides of the C2-C9 acids. [36, 134] Given the low volatility and high polarity of PFAS compounds, a derivatization step is essential prior to GC analysis. Various derivatization methods have been developed to convert PFAS into their methyl esters using reactions with diazomethane,[135, 136] methyl iodide, [137] methanolic BF3, [138] and methanol/MTBE/DCA. [139] Alongside this rapid and straightforward derivatization procedure, they employed various extraction matrices (acetonitrile, water, methanol, phosphate buffer) and detectors (GC-EI-MS, GC-ECD). The limits of detection (LOD) obtained using GC-ECD ranged from 0.06 to 1.80 mg/L, while GC-EI-MS achieved LODs ranging from 0.030 to 0.314 mg/L. The specific LODs depended on the matrix analyzed and the detector employed, as highlighted by Shafique et al.. [140] However, while derivatization methods have proven valuable for GC analysis of PFAS compounds, it is important to acknowledge certain limitations. The process of derivatization is time-consuming to implement, potentially impeding the efficiency of analysis, and can introduce variability in derivatization yields across samples.

Liquid chromatography mass spectrometry (LC-MS/MS): Developing analytical methods for underivatized TFA and other ultra-short chain PFAS using HPLC-MS techniques presents advantages. However, conventional reversed-phase liquid chromatography (RPLC) systems face challenges due to poor retention, separation, and peak resolution caused by the high polarity of these PFAS. Early elution with other polar matrix components and reduced ionization efficiency

further complicate analysis. Furthermore, pre-concentration procedures traditionally employed for long-chain PFAS are often unsuitable for the more polar and water-soluble ultra-short and short-chain PFAS. Thus, various alternative LC methods have been explored to analyze compounds, including ion exchange sorbents, normal phase liquid chromatography (NPLC), and carbon-based sorbents. [141] [142] [143] [144] However, it's important to note that these techniques have their own limitations. For example, carbon-based LC may pose challenges when dealing with large sample series due to the time required for equilibration between consecutive injections. [145] Ion-exchange chromatography relies on the analytes being in their ionized form during injection, which may not be easily achievable when dealing with analytes of varying properties, such as different pKa values. [146] Non-aqueous NPLC, which involves the retention of polar analytes on a polar stationary phase using a highly apolar mobile phase like hexane, can lead to excessive retention of highly hydrophilic compounds and poor solubility in the mobile phase. [147]

To address these challenges, a modified normal phase sorbent compatible with the introduction of water into the mobile phase composition can be utilized. This technique, known as Hydrophilic Interaction Chromatography (HILIC), has emerged as a powerful complementary method to RPLC for the retention and separation of highly polar analytes [148] [149] [150] [151] [152] In order to achieve a suitable method detection limit for water samples, a common approach involves an off-line pre-concentration step where 50-250 mL of the water sample is loaded onto solid phase extraction (SPE) cartridges specifically designed for this purpose, such as Oasis HLB, Isolute ENV+, or Hypersep Retain PEP. Elution is then carried out using a high organic solvent content, typically a mixture of acetonitrile and water (90:10 v/v), suitable for subsequent injection into the HILIC-MS system. [146] There is another alternative approach, i.e., online preconcentration coupled with HILIC-MS, which has the advantages of fewer pretreatment steps and faster turnaround time. This technique has been explored in a limited number of studies, mainly in bioanalytical applications and involving relatively small injection volumes, its potential for aqueous environmental samples is promising. [153] Previous studies have demonstrated the feasibility of on-line solid phase

extraction (SPE) coupled with HILIC-MS for analyzing polar pharmaceuticals in slightly larger sample volumes. [146, 153] However, despite the numerous advancements in HILIC-MS techniques, there is a noticeable gap in research regarding the investigation of sample pre-concentration coupled on-line to HILIC-MS for achieving faster turnaround times and improved sensitivity specifically for short-chain and ultra-short chain PFAS.

Other non-conventional analytical methods, such as ultra-performance convergence chromatography (UPC^2), [38] mixed-mode liquid chromatography (MMLC), [41 42] and supercritical fluid chromatography (SFC) [28 43 13] offer potential solutions, and SFC has demonstrated the lowest instrument detection limits for C1-C4 PFAS among these techniques, as reported by Björnsdotter et al., [28]. However, its limited popularity is attributed to the specific instrumentation and pressure conditions required.

2.5. PFAS Sample Preparation

The pre-treatment stage of PFAS analysis is the most crucial step in the entire analytical process and often the most time-consuming and labour-intensive. The primary objective of this stage is to remove unwanted matrix interferences and/or concentrate or dilute analytes of interest. The quality of the sample preparation methods can greatly affect the sensitivity, accuracy, and chromatographic separation of the subsequent instrumental analysis. A poorly prepared sample can result in a reduced signal-to-noise ratio, decreased detection sensitivity, and poor chromatographic peak shape, all of which can compromise the quality of the data generated. Therefore, it is imperative to use robust and validated pre-treatment methods to ensure the quality and integrity of PFAS analysis.

2.5.1. Aqueous Matrices

Two of the most commonly used pre-treatment techniques for water samples that contain low

levels of organics of interest are solvent-based extraction (SBE) and adsorbent-based extraction (ABE). [154] While both methods have advantages, ABE is gaining increasing attention due to its ability to achieve higher extraction yields with lower organic solvent consumption. Additionally, ABE offers a wide range of sorbents that can be selected based on the specific properties of the sample matrix. For more complex environmental liquid samples, solid-phase extraction (SPE) is often the preferred pre-treatment method. SPE enables efficient extraction and purification of the PFAS analytes from a large number of interfering compounds, which can cause ion suppression or enhancement during electrospray ionization. Eliminating the matrix interferences can significantly enhance the accuracy and sensitivity of subsequent PFAS analysis.

Commercially available adsorbents, such as weak anion exchange sorbents (WAX) and hydrophilic-lipophilic balance (HLB) polymeric sorbents, have been used for PFAS extraction, while bamboo charcoal-packed cartridge, [155] Sep-Pak Vac C18 [156] or Enviro-Clean CUCARB [157] are less commonly used. Although HLB has been used for PFCA extraction, it has been found to have low recoveries for short-chain PFCAs because of poor retention of certain hydrophilic compounds onto the sorbents. [158] In contrast, the effectiveness of the WAX adsorbent in retaining short-chain homologues has been well-established. The presence of tertiary amine functional groups on WAX sorbents makes them positively charged at lower pH levels (less than 4), enhancing their ability to retain anionic PFAS through electrostatic interactions. [156] Moreover, the WAX adsorbent is known for its high extraction efficiency for both neutral and acidic PFAS, making it a more reliable and preferred option for PFAS extraction.[159] Results have shown that the mixed-mode WAX sorbents are capable of extracting and fractionating various PFAS, including neutral, cationic, and zwitterionic PFAS. [160] To elute the different PFAS from WAX solvents, methanol can be used, where neutral, cationic, and zwitterionic PFAS can be eluted first, and then anions can be eluted with basic methanol. In addition, WAX cartridges have shown satisfactory recoveries for emerging PFAS such as perfluoroalkyl ether carboxylic acids (PFECAs), [161] chlorinated polyfluoroalkyl ether sulfonic acids (Cl-PFESAs), [162] sodium p-perfluorous

nonenoxybenzenesulfonate (OBS), [163] and fluorotelomer sulfonamide alkyl betaines (FTABs). [164] In addition, the use of multiple SPE cartridges with different sorbents has been explored, such as a combination of HLB, WAX, and cation exchange cartridges, to increase the chances of retrieving unknown PFAS that cannot be recovered using a single-phase SPE method. [165]

Traditional SPE requires large volumes of samples, which after the elution step, need to be evaporated to a small volume or dryness, and then re-dissolved in a water-methanol mixture solvent. This lengthy process increases the risk of introducing contamination at each step of the SPE. To overcome these limitations, online SPE coupled with LC-MS/MS offers a solution for shortening the pre-treatment duration and minimizing background contamination. This approach requires a smaller sample volume, e.g. 10 mL, and reduces the possibility of introducing contaminants at each step. [166] However, they may present greater matrix effects and other challenges. One example of such a pitfall is the risk of sorption artifacts for hydrophobic PFAS. This is mainly a concern for long-chain PFAS, as the high aqueous percentage of the final extracts submitted to LC-MS could lead to time-dependent sorption, resulting in dynamically changing detection limits. [113]

Direct injection in water analysis is another solution that eliminates the need for sample pre-treatment. However, this method requires an extended chromatographic analysis step to ensure the separation of the analytes from the interferences present in the matrix. Ciofi et al. [167] demonstrated the excellent detection limits (0.014-0.44 ng/L) on Sciex QTrap 5500 triple quadrupole mass spectrometry for direct injection analysis of 100 µL of waste, surface, and drinking water samples for nine perfluoroalkyl acids. Mottaleb et al. [168] used Sciex QTrap 6500 in direct injection mode for the determination of eight perfluorinated compounds, requiring only 5 µL of sample after centrifugation and filtration and achieved detection limits of 0.007 - 0.04 ng/mL. Moreover, solid-phase micro-extraction (SPME) has emerged as a technique that combines sampling, sorbent extraction, preconcentration, and injection in a single step. Huang et al. [159] proposed a novel

multiply monolithic fiber solid-phase microextraction (MMF-SPME) technique, which utilizes monolithic adsorbent (MA) combining fluorophilic and anion-exchange interactions to concentrate PFCAs, requiring only 20 mL of the sample volume.

2.5.2. Solid Matrices

Table S1 summarizes the various extraction methods used for PFAS, including legacy and novel ones. While some of these methods may appear similar, extracting cationic and zwitterionic PFAS in soil and sediment can be particularly challenging due to their unique properties and the presence of soil organic matter and clay content. [164, 169] These factors can impact extraction efficiency and potentially result in inaccurate measurements of PFAS concentrations in environmental samples. Moreover, extracting novel PFAS can present additional challenges, as their chemical structures and properties may differ from those of legacy PFAS. Novel PFAS, which have been developed as replacements for legacy PFAS, may have different levels of solubility, hydrophobicity, and reactivity, which can affect the choice of extraction method. Additionally, the complex nature of environmental matrices, such as soil and sediment, can further complicate the extraction process and require careful optimization of the method to achieve reliable and accurate results.

Mejia-Avendaño et al. [169] examined the impact of soil properties and the presence of hydrocarbon contamination on PFAS recovery performance. A MeOH/NH_4OH extraction method produced excellent extraction efficiency (70-120%) for most anionic PFAS under all soils and co-contaminants conditions. However, the extraction recoveries for betaine-based PFAS (PFOSB, PFOAB, and 6:2 FTAB) or quaternary amine based PFAS (PFOAAmS and PFOSAmS) were only 30%-60% in different soil types, and the recovery of betaines in clay loam soil was even lower (5-10%). The recoveries for some PFAS also decreased with increasing organic carbon content in the soil, especially when supplemented with petroleum cocontaminants. A MeOH/NaOH extraction method gave better recoveries for the novel PFAS but presented the drawback of higher detection limits and lower instrumental precision. Munoz et al. [164] further optimized extraction methods for

zwitterionic, cationic, and anionic PFAS in AFFF-impacted soils by performing extensive extraction tests with various extraction solvents, different pH modifiers, and concentrations of the latter. It was found that conventional analytical methods for extracting anionic PFAS from soil, such as methanol with low concentrations of base, severely underperformed for some of the newly identified zwitterionic and cationic PFAS. MeOH/HCl presented excellent recoveries for most cationic and zwitterionic PFAS, but the recoveries were less satisfactory for some anionic PFAS due to hydrolysis artefacts. MeOH/CH_3COONH_4 method was suggested as an appropriate compromise with acceptable recoveries and reduced risks of analyte interconversions.

Repeated use of AFFF-containing PFAS at firefighting stations and military bases/airports has not only caused serious contamination of the surrounding environment but also exposed the related infrastructure materials (i.e., concrete and asphalt) to severe PFAS contamination. Srivastava et al. [170] developed extraction methodology for the analysis of 22 target PFAS including short- and long-chain PFCAs and PFSAs and fluorotelomers in asphalt materials collected from military bases. The methanol-based extractants performed best due to their accuracy and precision, which were within the acceptable range (extraction efficiency between 70 and 130% and RSD < 20%). Baduel et al. [171] used MeOH/NH_3aq (99/1) as extraction solvents to extract PFAS from AFFF-impacted concrete, more than 60 PFAS representing 12 different fluorochemical classes were identified in the concrete extracts.

3. Materials and Methods

3.1. Chemicals and Standards

Certified standards of trifluoroacetic acid (TFA, ⩾99%), perfluoropropanoic acid (PFPrA, ⩾ 97%), perfluorobutanoic acid (PFBA, ⩾99%), and trifluoromethane sulfonic acid (TMS, ⩾99%) were purchased from Sigma-Aldrich Canada (Oakville, ON, Canada). Perfluoroethane sulfonic acid (PFEtS) was obtained from Apollo Scientific Ltd (Stockport, UK). Perfluoropentanoic acid (PFPeA), perfluoropropanesulfonic acid (PFPrS), and perfluorobutane sulfonic acid (PFBS) were purchased from Wellington Labs, Inc. (Whitby, ON, Canada). The n:3 acids (1:3 acid, 2:3 acid, and 3:3 acid) were obtained from Synquest Laboratories (Alachua, FL, USA).

TFA-$^{13}C_2$, PFBA-$^{13}C_4$, PFPeA-$^{13}C_5$, PFBS-$^{13}C_3$ were the isotope-labelled internal standards used in the present study. The association between the native analyte and the corresponding internal standard is provided in Table S2. TFA-$^{13}C_2$ was from Toronto Research Chemicals (Toronto, ON, Canada), while PFBA-$^{13}C_4$, PFPeA-$^{13}C_5$, and PFBS-$^{13}C_3$ were from Wellington Labs, Inc.

HPLC grade solvents, including water (H_2O), acetonitrile (ACN), and methanol (MeOH), were purchased from Fisher Scientific Canada (Whitby, ON, Canada). Formic acid (FA) (⩾98%), ammonium formate (⩾99%, LC-MS grade), and ammonium acetate (AmAc) (⩾99%, LC-MS grade) were purchased from Sigma-Aldrich Canada.

3.2. Sample collections

Method application was conducted on Forty-four surface water samples obtained through collaborators, covering different site contexts. Common to each sampling campaign, bottle

containers (0.5-L high-density polyethylene bottles) were rinsed at the analytical facilities with Milli-Q water, 50:50 MeOH/HPLC water, and HPLC water before use. Samples from a large Canadian river (n = 16) were collected in the summer of 2019 from aboard the *Lampsilis* research vessel. The samples were collected at ~1 m below the surface with a Niskin/Go-Flo sampler and stored refrigerated onboard until transfer to the analytical facilities. A field blank was also performed using ultrapure water passed through the Niskin/Go-Flo sampler. Surface water samples from tributaries to this large river were also available for screening, including rivers with relatively limited anthropogenic impacts (rivers A and B) and an urbanized river (river C). Surface water samples were also obtained from AFFF-impacted sites, including ditches or rivers/creeks near fire-training and fire-equipment testing areas of four airports in central and eastern Canada. [172] After their reception at the analytical facilities, all samples were stored at 4 °C until sample preparation and analysis.

3.3. Sample Preparation and Instrument Analysis

Surface water samples were filtered through glass fiber syringe filters (GFF, 0.3 μm) and a 5-mL aliquot of the filtrate was spiked with a mixture of isotopically-labelled internal standards to reach a concentration of 20 ng/L each. Samples were then analyzed at the Université de Montréal by on-line solid-phase extraction (SPE) coupled to liquid chromatography interfaced with high-resolution mass spectrometry (LC-HRMS).

A two-pump system was used for on-line pre-concentration and chromatographic separation, including a Thermo Dionex UltiMate™ 3000 pump and a Thermo Dionex UltiMate™ 3000 RS pump. The on-line SPE system was connected to the LC-HRMS system by a dual switching-column array consisting of six-port and ten-port valves (see a schematic of the system in Scheme S1). A 2-mL aliquot of the sample was injected into a 2 mL injection loop and loaded onto the on-line SPE column for sample pre-concentration. The flow rate for sample loading was 1 mL/min. After the sample loading step, the on-line SPE aqueous mobile phase was allowed to flow through

the cartridge for an additional 0.5 min (equivalent to a wash volume of 0.5 mL) to remove the matrix and salts. The analytes were then eluted in a back-flush mode at 0.5 mL/min with the LC-HRMS gradient. Analytes were retained using a Thermo Scientific Acclaim™ Trinity Q1 column thermostated at 40 °C, starting from 90/10 A/B, a strong solvent condition. The mobile phases were 25 mM ammonium acetate (A) and HPLC-water (B). Data were acquired using a Q-Exactive Orbitrap high-resolution mass spectrometer (Thermo Scientific, Waltham, MA, USA) operated in full scan MS negative electrospray ionization mode, with a resolution setting of 70,000 FWHM at *m/z* 200. Further method parameters are provided in SI Table S5.

3.4. Method validation and quality assurance/quality control

Filtration recoveries were evaluated in surface water, involving the following types of syringe filters: glass fiber (GFF), 0.3 µm, 25 mm, non-capsule (ADVANTEC); nylon (NY), 0.2 µm, 25 mm, capsule (Fisher Scientific); polyethersulfone (PES), 0.22 µm, 13 mm, capsule (Cole-Parmer Canada); and regenerated cellulose (RC), 0.2 µm, 13 mm, capsule (Fisher Scientific). The filtration recovery is derived from the area ratio of analytes in surface water samples spiked with target PFAS before filtration and reference samples spiked after filtration.

The online SPE recoveries of target PFAS were evaluated based on the procedure described by Vaudreuil et al. [146] On-line SPE recoveries were derived from an equivalent amount of analyte response submitted to online SPE large volume LC-MS (2000 µL) versus online SPE small volume LC-MS (50 µL).

Quantification of analytes was achieved using matrix-matched calibration curves constructed in a composite mixture of surface water samples from the Quebec province, including Lake Saint-Anne (SW1), the St. Lawrence River (SW2) and the Chateauguay River (SW3). Matrix-matching curves were constructed by adding increments of PFAS at 10 calibration levels (For TFA, PFPrA, PFBA, PFPeA, TMS, PFEtS, PFPrS, and PFBS: 0.05, 0.1, 0.5, 1, 2, 5, 10, 25, 50 and 100 ng/L; For 1:3

acid, 2:3 acid, and 3:3 acid: 1.05, 2.1, 5.5, 11, 22, 55, 110, 225, 550, and 1100 ng/L). In all cases, the isotope-labeled internal standards (ISs) were spiked to reach a final concentration of 20 ng/L (30 ng/L for $^{13}C_2$-TFA).

The method limit of detection (LOD) was determined following two approaches. In the first approach, ten procedural mQ-water blanks were injected; for those PFAS that were detectable in the blanks, the LOD was three times the standard deviation of the determined blank concentrations, and mLOQ was ten times the standard deviation. For those PFAS that were not present in blank samples, the second method was applied as follows. Several different low-level concentrations of PFAS (0.05-2 ng/L) were spiked into the surface water matrix to reach intensities between 1E4-1E5, and the mLOD was then derived as the concentration yielding a peak with an intensity of 1E4;[119] the mLOQ was then set as three times the mLOD.

Accuracy was evaluated by analyzing 5 quality control (QC) replicates at two concentration levels in surface water matrices, each spiked in triplicate (QC1: 7.5 ng/L for TFA, PFPrA, PFBA, PFPeA, TMS, PFEtS, PFPrS, and PFBS, 17.5 ng/L for 1:3 acid, 2:3 acid, and 3:3 acid; QC2: 75 ng/L for TFA, PFPrA, PFBA, PFPeA, TMS, PFEtS, PFPrS, and PFBS, and 575 ng/L for 1:3 acid, 2:3 acid, and 3:3 acid). Accuracy was determined by comparing quantified (measured) concentrations with theoretical (expected) spiked concentrations. Precision is the repeatability of a series of measurements expressed as percent relative standard deviation (%RSD). Intra-day precision corresponded to the %RSD of three QC samples analyzed during a single workday. The procedure was repeated on different weekdays, and the inter-day precision was derived from the overall %RSD (n = 9).

Matrix effects were assessed by comparing the slopes of calibration curves in the surface water matrix with those in matrix-free ultrapure water (mQ-water), following the same procedures as reported before. [146,173]

3.5. Statistical analyses

A design of experiments (DOE) was carried out for multiple response simultaneous optimization of the experimental conditions of the online SPE method used for the simultaneous determination of 5 PFAS. A modified Box-Behnken design was applied to investigate the effects of three important factors on online SPE for analyzing 5 PFAS. The factors were: sample loading volume, loading flow rate and wash volume. Fig. S20 describes the model of the modified Box-Behnken design (BBD) for the optimization of three factors in this study. In Table S6, columns 2-4 represent the three important factors and their coded levels, and columns 5-7 show the uncoded factor levels for all experiments. The relationship between natural variables and coded variables is as follows:

$$x_1 = \frac{Sample\ volume - (Sample\ volume_{max} + Sample\ volume_{min})/2}{(Sample\ volume_{max} - Sample\ volume_{min})/2}$$

$$x_2 = \frac{Flow\ rate - (Flow\ rate_{max} + Flow\ rate_{min})/2}{(Flow\ rate_{max} - Flow\ rate_{min})/2}$$

$$x_3 = \frac{Washing\ volume - (Washing\ volume_{max} + Washing\ volume_{min})/2}{(Washing\ volume_{max} - Washing\ volume_{min})/2}$$

The overall design matrix shows 15 runs randomly carried out trying to nullify the effect of lurking variables (n = 3 per condition).

The obtained experimental data were employed to build a model for each response, fitting them to a second-order polynomial function, responding to the general equation below:

$$y = \beta_0 + \sum_{i=1}^{k} \beta_i x_i + \sum_{i=1}^{k} \beta_{ii} x_i^2 + \sum_{1 \le i \le j}^{k} \beta_{ij} x_i x_j + \varepsilon$$

where β_0 is the constant term, and β_i, β_{ii}, and β_{ij} represent the coefficients of the first-order

terms, quadratic terms and interaction terms, respectively, and ε is the residual associated with the experiments, and *k* is the number of factors.

The DOE was conducted using JMP Pro 16. The modified BBD box was constructed using Python 3.9.6. The t-test results were also from Python 3.9.6. Results of the standard least square fit were obtained using JMP Pro 16. Related scripts are provided in the supporting information.

4. Results and Discussion

4.1. Optimization of LC conditions

4.1.1. Screening of LC columns

The study began with a screening of different analytical columns. Chromatographic properties and separation performance were examined on seven analytical columns. The relevant information for the analytical columns is shown in Table S3. Three analytical columns for reversed-phase liquid chromatography (RPLC), namely C18, C18-aQ and PFP, were first investigated (Figure S4). The C18 column is a conventional silica-based C18 column, the most commonly used analytical column in RPLC, where the retention decreases with the increasing polarity of the analyte. Unsurprisingly, TFA, PFPrA, PFBA, TMS, and PFEtS were eluted in less than 4 min, and the elution order of the five PFAS was consistent with the above. Although the peaks of 5 different PFAS were well separated, TFA was not adequately retained. Subsequently, a modified C18, C18-aQ (a polar end-capped C18 column), was tested. The results obtained for C18-aQ were similar to the conventional C18 but slightly worse than the conventional C18 in terms of retention and peak intensity (Figure 2). The PFP column uses pentafluorophenylpropyl as the stationary phase and spherical porous ultra-pure silica as the packing material, which can provide an alternative to the C18 column. The PFP column is particularly suitable for the separation of halogenated compounds and non-halogenated polar compounds. Among the three RPLC analytical columns, the PFP

column showed the highest retention for all five PFAS, but peak intensities were similar to those of C18. Overall, all three analytical columns separated the five different PFAS well, but all five PFAS eluted too early; none of the columns obtained a highly resolved TFA peak.

Four HILIC analytical columns were then investigated (Figure S5). Compared to RPLC, the retention order is often reversed, i.e., highly polar analytes are more strongly retained. The HILIC-AMIDE column is based on the support of spherical solid core ultrapure silica modified by amide. The HILIC-Syncronis analytical column consists of spherical porous ultrapure silica as the packing material and a zwitterionic stationary phase (the stationary phase has both quaternary ammonium and sulfonic groups). The results of the HILIC-AMIDE and HILIC-Syncronis columns were opposite to those of the C18 and C18-modified columns. Although all 5 PFAS acquired highly resolved peaks, they showed inadequate chromatographic separation and weakly retained peaks. For the HILIC-PEI column, the peaks of TFA and PFPrA were broad and not adequately resolved. Trinity-Q1 is a multifunctional column based on nanopolymer silica hybrid technology, providing reverse phase, weak anion exchange, and cation exchange retention mechanisms. The weak anion exchange function can provide good retention and separation for anionic species, whereas the weak cation exchange moiety effectively deactivates the undesirable interaction between the surface silanols and the analytes. Although not classified as a HILIC column, HILIC-Trinity-Q1 performed well under the HILIC mode regarding separation, peak resolution, and retention for analyzing ultra-short and short-chain PFAS. All five PFAS also had satisfactory peak heights (Figure S5 and Figure 2). The Trinity-Q1 was thus selected for the subsequent optimization experiments.

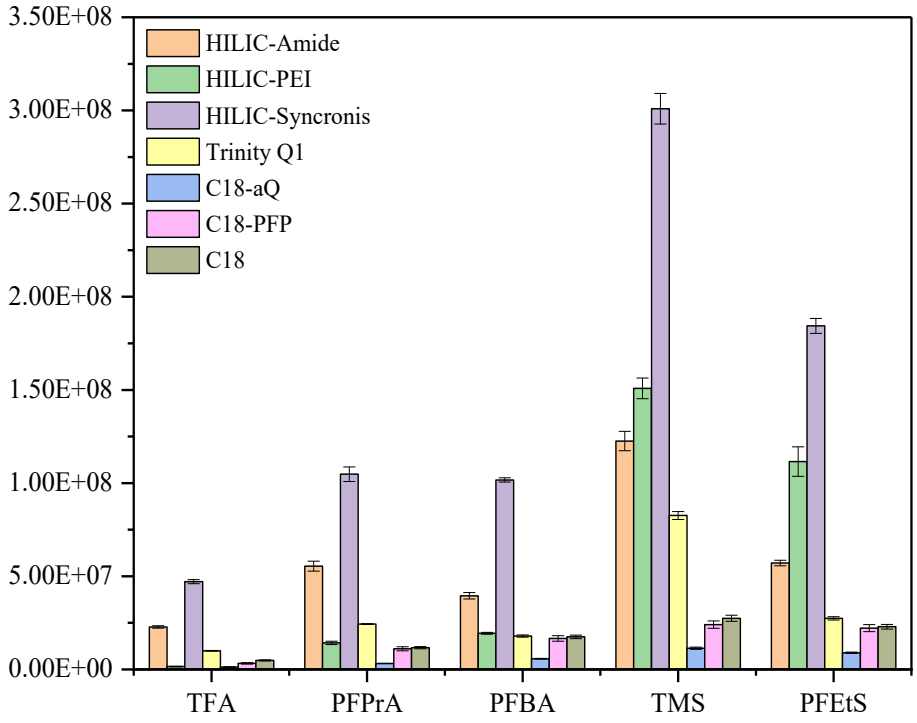

Figure 2 Peak intensities (signal height) of 5 PFAS using different LC analytical columns

4.1.2. Optimization of LC conditions

Flow rate. LC conditions were further optimized by investigating the effect of mobile phase flow rate on the chromatographic separation, peak shape (Figure S6) and peak height (Figure 3). For PFPrA, TMS, and PFEtS, the intensity increased with the increase in flow rate. Interestingly, for TFA, the change in peak height seemed to be independent of the flow rate over the tested range. In this study, since TFA is the most hydrophilic among the five tested PFAS and a relatively difficult compound to analyze in LC, priority was given to this compound to achieve the best chromatographic separation and intensity. Therefore, the optimal flow rate was determined to be 0.5 ml/min.

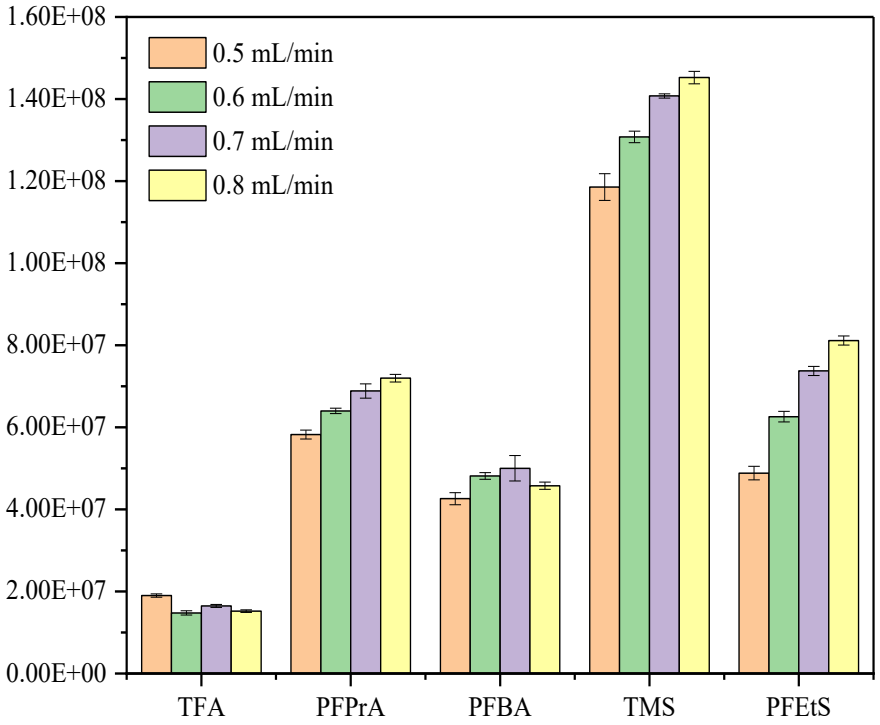

Figure 3 Effect of different sample loading flow rates on the peak intensities (signal height) of 5 PFAS

Mobile phase eluent composition. Ionic additives are commonly used in HILIC and RPLC to control the pH and ionic strength of the mobile phase, such as ammonium acetate (AmAc) and ammonium formate. They can also result in different chromatographic retention/elution. [149] In addition, it was reported that increasing the concentration of AmAc can improve the peak shape. [174] These findings indicate that optimizing the mobile phase composition is essential when developing analytical methods for ultrashort chain PFAS. In this study, the concentration of AmAc was varied between 5 and 50 mM (Figure 4). As the AmAc concentration increased, the retention times of the five PFAS decreased, and sharper peaks shapes were obtained (Figure S7). If considering only the peak intensity, 20 mM AmAc would be the best compromise for the five tested PFAS. However, chromatographic separation is another factor to consider. At 15 mM AmAc, better chromatographic separation was achieved than at 20 mM. For TFA, the peak intensity at an AmAc concentration of 15 mM was also slightly higher than at 20 mM. Therefore, the optimal

concentration of AmAc was determined to be 15 mM. The effect of the addition of formic acid (0.1% FA) was also investigated (Figure S8); as no improvement was noted, the addition of FA in the mobile phase was discarded.

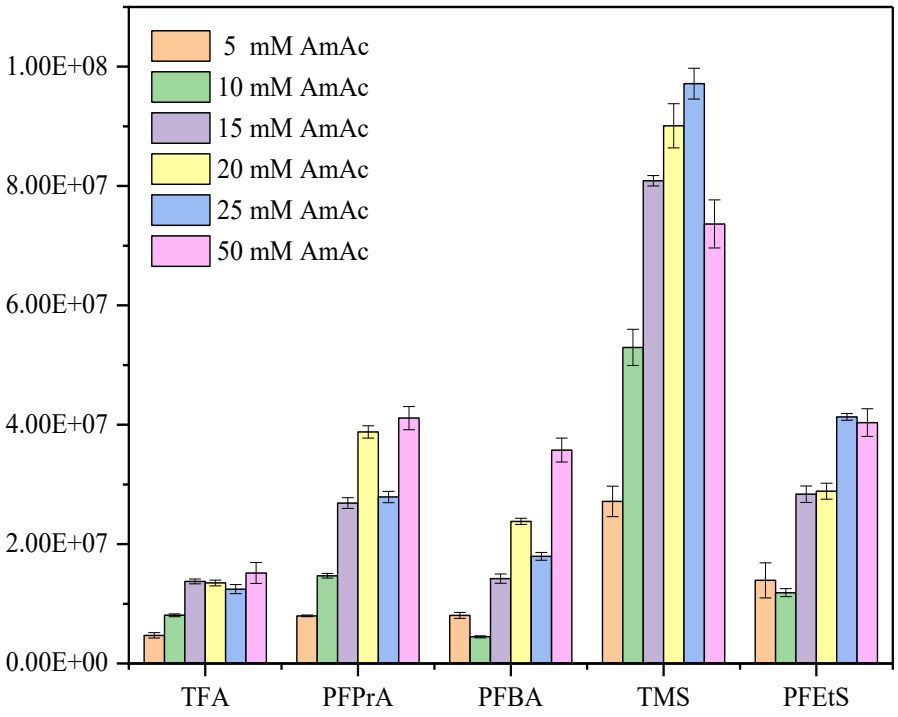

Figure 4 Effect of different mobile phase concentrations of ammonium acetate (AmAc) on the peak intensities (signal height) of 5 PFAS

4.2. Optimization of online SPE

4.2.1. Screening of online SPE conditions

One of the most promising strategies for minimizing sample preparation steps and achieving improved LC-MS instrumental sensitivity is the use of online SPE. As the technique requires the analyzed sample to be highly aqueous, it is typically not appropriate for long-chain hydrophobic PFAS due to time-dependent sorption onto the vial surface. [113] In contrast, ultra-short and short-

chain PFAS are likely amenable to online SPE analysis, as recently tested by Jacob and Helbling.[175] An appropriate SPE column is essential for quantitative extraction of the target analytes, matrix removal, and rapid transfer of analytes from the SPE column to the analytical column.[176] Developing the online pre-concentration method involved screening different enrichment columns and optimizing sample loading parameters (loading flow rate, loading mobile phase, wash volume, and sample injection volume), described as follows.

Screening of online SPE columns. In this study, five different SPE columns were evaluated by loading a 1 mL surface water sample spiked with 5 PFAS (1 ppb). The effect of sample acidification on extraction performance was also investigated. Representative chromatograms are shown in Figures S9 and S10, and peak intensities are in Figure 5. Of the five columns tested, Biotage with sample acidification and GCB without sample acidification resulted in higher peak intensities for all tested PFAS, especially for TFA. Thus, these two columns were selected for subsequent stability tests (Figure S11-12). With the GCB column, after 10 repeated injections, a loss of nearly 60% in peak intensity for the five PFAS was observed. In contrast, satisfactory stability was obtained using the Biotage column (Figure S12). The Biotage column was therefore selected for subsequent optimization.

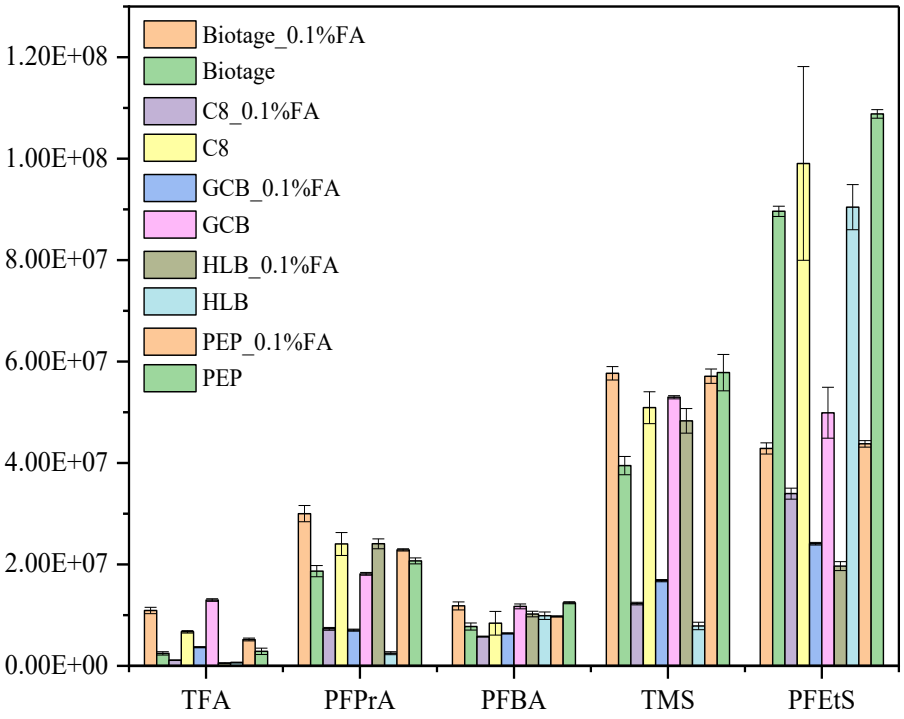

Figure 5 The effect of different online SPE columns on the peak intensities (signal height) of 5 PFAS

Online SPE and LC mobile phase composition. When online-SPE-LC-HRMS was performed using the optimized LC conditions (section 3.1) and the Biotage pre-concentration column, double peaks appeared for PFPrA and PFBA (Figure S13). Increasing the wash volume alone could increase the pH value in the SPE system, promoting the dissociation of the carboxylic acid to form the anion, which could explain the second peak of PFPrA and PFBA. By increasing the concentration of AmAc in the LC mobile phase solely, the double peaks of both PFPrA and PFBA disappeared, and the peak shapes of all five PFAS became increasingly sharp (Figure S14-S15), possibly because AmAc acts as an ion-pairing agent aiding chromatographic elution. [177] Additionally, when the amount of FA was increased in both the sample and mobile phases (thus lowering the pH), it could prevent the dissociation of PFPrA and PFBA. Combining an increased wash volume and the addition of FA to the mobile phase while maintaining a 0.1% FA concentration in the sample results in the disappearance of the double peaks for both PFPrA and

PFBA.

Next, the effect of different FA concentrations in the SPE loading phase was investigated. As shown in Figures S16 and S17, FA percentages in mQ-water ranged from 0 to 0.1% in the SPE loading phase, and all five PFAS displayed adequate chromatographic separation and peak shapes. In terms of peak intensity (Figure S18), perfluorocarboxylic acids (e.g., TFA, PFPrA, and PFBA) all showed the highest peak intensity when the percentage of FA was 0.0125%, and peak intensities gradually decreased as the percentage of FA increased. For perfluorosulfonic acids, TMS showed the highest peak intensity at 0.1% FA, followed by 0.0125% FA, and PFEtS showed the highest peak intensity at 0.05% FA, followed by 0.1% and 0.0125% FA. Therefore, 0.0125% FA in mQ-water of the SPE loading phase was selected.

Sample acidification. The addition of FA to the aqueous sample generally increased PFAS peak intensities compared to sample without acidification, with the largest effect for PFPrA and TMS (Figure S19). With the increase of FA concentration in the samples from 0.025% to 0.1%, the peak intensities of the 5 PFAS only varied marginally. TFA had the highest peak intensity for an FA content of 0.025%, while the remaining 4 PFAS had similar peak intensities at FA contents of 0.025% to 0.1%. Sample acidification with a content of 0.025% FA (i.e., pH ~4) was therefore selected for subsequent optimization of other online SPE parameters.

4.2.2. Optimization of other online SPE parameters

The online SPE step depends on several other parameters, including the sample volume loaded onto the SPE column (using different injection volumes and loop sizes) and the speed at which the sample is loaded (flow rate). A larger volume of sample passed through the SPE column does not always equate with signal improvement, as the least retained analytes could suffer breakthroughs with increasing loading volume, and matrix effects could also become more prominent. Another important parameter is the wash volume, i.e., the volume of the online SPE aqueous phase that flows through the SPE column after sample loading is completed and before starting the elution

from the SPE column to the analytical column. A larger wash volume could be useful to reduce matrix effects and remove salts but could also result in unwanted analyte losses (breakthrough). As these parameters may interact which each other, a traditional one-factor-at-a-time (OFAT) methodology may not be the best approach for optimization. Here, we simultaneously tested the effects of sample loading volume (tested in the range of 1 – 5 mL), loading speed (1 – 2 mL/min) and wash volume (0.5-1.5 mL), using a design of experiment (DOE) methodology (Section 2.5). A fractional BBD was used to reduce the total number of runs, and a response surface was fitted to the results for data visualization (see also Table S7 for corresponding regression coefficients, R^2, and p-values).

Figure S21 shows response surface contour plots of the 5 PFAS. TFA peak intensity decreased with increasing sample loading volume, while the other 4 PFAS showed increased intensities. TFA peak intensity also decreased with higher washing volume, while it had little effect on the other 4 PFAS. Thus, TFA peak intensity is maximum with minimum sample loading and washing volumes. The fitted model of TFA shows that the maximum peak intensity of TFA would be obtained when the sample volume is 1 ml, the flow rate is 1 ml/min, the washing volume is 0.5 ml, and the predicted value of its peak intensity is 4.86×10^6 (95% confidence interval, [4.63E+06-5.08E+06]); however, the minimum peak intensity values are obtained for the other 4 PFAS under such conditions. When the sample volume is increased to 2 ml, the prediction model shows that the peak intensity of TFA decreases slightly (3.75E+06), while the peak intensity of the other 4 PFAS increase to about twice their original value (Figure S22). Therefore, a sample volume of 2 ml, a flow rate of 1 ml/min, and a wash volume of 0.5 ml were selected as the best operating conditions for simultaneous analysis of the tested PFAS.

4.3. Assessment of filters

To decide which filter to use, different filters have been evaluated prior to the validation phase. After sample collection, surface water is often filtered as a pretreatment step to remove suspended

matter and reduce microbial levels. [178] However, improper selection of filter materials may bias the measured concentration of PFAS in surface water. For instance, Sörengård et al. [179] analyzed the filtration losses of 21 PFAS in milli-Q water and DOC-amended water and found average PFAS losses of 10-40%, depending on the syringe filter nature.

Our results suggest a limited influence of the filter material on the absolute recoveries of ultra-short and short-chain PFAS, in stark difference from trends for long-chain PFAS (Figure S23). [179] In the present study, recoveries for the GFF filter were 73–108% (standard deviation, SD = 0.51–6.0%), 72 –108% (SD = 1.1–19%) for NY, 65–105% (SD = 1.0–15%) for PES, and 69–110% (SD = 5.0–32%) for RC. Most compounds had recoveries within 80-110%, except PFBS with the PES filter (~65%) and PFBA regardless of filter type (~70%). Considering the need for high recoveries and suitable precision (i.e., small SDs), GFF was the more suitable filter for our study.

4.4. Analytical validation

Matrix-matched calibration, LOD, and LOQ. As shown in Table 1, the matrix-matched calibration curves yielded suitable coefficients of determination (R^2 range: 0.9913 – 0.9999) in surface water, meeting the acceptance criterion of $R^2 \geqslant 0.99$. [180] Method LODs ranged between 0.006 and 3.3 ng/L, and method LOQs between 0.019 and 11 ng/L. Compared to previously reported method LODs for TFA (Figure 6), earlier methods for TFA analysis were based on GC with mass spectrometry, and the GC method could achieve a lower LOD of a few ng/L. [17, 22] In addition, SFC-MS/MS not only eliminates the need for derivatization, a step required for TFA analysis by GC, but also achieves a much lower LOD. [28, 43] However, LC-MS/MS is more common than GC-MS or SFC-MS/MS in most laboratories. In this study, the LOD performance of TFA surpassed that of other LC-MS methods commonly employed in environmental waters. This improvement is particularly notable due to the utilization of a substantially lower sample volume compared to offline pre-concentration approaches (>100 mL). [37]

Table 1 Method validation data of 11 PFAS in a mixture of surface water, including method limits of detection (mLOD, ng/L) and method limits of quantification (mLOQ, ng/L), linear range and determination coefficients (R2) of matrix-matched calibration curves.

Compounds	LOD (ng/L)	LOQ (ng/L)	R-Square	Concentration Linearity (ng/L)
TFA	3.285	10.951	0.9924	LOQ-100
PFPrA	1.063	3.542	0.9997	LOQ-100
PFBA	0.685	2.285	0.9994	LOQ-100
PFPeA	1.191	3.970	0.9979	LOQ-100
TMS	0.008	0.025	0.9913	LOQ-100
PFEtS	0.006	0.019	0.9999	LOQ-100
PFPrS	0.017	0.050	0.9964	LOQ-100
PFBS	0.020	0.060	0.9969	LOQ-100
1:3_acid	0.205	0.614	0.9989	LOQ-1100
2:3_acid	1.544	4.632	0.9966	LOQ-1100
3:3_acid	2.850	8.549	0.9994	LOQ-1100

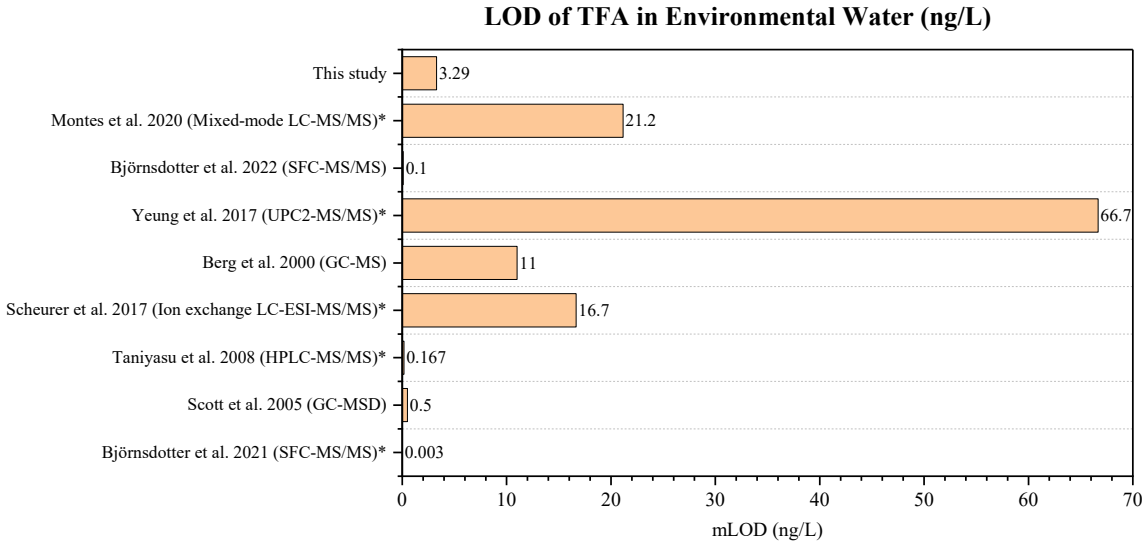

Figure 6 Method LOD (ng/L, mLOD) for the analysis of TFA in environmental water compared with literature data (*: Authors provided only mLOQ in their articles, we assume here that mLOQ is three times mLOD)

On-line SPE absolute extraction efficiency. Absolute extraction efficiencies (without surrogate internal standard correction) were between 40% and 128% at QC1, and between 24% and 125%

at QC2 (Table S8). Among these PFAS, TFA has a relatively poor absolute extraction efficiency in the online SPE due to its high polarity, which makes it difficult to retain on the SPE column during the loading and washing steps. However, as the matrix-matched calibration curve levels are also submitted to the online SPE process, and as labelled TFA was used for internal standardization, suitable whole-method accuracy can still be attained.

Accuracy and Precision. The overall accuracy of the matrix-matched spikes ranged from 71% to 130% (Table S9). This is within the EPA's acceptance criterion of 70-130% accuracy. [180] Intra-day precision ranged between 0.48% and 20.0%, and inter-day precision ranged between 0.92% and 19.0%, within the <30% guideline. [180]

4.5. Assessment of matrix effects

Assessment of matrix effects is essential when developing a robust quantification method. Standard lines were built in mQ-water, matrix-matched surface water, and surface water from different locations. As shown in Table S10, when matrix-matched surface water calibration curves to mQ water (matrix-free) curves, slight matrix suppression was observed for PFPrA (-10.27%), PFBA (-8.34%), PFPeA (-5.32%), and TMS (-6.83%). Other PFAS were affected by varying degrees of matrix enhancement, still within acceptance ranges (±30%); noteworthy exceptions were TFA, 1:3 acid and 2:3 acid, where the deviations exceeded the acceptance threshold. For this reason, we preferred using a matrix-matched calibration curve for more accurate quantitation.

Residual matrix effects were also tested to verify the suitability of calibration when applied to surface waters of different locations. Standard additions were constructed in three individual samples and compared to the slope of the matrix-matched calibration curve. The method showed limited residual matrix effects, further supporting the use of a composite surface water matrix for quantification.

4.6. Application to field samples of Canada

The developed analytical method was utilized to analyze ultra-short-chain and short-chain fluoroalkyl acids in a collection of surface water samples obtained in eastern Canada (Table 2). When considering the overall dataset (n = 44), five compounds had detection frequencies above 50%: TFA (89%, concentration range in positive samples = 4.6–220 ng/L), PFBA (61%, 0.53–33 ng/L), PFPeA (86%, 1.2–2100 ng/L), TMS (77%, 0.01–4.3 ng/L), and PFBS (100%, 0.07–450 ng/L). These results are similar to the concentrations of ultra-short-chain and short-chain PFAS previously reported in the literature (Table S11). For instance, Cahill et al. reported that TFA concentrations in surface waters of northern California, USA, increased from <9.5–295 ng/L to 23–2790 ng/L over two decades (1998-2021). [181]

Table 2 Concentrations (ng/L) of the targeted PFAS in field-collected surface water samples from Canada.

Type	Name	TF	PFP	PFB	PFP	T	PFE	PFP	PF	1:3	2:3	3:3
AFFF	River downstream	59	ND	0.85	12	1.1	0.03	0.09	2.6	ND	ND	ND
AFFF	River downstream	66	ND	ND	2.1	0.1	0.02	0.03	0.98	ND	ND	ND
AFFF	River downstream	46	ND	1.9	77	0.0	0.09	0.6	16	ND	ND	ND
AFFF	River downstream	59	ND	2.3	56	1.4	0.08	0.48	13	ND	ND	ND
AFFF	River upstream Airport	35	24	23	680	0.2	2.1	11	330	6.0	5.0	15
AFFF	River upstream Airport	60	1.3	0.57	3.0	0.1	0.02	0.04	1.3	ND	ND	ND
AFFF	River upstream Airport	60	1.1	0.53	4.6	0.1	0.02	0.04	1.7	ND	ND	ND
AFFF	River upstream Airport	47	21	20	560	0.2	1.9	9.7	290	5.2	4.1	9.9
AFFF	River upstream Airport	42	26	27	760	0.2	2.2	12	360	7.7	6.8	14
AFFF	River upstream Airport	43	4.3	11	180	0.0	0.04	0.46	17	ND	ND	ND
AFFF	River upstream Airport	48	0.99	0.75	15	0.1	0.04	0.18	5.0	ND	ND	ND
AFFF	Creek within Airport 1,	62	18	32	1300	0.3	3.0	18	450	ND	3.1	23
AFFF	Creek within Airport 1,	72	17	33	2100	0.2	2.1	13	340	11	5.9	18
AFFF	Creek within Airport 1,	54	14	28	1400	0.1	1.9	13	340	ND	4.5	18
AFFF	Creek within Airport 1,	46	6.8	16	810	0.0	0.83	6.2	160	ND	1.7	5.7
AFFF	Creek within Airport 1,	41	ND	5.1	240	0.0	0.04	0.67	26	ND	ND	ND
AFFF	Ditch downstream	16	ND	1.8	67	0.0	0.01	0.05	3.7	ND	ND	ND
AFFF	Ditch within Airport 3,	ND	4.4	11	580	0.0	0.01	0.15	12	ND	ND	ND
AFFF	Ditch within Airport 3,	ND	5.2	11	640	ND	0.01	0.14	13	ND	ND	ND

AFFF	Ditch within Airport 3,	8	6.0	14	740	0.0	0.01	0.18	16	ND	ND	ND
AFFF	Ditch within Airport 3,	41	ND	2.3	75	ND	0.01	0.10	7.8	ND	ND	ND
AFFF	Ditch within Airport 4,	93	7.7	16	500	ND	0.05	0.65	29	ND	ND	ND
AFFF	Ditch within Airport 4,	61	5.8	8.8	430	ND	0.07	0.60	26	ND	ND	ND
AFFF	Ditch within Airport 4,	62	5.0	8.0	410	ND	0.05	0.46	23	ND	ND	ND
AFFF	Ditch within Airport 4,	85	3.3	8.3	230	ND	0.02	0.30	15	ND	ND	ND
Background	River A	4.6	ND	ND	ND	ND	ND	ND	0.09	ND	ND	ND
Background	River B	11	ND	ND	ND	ND	ND	ND	0.18	ND	ND	ND
Highly	River C	22	ND	ND	1.6	ND	ND	ND	0.33	ND	ND	ND
Urban	River D, SW1	ND	ND	ND	ND	ND	ND	ND	0.47	10	ND	ND
Urban	River D, SW2	ND	ND	0.94	1.9	0.0	ND	ND	0.62	ND	ND	ND
Urban	River D, SW3	ND	ND	ND	1.3	0.7	ND	ND	0.69	5.4	ND	ND
Urban	River D, SW4	65	ND	ND	1.4	0.1	ND	ND	0.66	ND	ND	ND
Urban	River D, SW5	93	ND	1.1	2.7	0.1	ND	ND	0.77	ND	ND	ND
Urban	River D, SW6	46	ND	ND	ND	0.4	ND	ND	0.65	ND	ND	ND
Urban	River D, SW7	96	ND	ND	1.2	0.1	ND	ND	0.60	ND	ND	ND
Urban	River D, SW8	13	ND	1.1	1.5	0.1	ND	ND	0.52	4.8	ND	ND
Urban	River D, SW9	48	ND	ND	1.6	0.2	ND	ND	0.63	ND	ND	ND
Urban	River D, SW10	57	ND	ND	1.2	0.2	ND	ND	0.53	4.1	ND	ND
Urban	River D, SW11	59	ND	ND	ND	4.3	ND	ND	0.07	ND	ND	ND
Urban	River D, SW12	ND	ND	ND	ND	0.0	ND	ND	0.61	ND	ND	ND
Urban	River D, SW13	44	ND	ND	1.4	0.1	ND	ND	0.67	ND	ND	ND
Urban	River D, SW14	42	ND	ND	1.4	0.2	ND	ND	0.74	ND	ND	ND
Urban	River D, SW15	51	ND	ND	1.6	0.2	ND	ND	0.66	4.4	ND	ND
Urban	River D, SW16	40	ND	ND	1.4	0.2	ND	ND	0.68	ND	ND	ND

ND: Analyte not detected.

Some analytes had much higher detection frequencies and concentration levels in surface waters near airports with AFFF use (specifically: C3-C5 PFCAs and C2-C4 PFSAs) compared to the other surface waters targeted in this survey. For instance, concentrations of PFBS averaged 83 ng/L for AFFF-impacted rivers versus 0.53 ng/L for other rivers. The occurrence of C2-C4 PFSAs is likely related to the use of historical (ECF-based) AFFFs at fire-training area sites, which is also known to result in high levels of long-chain PFHxS (C6) and PFOS (C8) in groundwater as reported in Liu et al. [172] The detections of C3-C5 PFCAs could reflect the transformation of precursors to these

substances originally present in some AFFF formulations, such as 6:2 fluorotelomers. [182] Interestingly, ultra-short-chain TFA was detected at similar concentration ranges in AFFF-impacted rivers (<3–160 ng/L) and other rivers (<3–220 ng/L), with most values between 40–100 ng/L. A similar comment applies to the ultra-short-chain TMS. This could indicate that AFFFs are unlikely a major source of TFA and TMS to the environment and that diffuse sources (e.g., atmospheric deposition) may be preponderant over point sources for these ultra-short-chain PFAAs. Some high-production volume chemicals containing the -CF_3 moieties, such as novel refrigerants and pharmaceuticals, can generate TFA during environmental or engineered degradation processes, which could also explain the extensive occurrence of TFA in this study and other reports.

Four surface water samples from airport #1 all had detectable levels of 2:3 acid (1.7–5.9 ng/L) and 3:3 acid (5.7–23 ng/L), and one sample from the same airport also had 1:3 acid (11 ng/L). This is the first time that ultra-short-chain n:3 acids (n = 1, 2, 3) have been detected in environmental waters. These samples were collected from a creek within the airport boundary immediately downstream of the active fire-training area where fluorotelomer-based AFFFs are deployed. [172] Despite the absence of n:3 acids in AFFF formulations, it is probable that they resulted from the conversion of fluorotelomer precursors in the subsurface (soil/groundwater) and subsequently migrated to nearby surface waters. The short polyfluoroalkyl chain of these acids facilitated their high mobility. [183, 184, 185]

5. Conclusions

In this study, we developed a simple online SPE LC-HRMS method to quantitatively analyze 11 ultra-short and short-chain PFAS in surface water. The HILIC columns were expected to be the best-performing ones to retain and separate these PFAS, but the results show a multifunctional column performs better. This represents a significant improvement in analysis time compared with earlier approaches that relied on derivatization or offline SPE procedures. Online SPE achieved detection limits comparable to previous offline SPE – LC/MS approaches, thanks to the large sample volume injected into the system (2 mL) and instrument sensitivity. The method was successfully applied to field-collected surface water samples from Eastern Canada, including rivers downstream from AFFF source zones and other rivers. The AFFF-impacted rivers had C3-C5 PFCAs and C2-C4 PFSAs orders of magnitude higher than other rivers. For the first time, ultra-short-chain n:3 acids (n = 1, 2, 3) were detected in environmental water samples. In contrast, TFA (C2) and TMS (C1) were similar between the two groups of samples, suggesting that AFFFs are unlikely a significant source of these ultra-short-chain compounds to the environment and that diffuse sources (e.g., atmospheric deposition) may represent a key contamination pathway of surface waters. We encourage researchers to conduct further environmental studies of these ultra-short-chain and short-chain PFAS to document their occurrence, e-fate, and toxicity.

6. Supplementary Information

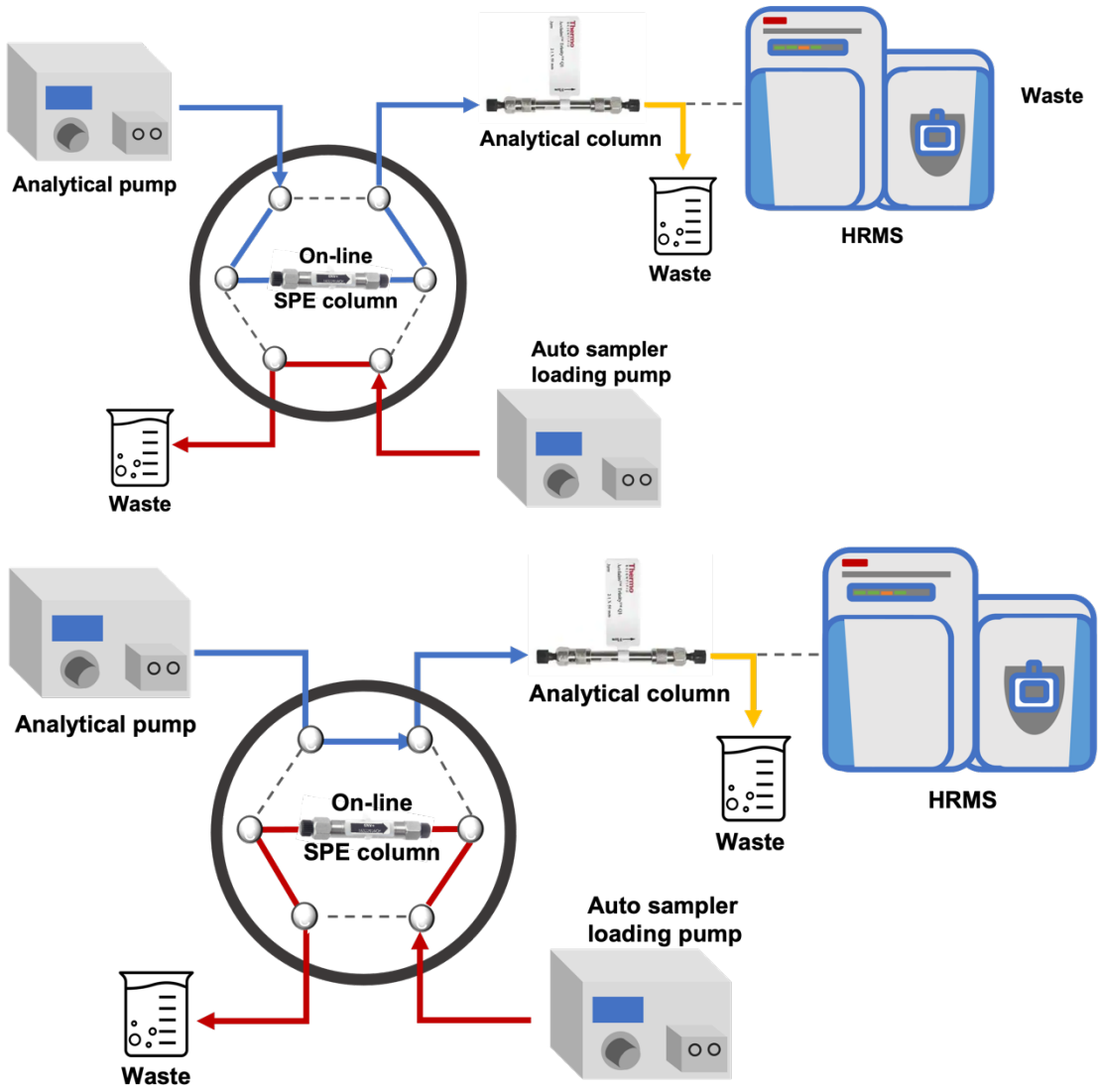

Scheme S1: Scheme of the online SPE and its connection to the LC-HRMS system

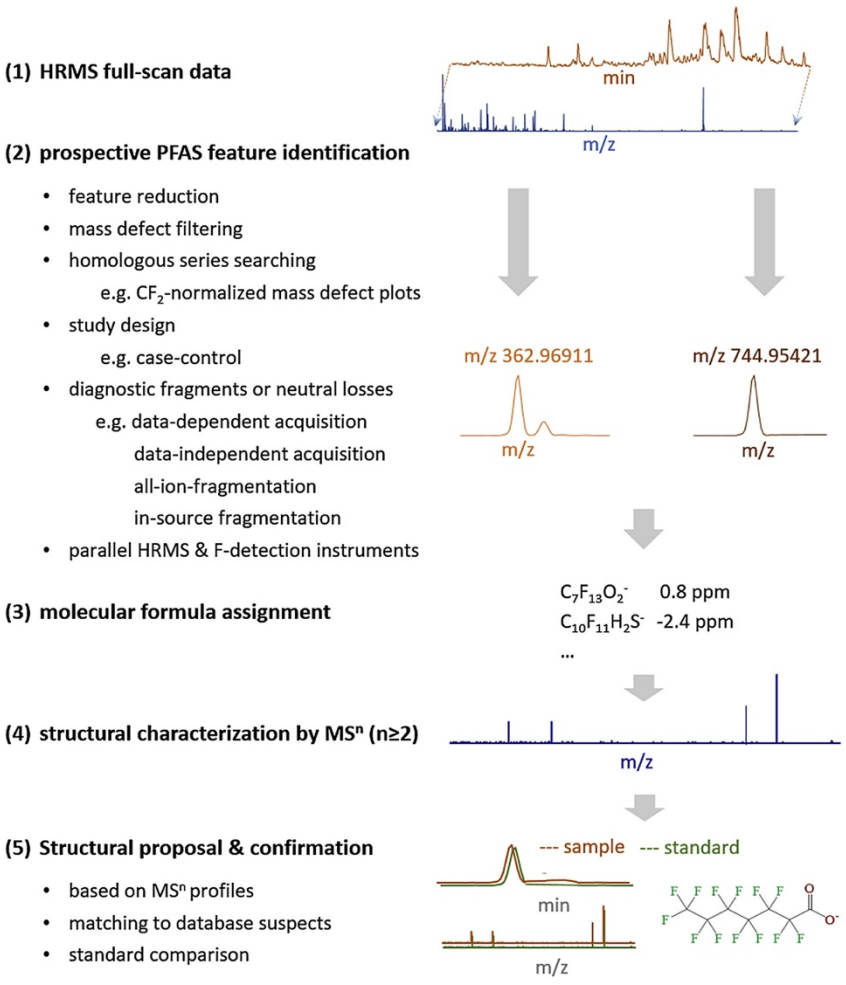

Figure S1 General schematic workflow of non-target PFAS analysis

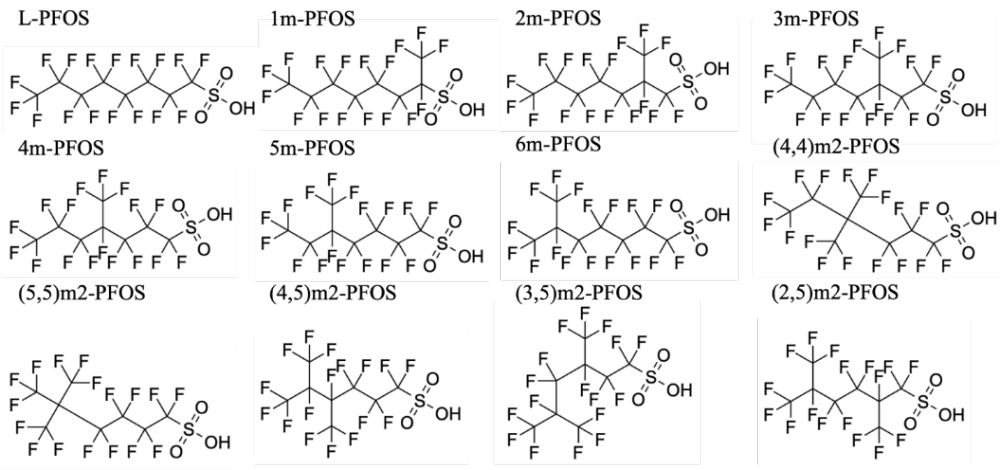

Figure S2 Structures of some common PFOS isomers

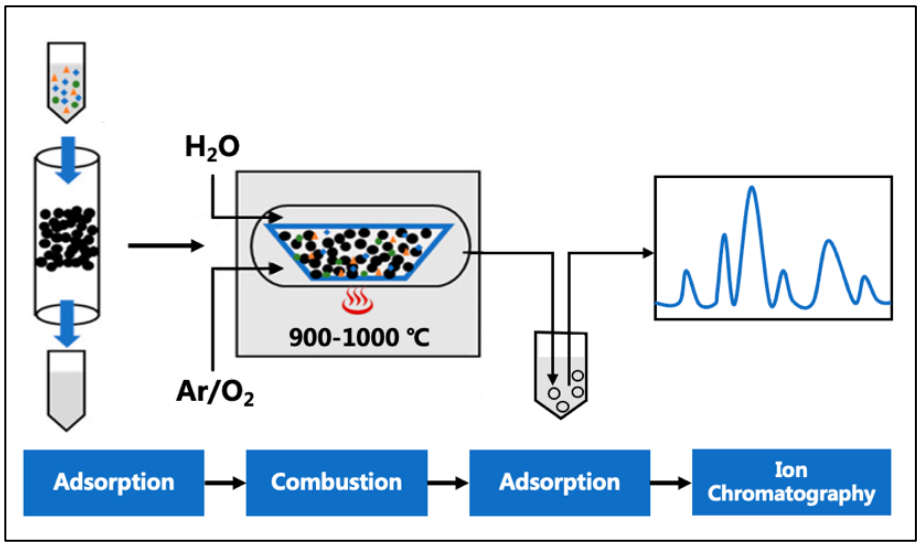

Figure S3 Schematic illustration of adsorbable organic fluorine (AOF)

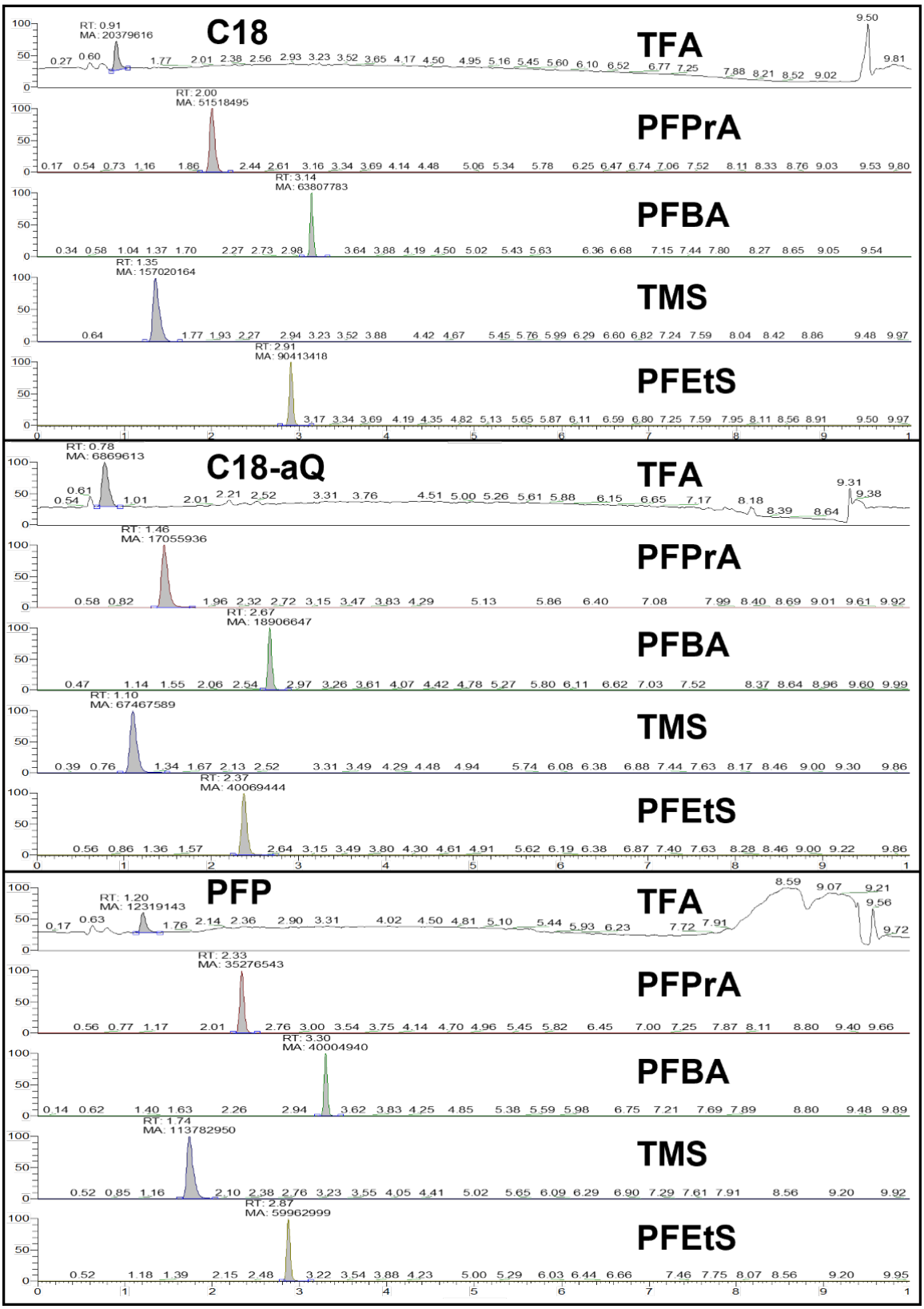

Figure S4 Chromatograms of 5 PFAS separated on different RPLC analytical columns

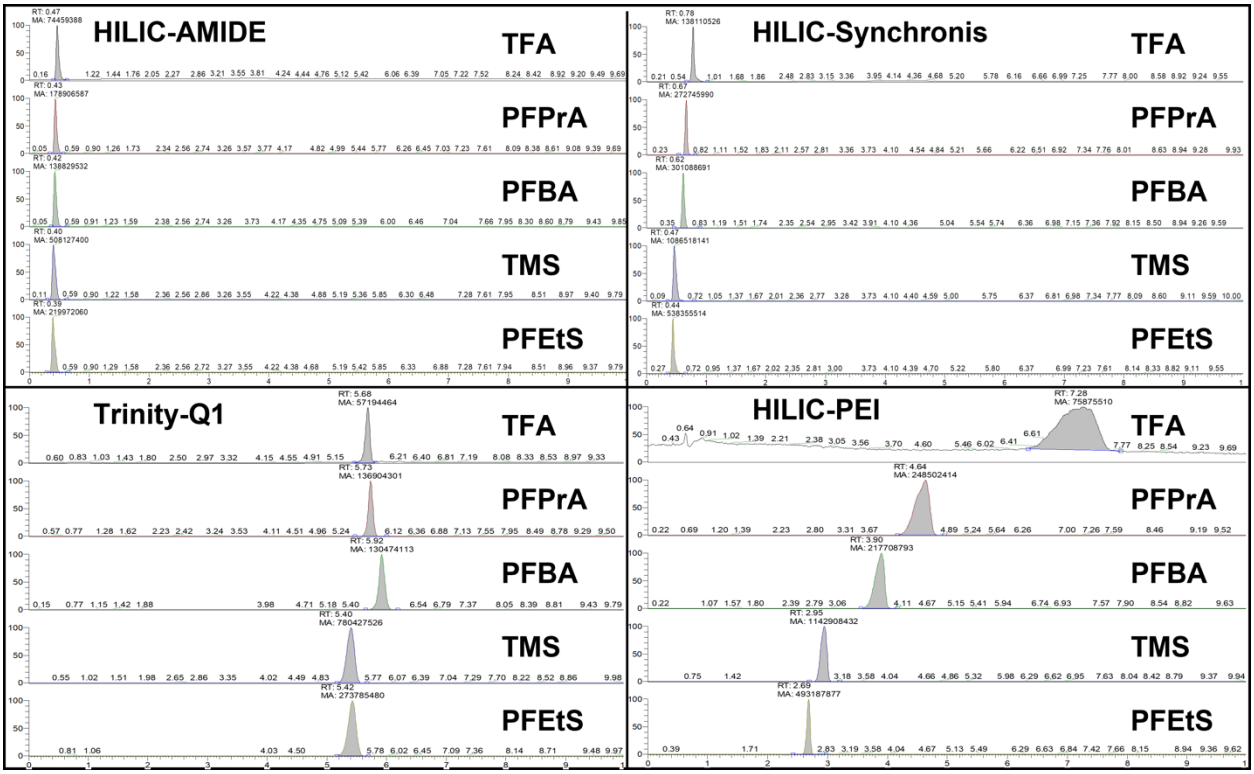

Figure S5 Chromatograms of 5 PFAS separated on different HILIC and multi-functional analytical columns

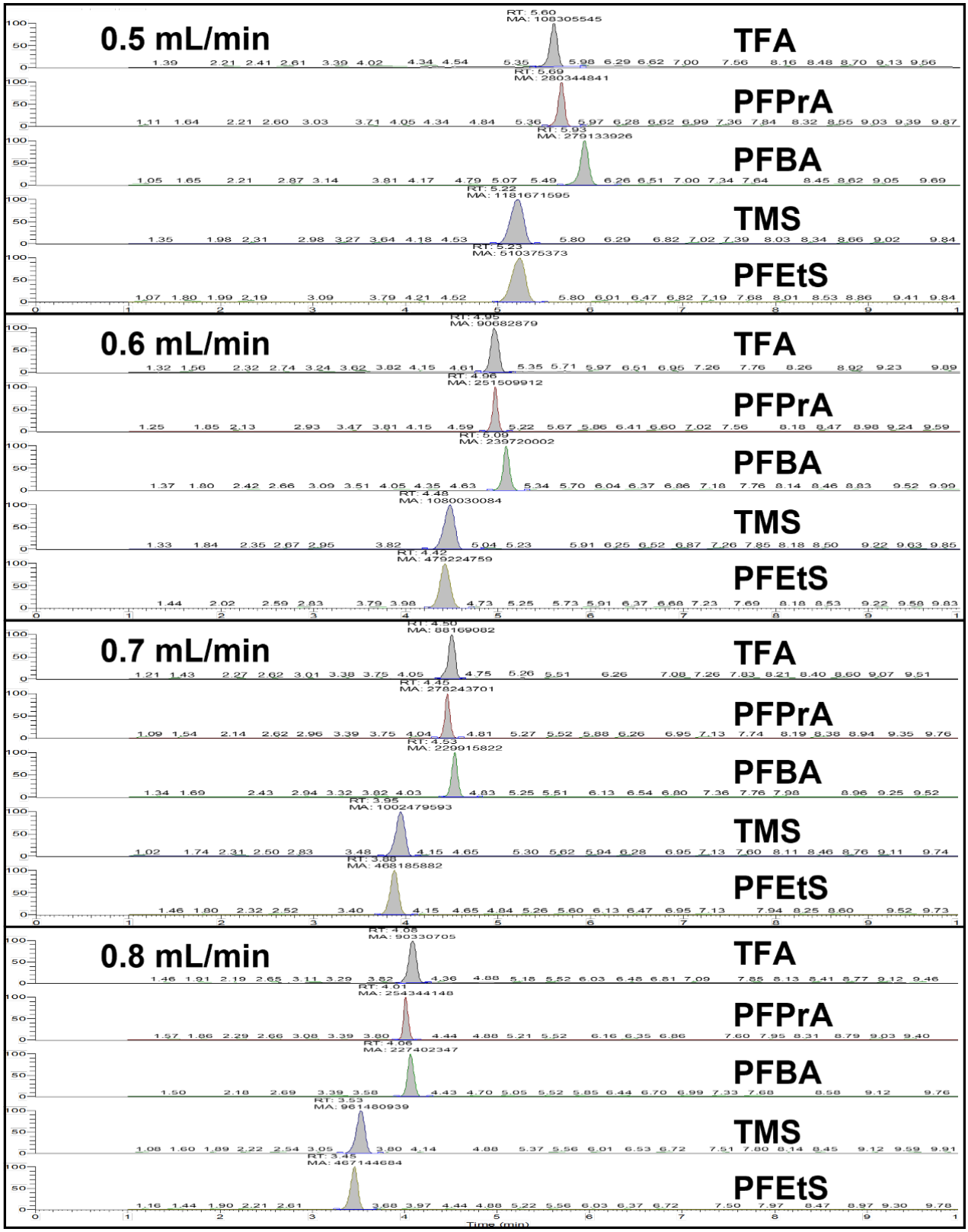

Figure S6 Chromatograms of 5 PFAS separated under different LC flow rates

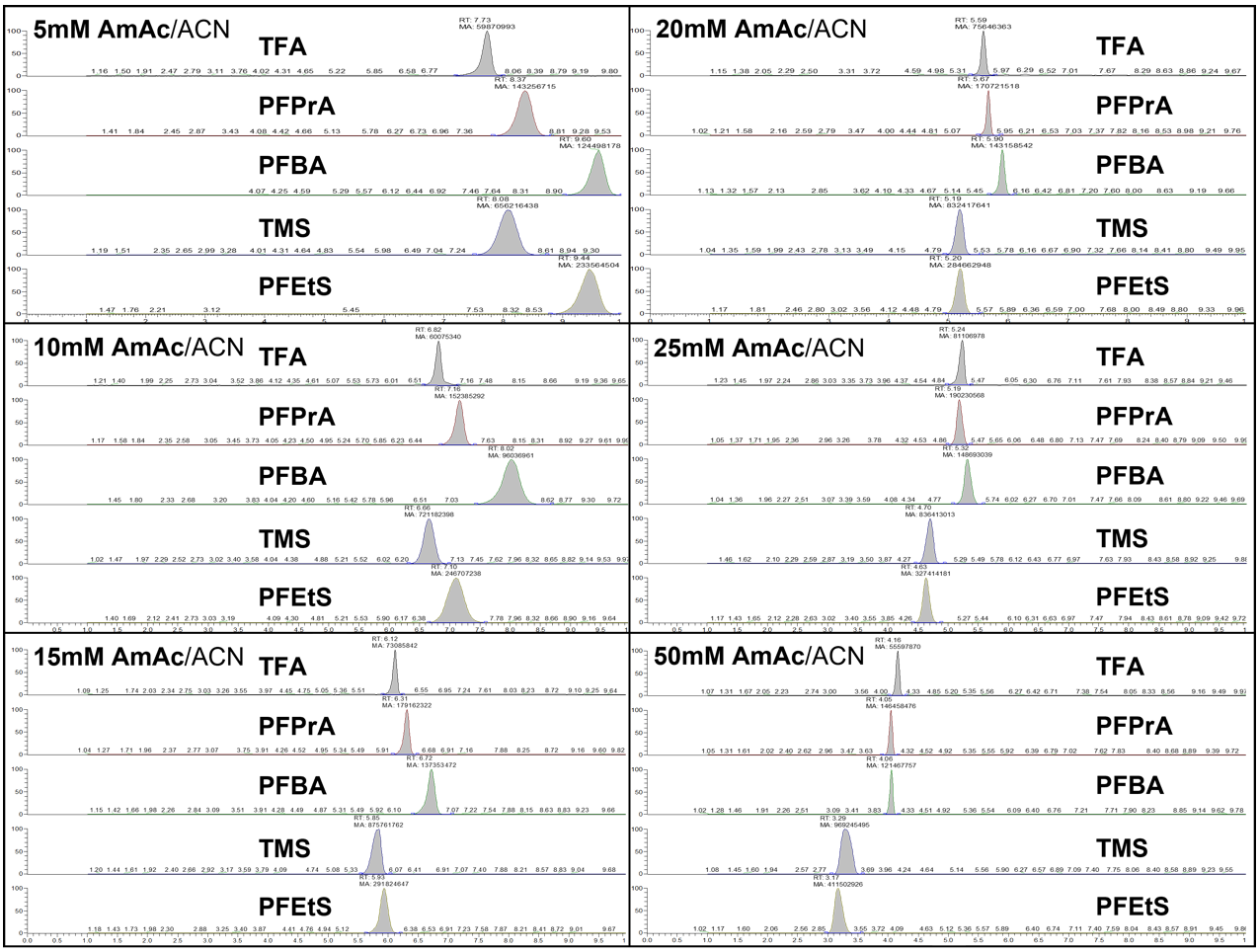

Figure S7 Chromatograms of 5 PFAS separated on different concentration of AmAc

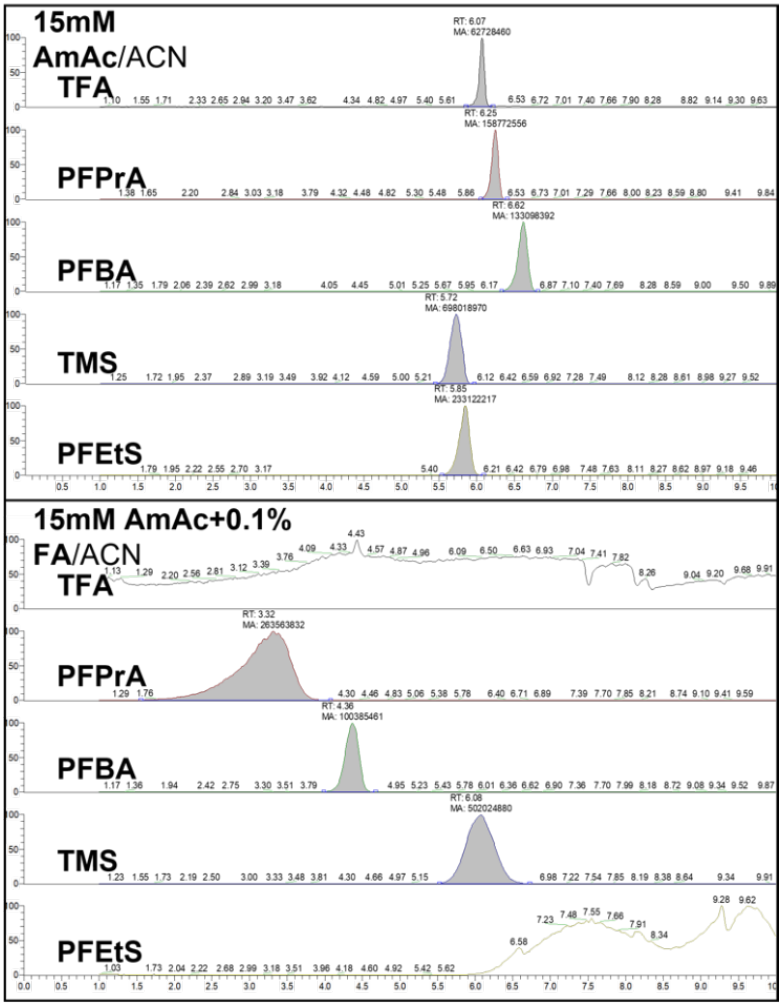

Figure S8 Chromatograms of 5 PFAS separated on the effect of the addition of formic acid (FA) in the mobile phase

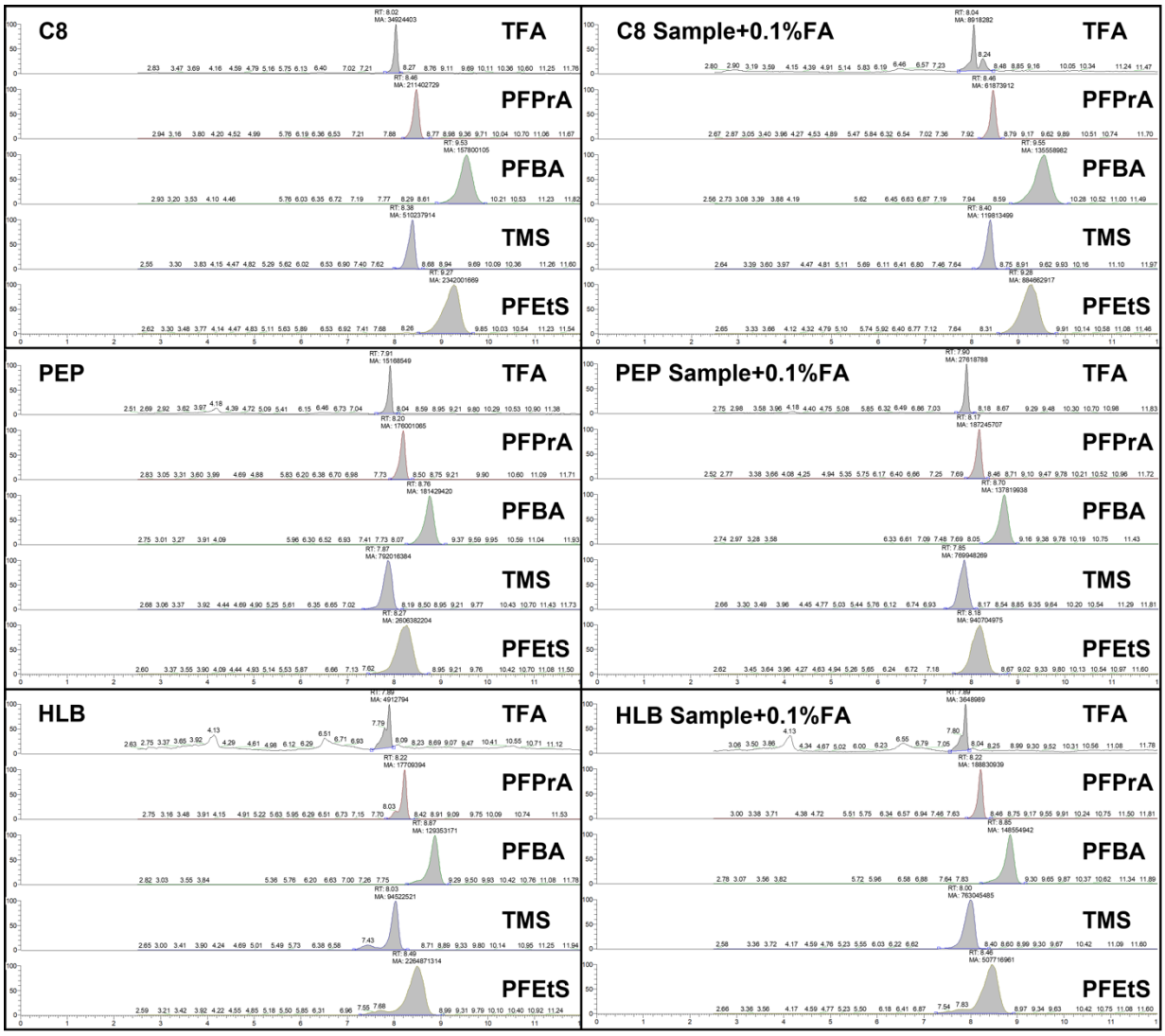

Figure S9 Chromatograms of 5 PFAS on the effect of different online SPE columns

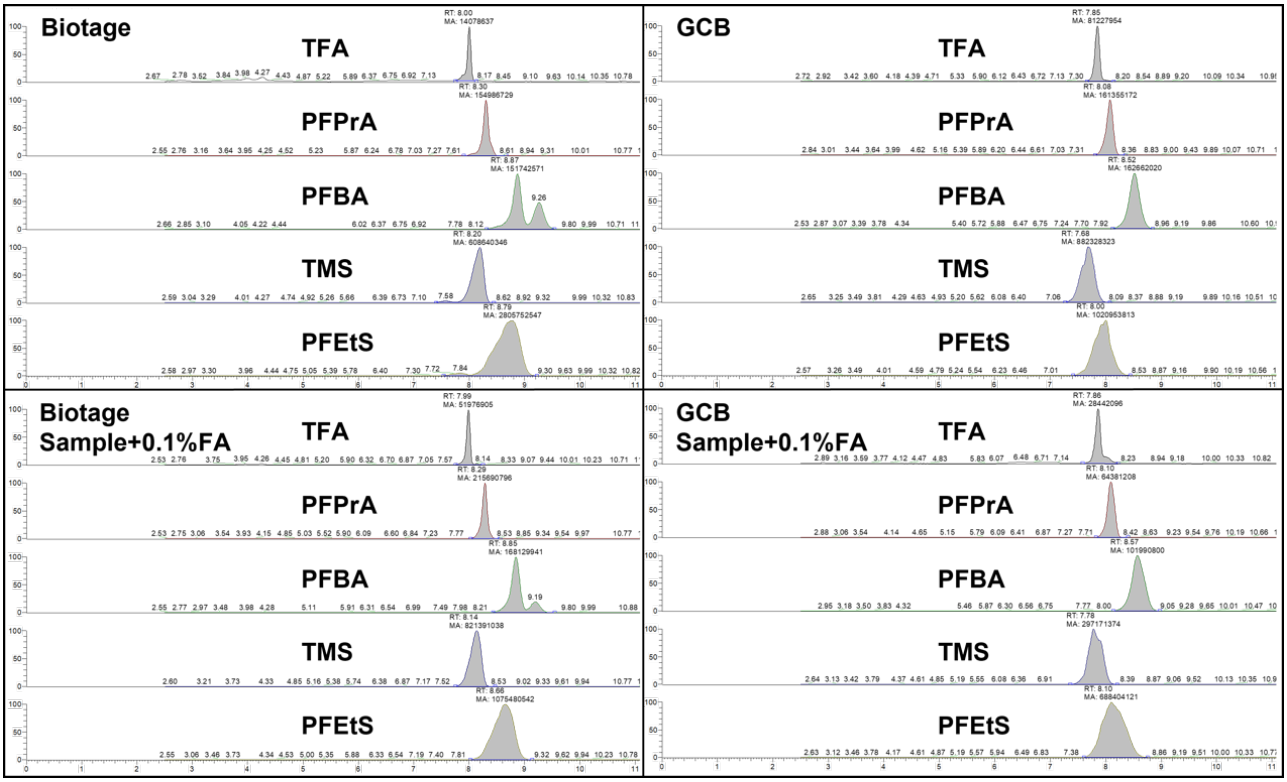

Figure S10 Chromatograms of 5 PFAS on the effect of different online SPE columns

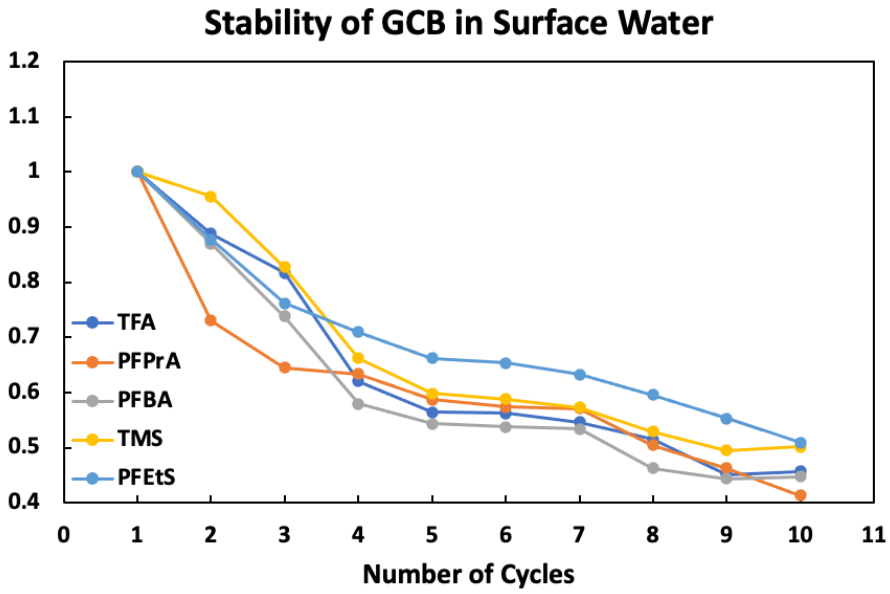

Figure S11 Stability of the online SPE column (GCB) in surface water

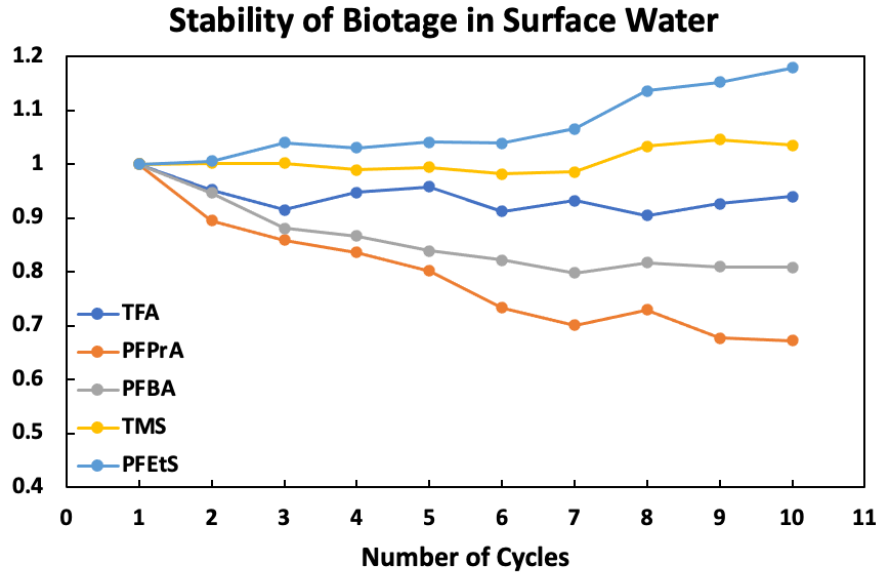

Figure S12 Stability of the online SPE column (Biotage) in surface water

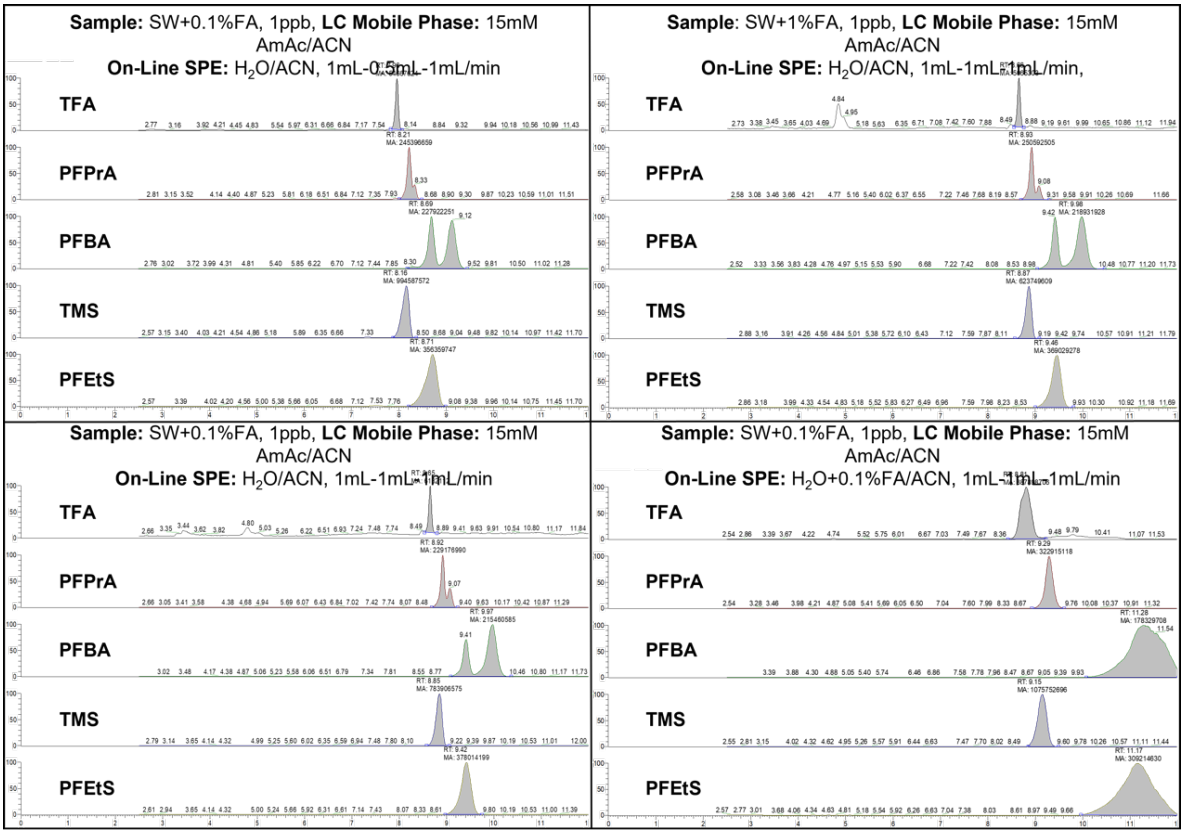

Figure S13 Chromatograms of 5 PFAS on the effect of SPE loading mobile phase

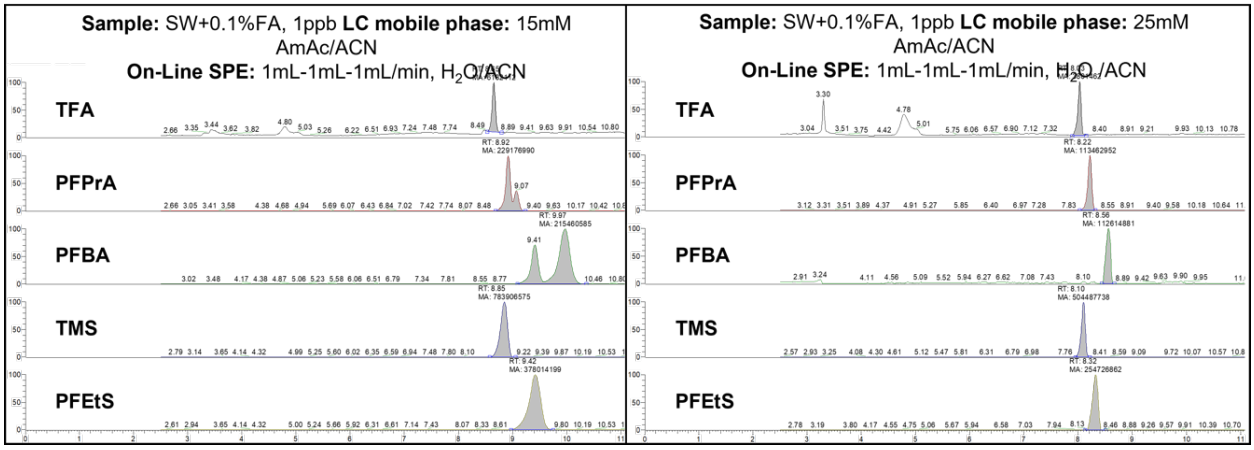

Figure S14 The effect of different LC mobile phases on chromatograms of 5 PFAS

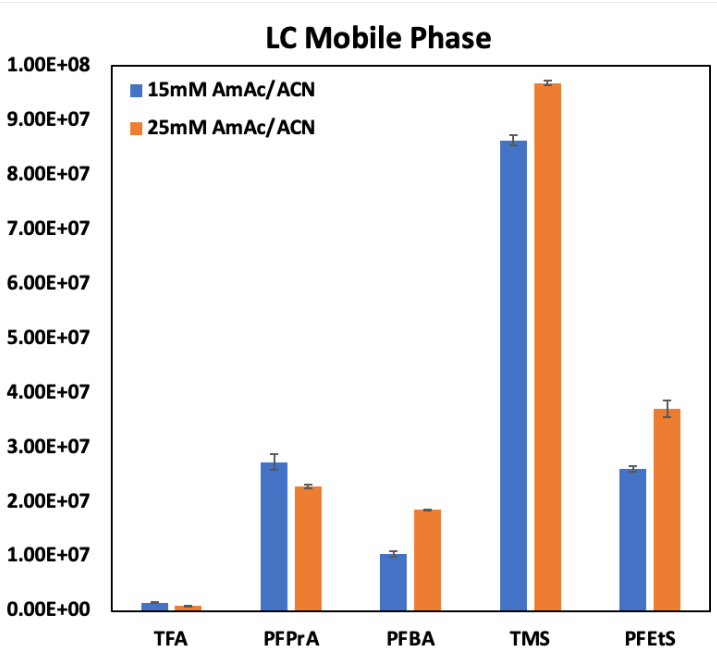

Figure S15 The effect of different LC mobile phases on peak intensities of 5 PFAS (n = 3)

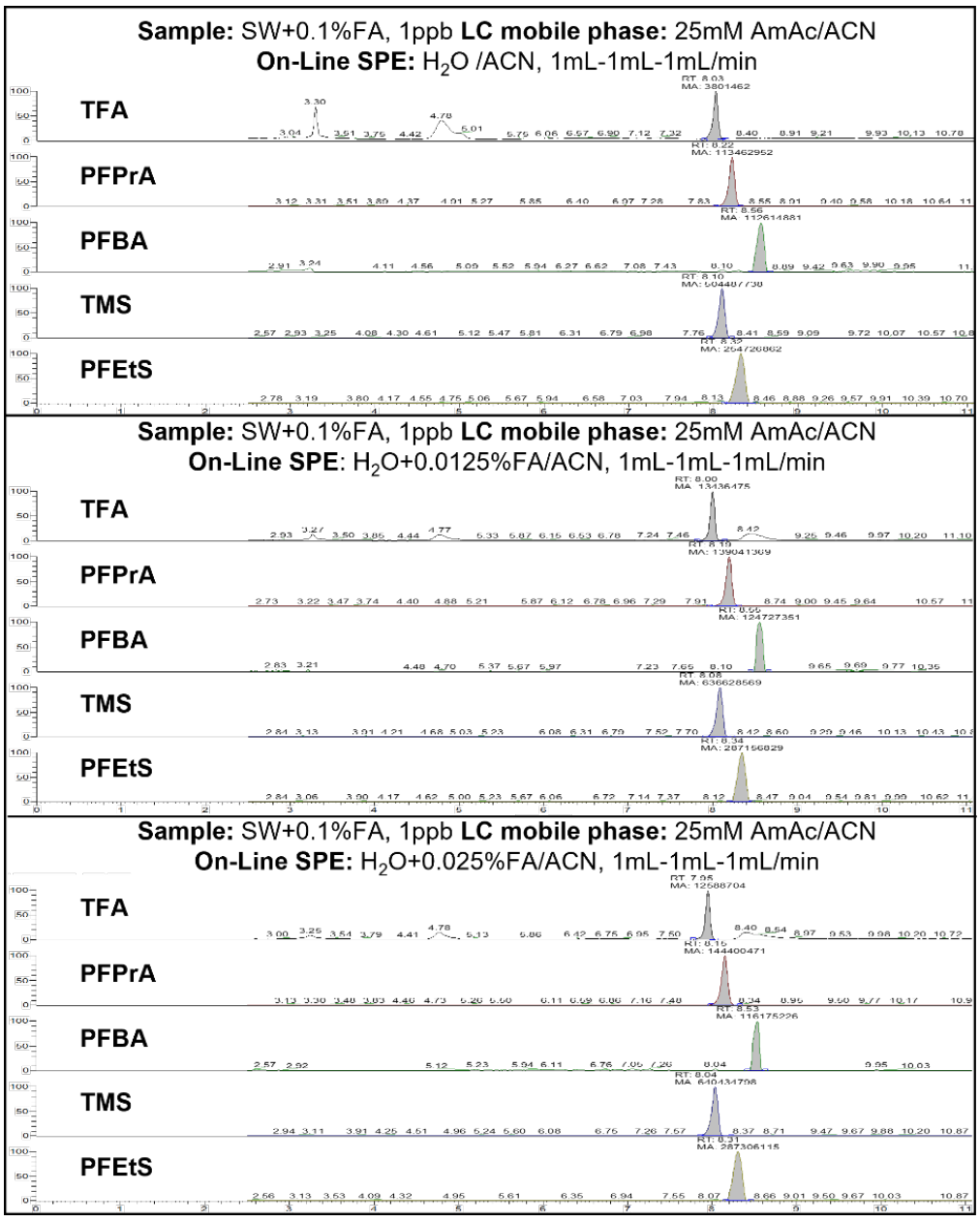

Figure S16 The effect of the percentage of FA in ACN of the SPE loading phase on the chromatograms of 5 PFAS

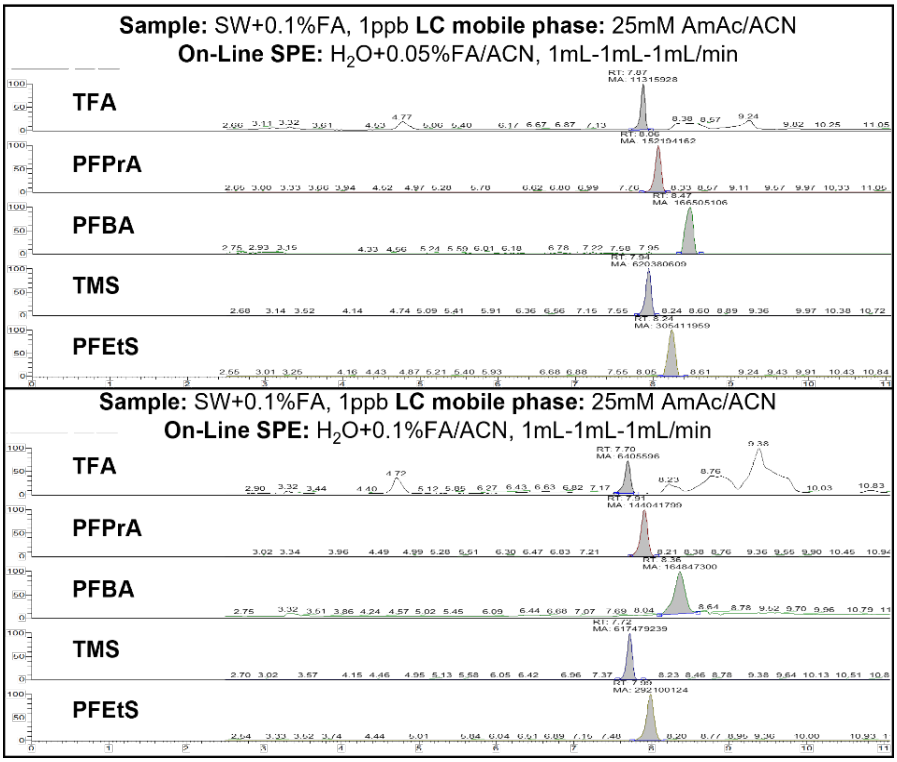

Figure S17 The effect of the percentage of FA in ACN of the SPE loading phase on the chromatograms of 5 PFAS

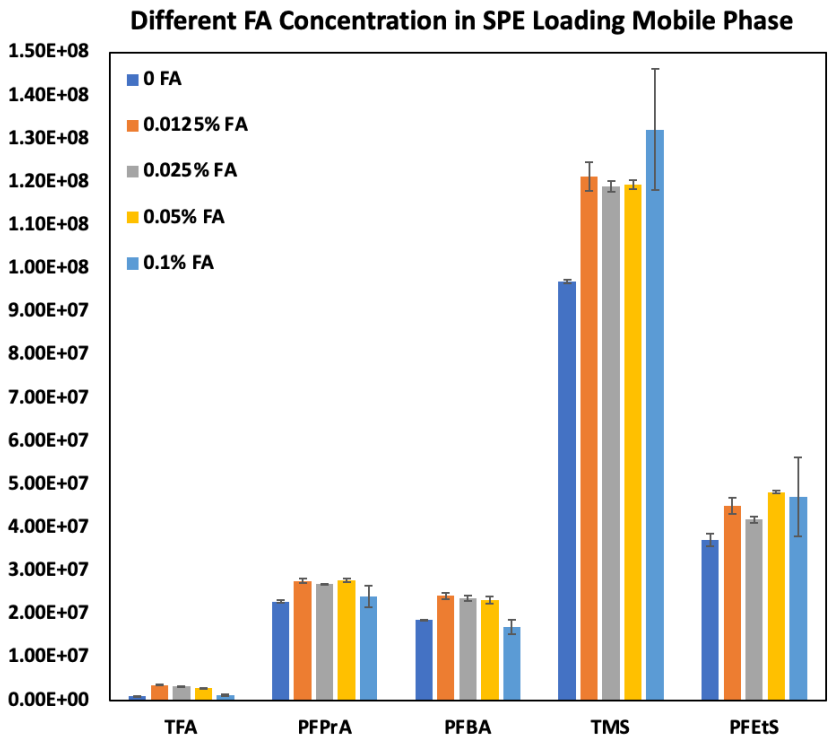

Figure S18 The effect of the percentage of FA in ACN of SPE loading phase on peak intensities of 5 PFAS (n = 3)

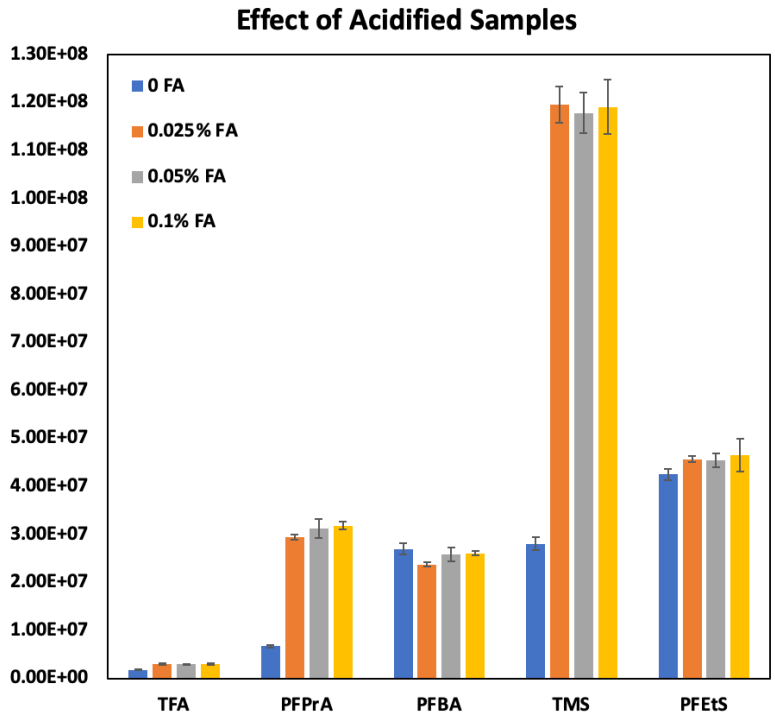

Figure S19 The effect of adding formic acid (FA) to surface samples on peak intensities of 5 PFAS (n = 3)

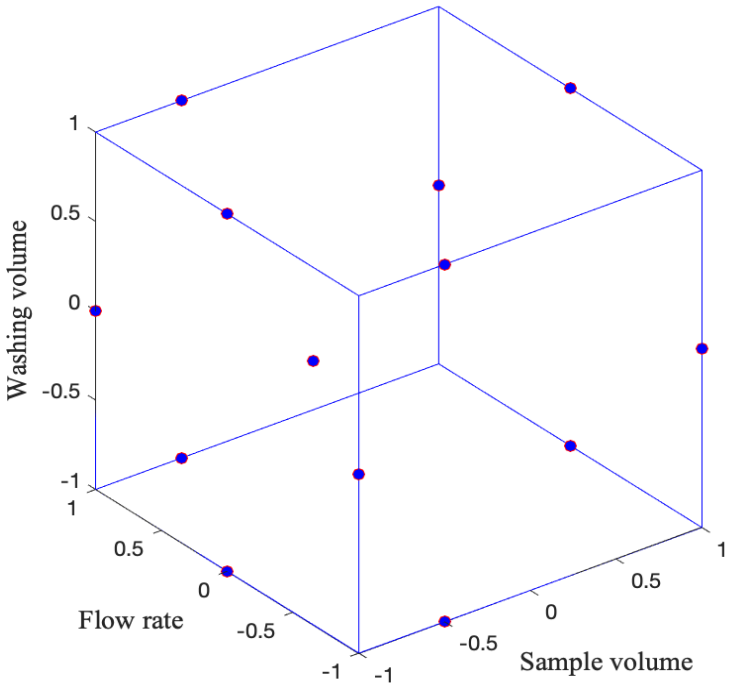

Figure S20 Modified Box-Behnken design

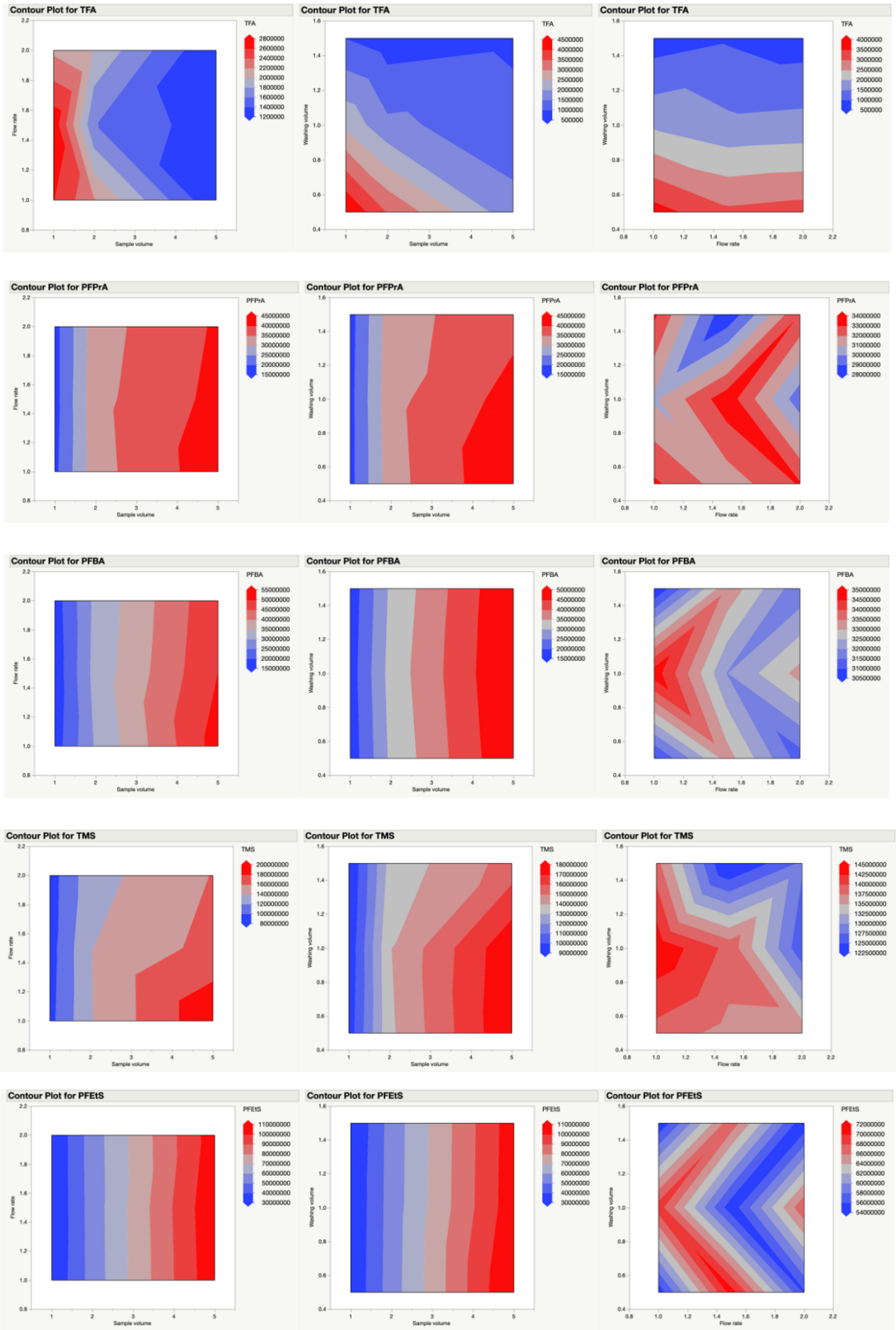

Figure S21 Contour plots showing the interactive impact of sample volume, washing volume, and flow rate on 5 PFAS.

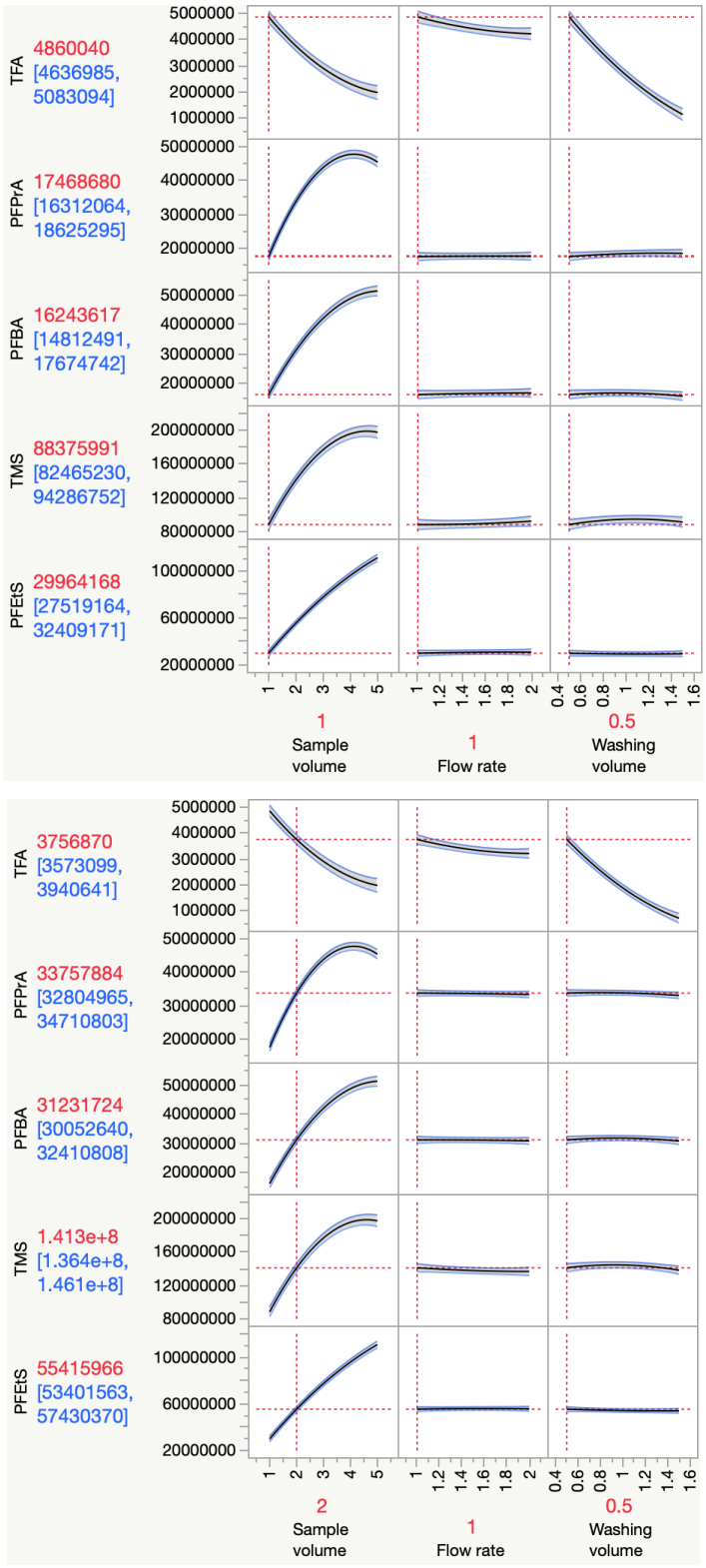

Figure S22 Fitting curves showing the interactive impact of sample volume, washing volume, and flow rate on 5 PFAS.

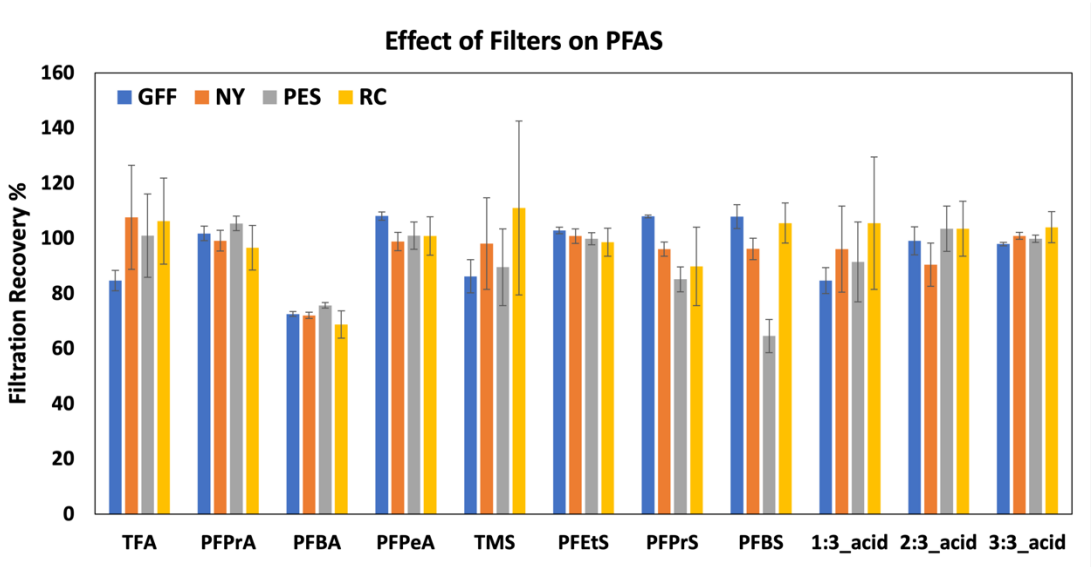

Figure S23 Filtration recovery of four types of filters for short-chain PFAS (n = 3)

Table S1 A summary of literature extraction methods of PFAS from environmental matrices

Matrices	Analytes	Extraction	Clean-up	Recovery	Ref.
Soil	51 PFAS adjacent to landfills	Methanolic ammonium hydroxide (0.3%)	ENVI-Carb	80%-120%	[186]
Soil	AFFFs	MeOH/NH_4OH MeOH/NaOH	ENVI-Carb graphite	**MeOH/NH_4OH:** For PFSAs, PFCAs, and FTSAs, 70-120%; For betaine-based PFAS (PFOSB, PFOAB, and 6:2 FTAB) and quaternary amine based compounds (PFOAAmS and PFOSAmS), 30-60%; For betaines in clay loam soil: ~5-10%. **MeOH/NaOH:** Betaines in the clay loam soil: 40-60% or higher.	[169]
Soil	AFFFs related anionic, cationic, and zwitterionic PFAS	0.1 M NH_4OH in methanol 0.5 M HCl in methanol	ENVI-Carb	70%-130%	[187]
Soil	AFFFs	4 mL of 100 mM of ammonium acetate in methanol	ENVI-Carb graphite cartridge		[172]
Soil	13 PFCAs, 6 PFSAs, FOUEA	Methanol	Phenomenex Strata™ C-18 cartridge	34-109 % in soil	[188]
Soil	86 PFAS (24 classes) related to AFFFs	MeOH/CH_3COONH_4	ENVI-Carb graphite cartridges	85-110%, except for 12:2 FTAB, 13:3 FTB, and 13:1:2 FTB (57-74%)	[164]
Sediment	13 PFCAs, 6 PFSAs, FOUEA	Methanol	Phenomenex Strata™ C-18 cartridge	45-103 % in sediment	[188]

Sediment	30 PFASs including 23 legacy PFASs and 7 novel cationic or zwitterionic PFASs	5 mL of basic methanol (NaOH 20 mM in MeOH)	ENVI-Carb graphite cartridges	60-110%	[189]
Concrete	15 PFASs including 11 PFCAs (C4-C14 PFCAs) and 4 PFSAs, (C4, C6, C8, C10 PFSAs), and 1 fluorotelomer sulfonate (FTS, 6:2)	Methanol	None	85%-120%	[190]
Concrete	AFFFs	MeOH/NH_3aq (99/1)	ENVI-Carb	35%-145%	[171]
Concrete	PFHxA, PFOA, PFHxS, PFOS, 6:2 FTS	Ammonia methanol (2%) and acetone	Envi-carb carbon cartridge		[191]
Concrete	36 PFAS from AFFFs	0.2% ammonia/methanol	ENVI-CarbTM		[192]
Asphalt	22 PFAS	Methanol/1% NH_3	3 ml Bond Elut carbon cartridge	70%-130%	[170]

Table S2 Current analytical techniques of ultra-short-chain and short chain PFAS

PFAS	Instruments	Analytical columns	Mobile phases	LOD	Internal Standard	Prep.	Recovery	Matrices	Ref.
PFEtS	LC-qTOF-MS	4.6 x 12.5 mm x 5 µm Zorbax silica guard column 4.6 x 12.5 mm x 5 µm Zorbax propylamine (NH_2) guard column Agilent 4.6 x 100 mm x 3.5 µm Zorbax Eclipse Plus C18 analytical column	A: 3% MeOH in HPLC-water B: 10 mM CH_3COONH_4 in HPLC-MeOH	0.8 ng/L	[$^{18}O_2$]PFHxS	LLE		AFFFs Groundwater	[29]
PFPrS	LC-qTOF-MS	4.6 x 12.5 mm x 5 µm Zorbax silica guard column 4.6 x 12.5 mm x 5 µm Zorbax propylamine (NH_2) guard column Agilent 4.6 x 100 mm x 3.5 µm Zorbax Eclipse Plus C18 analytical column	A: 3% MeOH in HPLC-water B: 10 mM CH_3COONH_4 in HPLC-MeOH	2.7 ng/L	[$^{18}O_2$]PFHxS	LLE		AFFFs Groundwater	[29]
TFA	SFC-MS/MS	3.0 x 150 mm x 1.7 µm SFC Torus DIOL column at 50 °C	A: CO_2 B: 0.1% NH_4OH in MeOH	0.009 ng/L (LOQ)	^{13}C-M2TFA	SPE		Surface snow	[28]
PFPrA	SFC-MS/MS	3.0 x 150 mm x 1.7 µm SFC Torus DIOL column at 50 °C	A: CO_2 B: 0.1% NH_4OH in MeOH	0.009 ng/L (LOQ)	^{13}C-M4PFBA	SPE		Surface snow	[28]
TMS	SFC-MS/MS	3.0 x 150 mm x 1.7 µm SFC Torus DIOL column at 50 °C	A: CO_2 B: 0.1% NH_4OH in MeOH	0.009 ng/L (LOQ)	^{13}C-M3PFBS	SPE		Surface snow	[28]
PFEtS	SFC-MS/MS	3.0 x 150 mm x 1.7 µm SFC Torus DIOL column at 50 °C	A: CO_2 B: 0.1% NH_4OH in MeOH	0.009 ng/L (LOQ)	^{13}C-M3PFBS	SPE		Surface snow	[28]
PFPrS	SFC-MS/MS	3.0 x 150 mm x 1.7 µm SFC Torus DIOL column at 50 °C	A: CO_2 B: 0.1% NH_4OH in MeOH	0.009 ng/L (LOQ)	^{13}C-M3PFBS	SPE		Surface snow	[28]
TFA	GC-MSD			0.5 ng/L				Sea water	[193]
PFEtS	HPLC-MS/MS	2.0 mm × 150 mm × 5 µm mixed mode ion-exchange	A: 50 mM ammonium acetate (pH 9)	0.1 ng/L (LOQ)		SPE		Rainwater	[37]

		column, RSpak JJ-50 2D, at 40 °C	B: MeOH; 20/80 (v/v)						
PFPrS	HPLC-MS/MS	2.0 mm × 150 mm × 5 μm mixed mode ion-exchange column, RSpak JJ-50 2D, at 40 °C	A: 50 mM ammonium acetate (pH 9) B: MeOH; 20/80 (v/v)	0.5 ng/L (LOQ)		SPE		Rainwater	[37]
TFA	HPLC-MS/MS	2.0 mm × 150 mm × 5 μm mixed mode ion-exchange column, RSpak JJ-50 2D, at 40 °C	A: 50 mM ammonium acetate (pH 9) B: MeOH; 20/80 (v/v)	0.5 ng/L (LOQ)		SPE		Rainwater	[37]
PFPrA	HPLC-MS/MS	2.0 mm × 150 mm × 5 μm mixed mode ion-exchange column, RSpak JJ-50 2D, at 40 °C	A: 50 mM ammonium acetate (pH 9) B: MeOH; 20/80 (v/v)	0.1 ng/L (LOQ)		SPE		Rainwater	[37]
TFA	Ion exchange LC-ESI-MS/MS	Dionex IonPac AS17-C column (2 mm × 250 mm), at 40 °C	A: 50 mM ammonium bicarbonate in HPLC-Water B: MeOH	0.05 μg/L (LOQ)	$^{13}C_2$-TFA			Surface water/River water/beer/tea	[194, 195]
TFA	GC-MS						101.8%	Air	[32]
TFA[#]	LC-MS/MS	Rspak JJ-50 2D column (2.0 mm × 150 mm × 5 μm)	A: 20% 50 mM CH_3COONH_4 in water B: 80% MeOH and 20% water.	50 (gas) 2.6 (particle) pg/m^3				Air	[33]
TFA[#]	GC-MS			128 (gas) 30 (particle) pg/m^3				Air	[33]
TFA	GC-MS							urban landscape waters/tap water/snow	[33, 34]
TFA	UPLC-MS/MS	RP18 column (2.1 mm × 100 mm × 1.7 μm, pore size 130 Å	A: 2 mM ammonium acetate B: MeOH	0.77 ng/L	[1,2-^{13}C] PFHxA	SPE	93.6 ±0.6%	Reaction solution	[196]
TFA	GC-MS			0.3 ng/L (iLOD) 11 ng/L (MDL)			96%-103%	Rain/snow/surface water/groundwater/wastewater	[35]
TFA	HPLC-MS/MS	Ion-exchange RSpak JJ-50 2D column (150 mm × 2.0 mm × 5 μm) at 45 °C	80% MeOH in Milli-Q water containing 50 mM ammonium acetate (at	0.123/3[a] ng/mL	$^{13}C_4$-PFBA	SPE	128.4%	Serum	[197]

			pH=9)						
PFPrA	HPLC-MS/MS	Ion-exchange RSpak JJ-50 2D column (150 mm × 2.0 mm × 5 μm) at 45 °C	80% MeOH in Milli-Q water containing 50 mM ammonium acetate (at pH=9)	0.071/3[a] ng/mL	$^{13}C_4$-PFBA	SPE	102.3%	Serum	[197]
TFA	SFC-MS/MS		A: CO_2 B: 0.1% NH4OH in MeOH	Surface water and effluent: 0.10 Lake water: 0.05 Atmospheric deposition: 0.10 ng/L	$^{13}C_2$-TFA	SPE	80 ± 22%	Surface water and effluent/Lake water/Atmospheric deposition	[43]
PFPrA	SFC-MS/MS		A: CO_2 B: 0.1% NH4OH in MeOH	Surface water and effluent: 0.60 Lake water: 0.30 Atmospheric deposition: 0.10 ng/L	^{13}C-M4PFBA	SPE	72 ± 12%	Surface water and effluent/Lake water/Atmospheric deposition	[43]
TMS	SFC-MS/MS		A: CO_2 B: 0.1% NH4OH in MeOH	Surface water and effluent: 0.10 Lake water: 0.05 Atmospheric	^{13}C-M3PFBS	SPE	87 ± 21%	Surface water and effluent/Lake water/Atmospheric deposition	[43]

				deposition: 0.10 ng/L					
TFA	UPC^2-MS/MS	UPC2 Torus DIOL column (3.0 mm × 150 mm, 1.7 µm) at 40 °C	A: Supercritical CO_2 B: 0.1% NH4OH in MeOH	0.2 ng/mL (MQL)			86%	Rain/River water	[38]
PFPrA	UPC^2-MS/MS	UPC2 Torus DIOL column (3.0 mm × 150 mm, 1.7 µm) at 40 °C	A: Supercritical CO_2 B: 0.1% NH4OH in MeOH	0.2 ng/mL (MQL)			86%	Rain/River water	[38]
PFEtS	UPC^2-MS/MS	UPC2 Torus DIOL column (3.0 mm × 150 mm, 1.7 µm) at 40 °C	A: Supercritical CO_2 B: 0.1% NH4OH in MeOH	0.2 ng/mL (MQL)			86%	Rain/River water	[38]
PFPrS	UPC^2-MS/MS	UPC2 Torus DIOL column (3.0 mm × 150 mm, 1.7 µm) at 40 °C	A: Supercritical CO_2 B: 0.1% NH4OH in MeOH	0.2 ng/mL (MQL)			86%	Rain/River water	[38]
TFA	Mixed-mode LC-MS/MS (MMLC-MS/MS)	Mixed-mode WAX-1 column (50 × 3 mm I.D., particle size 3 µm) at 40 °C	A: Ultrapure water B: acetonitrile C: 1 M aqueous CH_3COONH_4 at pH 5.5	0.56 ng/mL (IQL) 63.5 ng/L (MQL)	$^{13}C_4$PFBA	SPE	85% (River water) 92% (Ultrapure water)	Ultrapure water/River water	[42]
PFPrA	Mixed-mode LC-MS/MS (MMLC-MS/MS)	Mixed-mode WAX-1 column (50 × 3 mm I.D., particle size 3 µm) at 40 °C	A: Ultrapure water B: acetonitrile C: 1 M aqueous CH_3COONH_4 at pH 5.5	0.17 ng/mL (IQL)	13C4PFBA	SPE	93% (River water) 102% (Ultrapure water)	Ultrapure water/River water	[42]
TMS	Mixed-mode LC-MS/MS (MMLC-MS/MS)	Mixed-mode WAX-1 column (50 × 3 mm I.D., particle size 3 µm) at 40 °C	A: Ultrapure water B: acetonitrile C: 1 M aqueous CH_3COONH_4 at pH 5.5	0.02 ng/mL (IQL)	13C4PFBA	SPE	114% (River water) 95% (Ultrapure water)	Ultrapure water/River water	[42]
PFEtS	Mixed-mode LC-MS/MS (MMLC-MS/MS)	Mixed-mode WAX-1 column (50 × 3 mm I.D., particle size 3 µm) at 40 °C	A: Ultrapure water B: acetonitrile C: 1 M aqueous CH_3COONH_4 at pH 5.5	0.02 ng/mL (IQL)	18O2PFHxS	SPE	90% (River water) 103% (Ultrapure water)	Ultrapure water/River water	[42]
PFPrS	Mixed-mode	Mixed-mode WAX-1	A: Ultrapure water	0.06	18O2PFHxS	SPE	92%	Ultrapure	[42]

	LC-MS/MS (MMLC-MS/MS)	column (50 × 3 mm I.D., particle size 3 μm) at 40 °C	B: acetonitrile C: 1 M aqueous CH_3COONH_4 at pH 5.5	ng/mL (IQL)			(River water) 104% (Ultrapure water)	water/River water	
PFPrA	LC-MS/MS	a solid-core C18 column (100 mm x 2.1mm; 2.6 μm)	a water-MeOH gradient with a 2 mM ammonium acetate and 0.1% v/v acetic acid additive	0.45 ng/L (MDL)	[13C4] PFBA	SPE		Bottled water	[27]
PFPrS	LC-MS/MS	a solid-core C18 column (100 mm x 2.1mm; 2.6 μm)	a water-MeOH gradient with a 2 mM ammonium acetate and 0.1% v/v acetic acid additive	0.11 ng/L (MDL)	[13C3] PFBS	SPE		Bottled water	[27]
TMS	LC-MS	An Obelisc N column (2.1 mm × 150 mm, 5 μm particle size)	A: 40% acetonitrile (0.2% formic acid) B: 60% water (0.2% formic acid)	5.4 ng/L (LOQ)	M3PFBS	SPE		LC-MS Water	[41]
TMS	MMLC-MS	An Obelisc N column (2.1 mm × 150 mm, 5 μm particle size)	A: acetonitrile (0.2% formic acid) B: water (0.2% formic acid)	11 ng/L (LOQ)	M3PFBS	SPE	92%	LC-MS Water	[41]
TFA	LC-MS/MS	Kinetex C18 column (100 × 3 mm, 2.6 μm, 100 Å) Obelisc N column (150 × 2.1 mm, 100 Å, 5 μm)	C18 A: 2 mM ammonium formate and 0.2% formic acid in water/MeOH (4:1, v/v) C18 B: 2 mM ammonium formate in MeOH) ObN A: 2.5 mM ammonium acetate and 0.3% acetic acid in water/ACN (3:2, v/v) ObN B: 20 mM ammonium acetate in water/acetonitrile (ACN; 1:9, v/v))	Demineralised Water: 3.3 ng/L Natural spring Water: 5.5 ng/L	TFA-M1	SPE	TW: 97 ± 0.7% GW: 99 ± 4.4% SW: 101 ± 1.4%	Surface water/groundwater/drinking water/Tap water	[174]
PFPrA	LC-MS/MS	Kinetex C18 column (100 × 3 mm, 2.6 μm, 100 Å) Obelisc N column (150 × 2.1 mm, 100 Å, 5 μm)	C18 A: 2 mM ammonium formate and 0.2% formic acid in water/MeOH (4:1, v/v) C18 B: 2 mM ammonium formate in MeOH)	Demineralised Water: 1.0 ng/L Natural spring	PFBA-M4	SPE	TW: 95 ± 2.3 % GW: 83 ± 2.1% SW: 104 ± 4.5%	Surface water/groundwater/drinking water/Tap water	[174]

			ObN A: 2.5 mM ammonium acetate and 0.3% acetic acid in water/ACN (3:2, v/v) ObN B: 20 mM ammonium acetate in H2OmQ/acetonitrile (ACN; 1:9, v/v))	Water: 0.9 ng/L					
TFA	LC-MS/MS	Acclaim Polar Advantage II C18-analytical column (4.6 mm i.d., 25 cm length)	The mobile phase consisted of a mixture of 20 mM boric acid (pH 8.0) and 95% acetonitrile	1 mg/L				Microbial reaction solution	[198]
PFPrA	LC-MS/MS	Acclaim Polar Advantage II C18-analytical column (4.6 mm i.d., 25 cm length)	The mobile phase consisted of a mixture of 20 mM boric acid (pH 8.0) and 95% acetonitrile	1 mg/L				Microbial reaction solution	[198]
TMS	HPLC-MS/MS (HILIC)	a Nucleodur HILIC column (150 × 2.1 mm; 5 µm)	An acetonitrile-water gradient containing 5 mM ammonium formate at pH 3.0			SPE		Environmental water	[55]
TMS	Mixed-mode LC (MMLC)-HRMS	Acclaim Trinity P1 (2.6 µm particle size; 3 mm internal diameter, in both 50 and 100 mm length format)	a simultaneous binary gradient from low organic content (2% ACN) and buffer (5 mM CH_3COONH_4, pH 5.5) to high organic (80% ACN) and buffer (20 mM CH_3COONH_4, pH 5.5) in 10 min, with a final isocratic time of 15 min.			SPE		Surface /Ground/Drinking water/effluent wastewater	[199]
TFA	HPLC-MS/MS	ion-exchange RSpak JJ-50 2D column (2.0 mm i.d. × 150 mm length, 5 µm) at 30 ℃	A: 20% of 50 mM CH_3COONH_4 (at pH 9) B: 80% of methanol	96 ng/L (iLOD)	13C-TFA/13C4-PFBA[c]	SPE	Low recovery	Precipitation	[14]
PFPrA	HPLC-MS/MS	ion-exchange RSpak JJ-50 2D column (2.0 mm i.d. × 150 mm length, 5 µm) at 30 ℃	A: 20% of 50 mM CH_3COONH_4 (at pH 9) B: 80% of methanol	12 ng/L (iLOD)	13C4-PFBA[c]	SPE	Low recovery	Precipitation	[14]
TFA	HPLC-MS/MS	150mm×2.1mm Hyperdil Gold C18 column (3-µm	A: methanol B: 2mM CH_3COONH_4			SPE		Sediment/soil/sludge	[15]

		pore size)							
PFPrA	HPLC-MS/MS	150mm×2.1mm Hyperdil Gold C18 column (3-µm pore size)	A: methanol B: 2mM CH_3COONH_4			SPE		Sediment/soil/sludge	15
TFA	HPLC-MS/MS	A RSpak JJ-50 2D ion-exchange column (2 mm i.d. × 150 mm, 5µm) at 40 C°	20% of 50 mM ammonium acetate (at pH 9) and 80% of methanol (v/v)	Leaf: 0.25/1.92 ng/g dw / ng/g lipid Air: 0.02 pg/m^3 PM: 0.66 ng/g (MDL)			Leaf: 85±9% Air: 90±4% Dry deposition : 88±2%		200
PFPrA	HPLC-MS/MS	A RSpak JJ-50 2D ion-exchange column (2 mm i.d. × 150 mm, 5µm) at 40 C°	20% of 50 mM ammonium acetate (at pH 9) and 80% of methanol (v/v)	Leaf: 0.29/2.23 ng/g dw / ng/g lipid Air: 0.02 pg/m^3 PM: 0.69 ng/g (MDL)			Leaf: 92±5% Air: 89±5% Dry deposition : 93±3%		200
PFPrA	HPLC-MS/MS	Raptor C18 2.7 µm, 100 mm x 3.0 mm PFAS delay column, 40 °C	A: 5 mM ammonium acetate in water B: Methanol				Reagent water: 103%		201
PFPrS	HPLC-MS/MS	Raptor C18 2.7 µm, 100 mm x 3.0 mm PFAS delay column, 40 °C	A: 5 mM ammonium acetate in water B: Methanol				Reagent water: 99.1%		201

Table S3 Information of PFAS analyzed in this study

Compounds	Structure	Mass	Internal Standards
TFA	CF_3COO-	112.98449	TFA-^{13}C2
PFPrA	CF_3CF_2COO-	162.9813	PFBA-^{13}C4
PFBA	$CF_3CF_2CF_2COO$-	212.9781	PFBA-^{13}C4
PFPeA	$CF_3CF_2CF_2CF_2COO$-	262.97491	PFPeA-^{13}C5
TMS	CF_3SO_3-	148.95148	PFBA-^{13}C4
PFEtS	$CF_3CF_2SO_3$-	198.94828	PFBA-^{13}C4
PFPrS	$CF_3CF_2CF_2SO_3$-	248.94509	PFBA-^{13}C4
PFBS	$CF_3CF_2CF_2CF_2SO_3$-	298.94189	PFBS-^{13}C3
1:3 acid	$CF_3CH_2CH_2COO$-	141.01579	PFPeA-^{13}C5
2:3 acid	CF_3CF_2-CH_2CH_2COO-	191.0126	PFPeA-^{13}C5
3:3 acid	$CF_3CF_2CF_2$-CH_2CH_2COO-	241.0094	PFPeA-^{13}C5

Table S4 Information of analytical columns used in this study

Column	Dimension Size (mm)	Particle Size (μm)	Product Number	Manufacturer
C18	100 × 2.1	1.9	25002-102130	Thermo Scientific
C18-aQ	100 × 2.1	3	25303-102130	Thermo Scientific
C18-PFP	100 × 2.1	1.9	25402-102130	Thermo Scientific
HILIC-Amide	100 × 2.1	2.6	16726-102130	Thermo Scientific
HILIC-Syncronis	100 × 2.1	1.7	97502-102130	Thermo Scientific
Trinity Q1	100 × 2.1	3	079717	Thermo Scientific
HILIC-PEI	100 × 2.1	1.9	26502-102130	Thermo Scientific

Table S5 Information of SPE columns used in this study

Column	Dimension Size (mm)	Particle Size (μm)	Product Number	Manufacturer
C8	20 × 2.1	5	25205-022130	Thermo Scientific
HLB	20 × 2.1	5	186002034	Waters
Biotage	30 × 2.1	40	OSPE-916-32150	Biotage
GCB	20 × 2.1	7	35007-022130	Thermo Scientific
PEP	20 × 2.1	Not provided	60312-201	Thermo Scientific

Table S6 Details on the online-SPE-LC-HRMS method in surface water

UHPLC-HRMS system	Dionex Ultimate 3000 UHPLC chain Thermo Q-Exactive Orbitrap high-resolution mass spectrometer, heated electrospray ionization source (negative ion mode)			
Separation column	Acclaim Trinity Q1 LC column (100 × 2.1 mm, 3 μm particle size, Thermo Scientific)			
Column oven temperature	35°C			
HPLC mobile phases	A: 25mM AmAc in HPLC-water B: Acetonitrile Mobile phase flow rate 450 μL/min			
HPLC gradient	Time (min)	% A	% B	
	0.0	10	90	
	3.5	10	90	
	9.5	70	30	
	10.5	70	30	
	12.5	10	90	
	15.0	10	90	
Injection Volume	2000 μL			
On-line SPE mobile phases	A: 0.0125% FA in HPLC-water B: Acetonitrile			
On-line SPE gradient	Time (min)	% A	% B	Flow rate μL/min
	0.0	100	0	1000
	2.5	100	0	1000
	2.6	0	100	1500
	8.9	0	100	1500
	9.0	100	0	1500
	14.5	100	0	1500
	15.0	100	0	1000
Source	Sheath gas flow rate 45 a.u.			

	Aux gas flow rate 15 a.u. Sweep gas flow rate 0 a.u. Negative spray voltage (|V|) 3600 Capillary temperature (°C) 320 Vaporizer temperature (°C) 350 S-lens RF level 55
Q-Exactive Orbitrap settings	Full Scan MS mode Scan range (m/z) 100-400 Resolution 70,000 Max. Inject Time (ms) 100

Table S7 The model of modified Box-Behnken design for optimization of three factors

Run number	Coded factors			Uncoded factors		
	Sample volume	Flow rate	Washing volume	Sample volume (mL)	Flow rate (mL/min)	Wash volume (mL)
1	-1	-1	0	1	1	1
2	-1	0	-1	1	1.5	0.5
3	-1	0	1	1	1.5	1.5
4	-1	1	0	1	2	1
5	-0.5	-1	-1	2	1	0.5
6	-0.5	-1	1	2	1	1.5
7	-0.5	0	0	2	1.5	1
7	-0.5	0	0	2	1.5	1
9	-0.5	0	0	2	1.5	1
10	-0.5	1	-1	2	2	0.5
11	-0.5	1	1	2	2	1.5
12	1	-1	0	5	1	1
13	1	0	-1	5	1.5	0.5
14	1	0	1	5	1.5	1.5
15	1	1	0	5	2	1

Note: Columns 2-4 represent the three important factors and their coded levels, columns 5-7 show the uncoded factor levels for all experiments.

Table S8 Models fitting results for 5 PFAS based on actual values and predicted values

Responses (Peak intensity)	Regression		t-test	
	R-square	p-value	t-value	p-value
TFA	0.980229	< 0.0001	2.9528e-15	0.9999
PFPrA	0.991561	< 0.0001	5.9355e-15	0.9999
PFBA	0.993329	< 0.0001	-1.4211e-15	0.9999
TMS	0.982156	< 0.0001	4.5144e-15	0.9999
PFEtS	0.996566	< 0.0001	0.0	1.0

Table S9 SPE absolute recovery of 11 PFAS using the developed online-SPE-LC HRMS method at two concentration levels

Compounds	SPE Recovery (%)	
	QC1	QC2
TFA	40.4 ±8.7	24.3 ±2.6
PFPrA	115 ±4.0	110 ±1.6
PFBA	109 ±3.6	96.6 ±0.9
PFPeA	128±2.5	112 ±0.9
TMS	49.0 ±0.8	47.5 ±4.4
PFEtS	91.1 ±3.6	92.3 ±1.0
PFPrS	97.3 ±1.2	109 ±1.0
PFBS	123 ±14	125 ±0.8
1:3 acid	122 ±7.8	99.7 ±0.5
2:3 acid	91.1 ±6.4	83.4 ±1.3
3:3 acid	116 ±1.8	110 ±0.4

Note: QC1: 7.5 ng/L for TFA, PFPrA, PFBA, PFPeA, TMS, PFEtS, PFPrS, and PFBS, 17.5 ng/L for 1:3 acid, 2:3 acid, and 3:3 acid; QC2: 75 ng/L for TFA, PFPrA, PFBA, PFPeA, TMS, PFEtS, PFPrS, and PFBS, 575 ng/L for 1:3 acid, 2:3 acid, and 3:3 acid

Table S10 Method validation data of 11 PFAS in mixture of surface water, including accuracy (mean ± STDEV) and intra-day/inter-day precision (RSD%) of matrix spikes at two concentration levels

Compounds	QC Accuracy (%)		QC Precision (%) Intra-day		QC Precision (%) Inter-day	
	QC1	QC2	QC1-3	QC2-3	QC1-9	QC2-9
TFA	124 ± 25.0	98.4 ± 7.40	20.0%	7.52%	19.0%	10.8%
PFPrA	106 ± 6.00	101.0 ± 2.00	6.00%	2.12%	7.07%	8.19%
PFBA	103±1.16	98.9±3.86	1.12%	3.90%	2.52%	3.27%
PFPeA	106±1.54	100.8±0.57	1.45%	0.57%	2.63%	1.33%
TMS	123±3.98	100.9±4.44	3.22%	4.39%	6.89%	8.18%
PFEtS	108±1.59	98.6±2.12	1.47%	2.15%	2.82%	1.78%
PFPrS	100±0.48	99.2±7.79	0.48%	7.85%	0.92%	6.18%
PFBS	106±4.35	100±1.75	4.07%	1.74%	3.97%	1.27%
1:3_acid	70.5±2.86	100±3.40	4.06%	3.38%	7.79%	2.48%
2:3_acid	129±1.86	95.0±4.18	1.43%	4.40%	8.32%	6.08%
3:3_acid	114±6.75	98.1±4.55	5.92%	4.64%	6.45%	5.45%

Note: QC1: 7.5 ng/L for TFA, PFPrA, PFBA, PFPeA, TMS, PFEtS, PFPrS, and PFBS, 17.5 ng/L for 1:3 acid, 2:3 acid, and 3:3 acid; QC2: 75 ng/L for TFA, PFPrA, PFBA, PFPeA, TMS, PFEtS, PFPrS, and PFBS, 575 ng/L for 1:3 acid, 2:3 acid, and 3:3 acid

Table S11 Absolute and residual matrix effect of 11 PFAS in surface water

Compounds	Absolute matrix effect	Residual matrix effect		
		SW1	SW2	SW3
TFA	39.4%	-28.1%	0.83%	-27.8%
PFPrA	-10.3%	1.08%	-18.2%	-4.82%
PFBA	-8.34%	-14.7%	-4.34%	-13.4%
PFPeA	-5.32%	-0.28%	-1.55%	1.14%
TMS	-6.83%	10.8%	-13.2%	-7.53%
PFEtS	8.05%	-11.6%	1.92%	-2.89%
PFPrS	12.1%	-14.0%	-1.89%	-9.46%
PFBS	1.59%	-5.38%	-4.26%	-3.83%
1:3_acid	20.0%	-3.44%	6.23%	-4.32%
2:3_acid	31.7%	-2.97%	8.56%	-1.25%
3:3_acid	31.0%	6.94%	-2.78%	3.37%

Note: The absolute matrix effect is calculated versus the slope of the corresponding mQ-water, residual matrix effect is calculated versus the slope of the corresponding mixture of SW1, SW2, and SW3.

Table S12 A summary of the occurrence of ultra-short-chain and short-chain PFAS in the environment as reported in the literature

PFAS Concentration	Location	Ref.
TFA		
10-130 pg/m^3	Air	23
0.02-2400 ng/L	Precipitation	23 38 22
0.01-140 000 ng/L	Surface water	23 38 22 174 16 202
up to 7500 ng/L	Groundwater	174
16-11 00 ng/L	Tap water	22 174
<100-210 000 ng/L	Wastewater effluent	22
8000-181000 pg/L	Sea/Ocean in Arctic Ocean 1998	17
17000-200000 pg/L	Sea/Ocean in Atlantic Ocean 2002	17
1000-230000 pg/L	Sea/Ocean in Pacific Ocean 1999	17
500-50000 pg/L	Sea/Ocean in Mediterranean Sea 2005	17
65000 pg/L	Precipitation in Tsukuba city and Kawaguchi city, Japan, 2007	37
22-1800 ng/m^2	Surface snow in Norwegian Arctic, 2019	28
14000 ng/L	Water connected to know and suspected point sources in Sweden, 2019	13
0.3-6.0 ug/L	Surface water in Germany, 2022	203
0.4-12.4 ug/L	Blank filtrate in Germany, 2022	203
0.4-4.2 ug/L	Raw water in Germany, 2022	203
<0.2-10.7 ug/L	Groundwater in Germany, 2022	203
<9.5-295 ng/L	Surface water Northern California, USA, 1998	181
23.1-2790 ng/L	Surface water Northern California, USA, 2021	181
PFPrA		
unknown	Tap water	204
0.02-120 ng/L	Precipitation	38
<0.005-0.11 ng/L	Surface water	38
1.1-41 ng/L	Wastewater influent	205
0.9-38 ng/L	Wastewater effluent	205
9500 pg/L	Precipitation in Tsukuba city and Kawaguchi city, Japan, 2007	37
0.79-16 ng/m^2	Surface snow in Norwegian Arctic, 2019	28
53000 ng/L	Water connected to know and suspected point sources in Sweden, 2019	13

<0.003-0.0340 ug/L	Surface water in Germany, 2022	203
<0.003-0.0210 ug/L	Blank filtrate in Germany, 2022	203
<0.003-0.0360 ug/L	Raw water in Germany, 2022	203
<0.003-0.1790 ug/L	Groundwater in Germany, 2022	203
80.3-5250 ng/L	Sierra Nevada Foothills, Surface water Northern California, USA, 2021	181
PFBA		
2100 pg/L	Sea/Ocean in Shandong peninsula, China, 2012	206
26000 pg/L	Lambro River, Italy, 2011-2012	166
9000 pg/L	Samondogawa River, Japan, 2010-2012	207
24000000 pg/L	Groundwater in Military bases, USA, 1942-1990	208
3700000 pg/L	Groundwater in AFFF-impacted site, USA, 2014-2016	209
900 pg/L	Precipitation in Tsukuba city and Kawaguchi city, Japan, 2007	37
0.19-170 ng/m^2	Surface snow in Norwegian Arctic, 2019	28
<0.00042-0.0184 ug/L	Surface water in Germany, 2022	203
<0.00042-0.0231 ug/L	Blank filtrate in Germany, 2022	203
<0.00042-0.0098 ug/L	Raw water in Germany, 2022	203
<0.00042-0.0053 ug/L	Groundwater in Germany, 2022	203
PFPeA		
69000000 pg/L	Groundwater in Military bases, USA, 1942-1990	208
5200000 pg/L	Groundwater in AFFF-impacted site, USA, 2014-2016	209
39000 pg/L	Drinking water in Ruhr area, Germany, 2006	210
400 pg/L	Precipitation in Tsukuba city and Kawaguchi city, Japan, 2007	37
<0.000042-0.0088 ug/L	Surface water in Germany, 2022	203
0.0003-0.0105 ug/L	Blank filtrate in Germany, 2022	203
0.0009-0.0091 ug/L	Raw water in Germany, 2022	203
<0.000042-0.0026 ug/L	Groundwater in Germany, 2022	203
<129-233 ng/L	Surface water Northern California, USA, 2021	181
TMS		
up to 1000 ng/L	Surface water, Groundwater	40
1.5-57 ng/m^2	Surface snow in Norwegian Arctic, 2019	28

940 ng/L	Water connected to know and suspected point sources in Sweden, 2019	[13]
<0.0005-2.1125 ug/L	Surface water in Germany, 2022	[203]
0.0011-0.8626 ug/L	Blank filtrate in Germany, 2022	[203]
0.0026-0.0276 ug/L	Raw water in Germany, 2022	[203]
0.0005-0.0054 ug/L	Groundwater in Germany, 2022	[203]
PFEtS		
1.4-17 ng/L	Wastewater influent	[205]
0.08-11 ng/L	Wastewater effluent	[205]
0.9 ng/L	Tap water	[204]
7 000 000-13000 000 ng/L	AFFF	[29]
11-75000 ng/L	Groundwater near 11 military training sites between 2011 and 2014 in the United States	[29]
1700 ng/L	Water connected to know and suspected point sources in Sweden, 2019	[13]
PFPrS		
Unknown	Tap water	[204]
0.05-7.5 ng/L	Wastewater influent	[205]
0.05-4.1 ng/L	Wastewater effluent	[205]
120 000 000-270 000 000 ng/L	AFFF	[29]
19-63000 ng/L	Groundwater near 11 military training sites between 2011 and 2014 in the United States	[29]
15000 ng/L	Water connected to know and suspected point sources in Sweden, 2019	[13]
<0.000042-0.0004 ug/L	Surface water in Germany, 2022	[203]
<0.000125-0.0003 ug/L	Blank filtrate in Germany, 2022	[203]
<0.000042-0.0004 ug/L	Raw water in Germany, 2022	[203]
<0.000042-0.0013 ug/L	Groundwater in Germany, 2022	[203]
PFBS		
1100 pg/L	Sea/Ocean in Shandong peninsula, China, 2012	[206]
5554 pg/L	Ganges River in India, 2014	[211]
2600 pg/L	River Elbe, Germany, 2007	[212]
2200 pg/L	Llobregat River, Spain, 2010	[213]
33000 pg/L	Lambro River, Italy, 2011-2012	[166]
2000 pg/L	Samondogawa River, Japan, 2010-2012	[207]
4300000 pg/L	Groundwater in Military bases, USA, 1942-1990	[208]

1800000 pg/L	Groundwater in AFFF-impacted site, USA, 2014-2016	[209]
12000 pg/L	Drinking water in Ruhr area, Germany, 2006	[210]
0.0005-0.0172 ug/L	Surface water in Germany, 2022	[203]
0.0003-0.0141 ug/L	Blank filtrate in Germany, 2022	[203]
0.0004-0.0040 ug/L	Raw water in Germany, 2022	[203]
<0.00004-0.0045 ug/L	Groundwater in Germany, 2022	[203]

References

1. Liu, Y.; Pereira, A. D. S.; Martin, J. W., Discovery of C5–C17 Poly- and Perfluoroalkyl Substances in Water by In-Line SPE-HPLC-Orbitrap with In-Source Fragmentation Flagging. *Analytical Chemistry* **2015,** *87* (8), 4260-4268.
2. Giesy, J. P.; Kannan, K., Global Distribution of Perfluorooctane Sulfonate in Wildlife. *Environmental Science & Technology* **2001,** *35* (7), 1339-1342.
3. Sun, M.; Arevalo, E.; Strynar, M.; Lindstrom, A.; Richardson, M.; Kearns, B., Legacy and emerging perfluoroalkyl substances are important drinking water contaminants in the Cape Fear River watershed of North Carolina. *Environmental Science & Technology Letters* **2016,** *3* (12), 415-419.
4. Schultz, M. M.; Higgins, C. P.; Huset, C. A.; Luthy, R. G.; Barofsky, D. F.; Field, J. A., Fluorochemical mass flows in a municipal wastewater treatment facility. *Environmental Science & Technology* **2006,** *40* (23), 7350-7357.
5. Venkatesan, A. K.; Halden, R. U., National inventory of perfluoroalkyl substances in archived US biosolids from the 2001 EPA National Sewage Sludge Survey. *Journal of Hazardous Materials* **2013,** *252*, 413-418.
6. Lang, J. R.; Allred, B. M.; Field, J. A.; Levis, J. W.; Barlaz, M. A., National Estimate of Per- and Polyfluoroalkyl Substance (PFAS) Release to U.S. Municipal Landfill Leachate. *Environmental Science & Technology* **2017,** *51* (4), 2197-2205.
7. L.A., D. A.; S.A., M., Identification of novel fluorinated surfactants in aqueous film forming foams and commercial surfactant concentrates. *Environmental Science & Technology* **2014,** *48*, 121-129.
8. Xu, L.; Shi, Y. L.; Li, C. X.; Song, X. W.; Qin, Z. F.; Cao, D.; Cai, Y. Q., Discovery of a Novel Polyfluoroalkyl Benzenesulfonic Acid around Oilfields in Northern China. *Environmental Science & Technology* **2017,** *51* (24), 14173-14181.
9. Ateia, M.; Maroli, A.; Tharayil, N.; Karanfil, T., The overlooked short- and ultrashort-chain poly- and perfluorinated substances: A review. *Chemosphere* **2019,** *220*, 866-882.
10. Wang, Z.; DeWitt, J. C.; Higgins, C. P.; Cousins, I. T., A Never-Ending Story of Per- and Polyfluoroalkyl Substances (PFASs)? *Environmental Science & Technology* **2017,** *51* (5), 2508-2518.
11. Olsen, G. W.; Chang, S.-C.; Noker, P. E.; Gorman, G. S.; Ehresman, D. J.; Lieder, P. H.; Butenhoff, J. L., A comparison of the pharmacokinetics of perfluorobutanesulfonate (PFBS) in rats, monkeys, and humans. *Toxicology* **2009,** *256* (1), 65-74.
12. Cousins, I. T.; Vestergren, R.; Wang, Z.; Scheringer, M.; McLachlan, M. S., The precautionary principle and chemicals management: The example of perfluoroalkyl acids in groundwater. *Environment international* **2016,** *94*, 331-340.
13. Björnsdotter, M. K.; Yeung, L. W. Y.; Kärrman, A.; Jogsten, I. E., Ultra-Short-Chain Perfluoroalkyl Acids Including Trifluoromethane Sulfonic Acid in Water Connected to Known and Suspected Point Sources in Sweden. *Environmental Science & Technology* **2019,** *53* (19), 11093-11101.
14. Chen, H.; Zhang, L.; Li, M.; Yao, Y.; Zhao, Z.; Munoz, G.; Sun, H., Per- and

polyfluoroalkyl substances (PFASs) in precipitation from mainland China: Contributions of unknown precursors and short-chain (C2C3) perfluoroalkyl carboxylic acids. *Water Research* **2019,** *153*, 169-177.
15. Li, F.; Zhang, C.; Qu, Y.; Chen, J.; Chen, L.; Liu, Y.; Zhou, Q., Quantitative characterization of short- and long-chain perfluorinated acids in solid matrices in Shanghai, China. *Science of The Total Environment* **2010,** *408* (3), 617-623.
16. Scheurer, M.; Nödler, K.; Freeling, F.; Janda, J.; Happel, O.; Riegel, M.; Müller, U.; Storck, F. R.; Fleig, M.; Lange, F. T.; Brunsch, A.; Brauch, H.-J., Small, mobile, persistent: Trifluoroacetate in the water cycle – Overlooked sources, pathways, and consequences for drinking water supply. *Water Research* **2017,** *126*, 460-471.
17. Scott, B. F.; Macdonald, R. W.; Kannan, K.; Fisk, A.; Witter, A.; Yamashita, N.; Durham, L.; Spencer, C.; Muir, D. C. G., Trifluoroacetate Profiles in the Arctic, Atlantic, and Pacific Oceans. *Environmental Science & Technology* **2005,** *39* (17), 6555-6560.
18. Ellis, D. A.; Mabury, S. A.; Martin, J. W.; Muir, D. C. G., Thermolysis of fluoropolymers as a potential source of halogenated organic acids in the environment. *Nature* **2001,** *412* (6844), 321-324.
19. Ellis, D. A.; Martin, J. W.; De Silva, A. O.; Mabury, S. A.; Hurley, M. D.; Andersen, M. P. S.; Wallington, T. J., Degradation of fluorotelomer alcohols: A likely atmospheric source of perfluorinated carboxylic acids. *Environmental Science & Technology* **2004,** *38* (12), 3316-3321.
20. Kazil, J.; McKeen, S.; Kim, S. W.; Ahmadov, R.; Grell, G. A.; Talukdar, R. K.; Ravishankara, A. R., Deposition and rainwater concentrations of trifluoroacetic acid in the United States from the use of HFO-1234yf. *Journal of Geophysical Research-Atmospheres* **2014,** *119* (24), 14059-14079.
21. Solomon, K. R.; Velders, G. J. M.; Wilson, S. R.; Madronich, S.; Longstreth, J.; Aucamp, P. J.; Bornman, J. F., Sources, fates, toxicity, and risks of trifluoroacetic acid and its salts: Relevance to substances regulated under the Montreal and Kyoto Protocols. *Journal of Toxicology and Environmental Health-Part B-Critical Reviews* **2016,** *19* (7), 289-304.
22. Berg, M.; Muller, S. R.; Muhlemann, J.; Wiedmer, A.; Schwarzenbach, R. P., Concentrations and mass fluxes of chloroacetic acids and trifluoroacetic acid in rain and natural waters in Switzerland. *Environmental Science & Technology* **2000,** *34* (13), 2675-2683.
23. Jordan, A.; Frank, H., Trifluoroacetate in the Environment. Evidence for Sources Other Than HFC/HCFCs. *Environmental Science & Technology* **1999,** *33* (4), 522-527.
24. Wang, Q.; Wang, X.; Ding, X., Rainwater trifluoroacetic acid (TFA) in Guangzhou, South China: Levels, wet deposition fluxes and source implication. *Science of The Total Environment* **2014,** *468-469*, 272-279.
25. Wujcik, C. E.; Zehavi, D.; Seiber, J. N., Trifluoroacetic acid levels in 1994–1996 fog, rain, snow and surface waters from California and Nevada. *Chemosphere* **1998,** *36* (6), 1233-1245.
26. von Sydow, L. M.; Grimvall, A. B.; Borén, H. B.; Laniewski, K.; Nielsen, A. T., Natural Background Levels of Trifluoroacetate in Rain and Snow. *Environmental Science & Technology* **2000,** *34* (15), 3115-3118.
27. S.J. Chow, N. O., J.G. Jacangelo, K.J. Schwab, Detection of ultrashort-chain and other per-

and polyfluoroalkyl substances (PFAS) in U.S. bottled water. *Water Res.* **2021,** *201*, 117292.
28. Maria K. Björnsdotter, W. F. H., Roland Kallenborn, Ingrid Ericson Jogsten, Jack D. Humby, Anna Kärrman, Leo W. Y. Yeung, Levels and Seasonal Trends of C1–C4 Perfluoroalkyl Acids and the Discovery of Trifluoromethane Sulfonic Acid in Surface Snow in the Arctic. *Environmental Science & Technology* **2021,** *55* (23), 15853-15861.
29. A., K.; Barzen-Hanson; Field, J. A., Discovery and Implications of C2 and C3 Perfluoroalkyl Sulfonates in Aqueous Film-Forming Foams and Groundwater. *Environmental Science & Technology Letters* **2015,** *2* (4), 95-99.
30. Pickard, H. M.; Criscitiello, A. S.; Persaud, D.; Spencer, C.; Muir, D. C. G.; Lehnherr, I.; Sharp, M. J.; De Silva, A. O.; Young, C. J., Ice Core Record of Persistent Short-Chain Fluorinated Alkyl Acids: Evidence of the Impact From Global Environmental Regulations. *Geophysical Research Letters* **2020,** *47* (10).
31. Duan, Y.; Sun, H.; Yao, Y.; Meng, Y.; Li, Y., Distribution of novel and legacy per-/polyfluoroalkyl substances in serum and its associations with two glycemic biomarkers among Chinese adult men and women with normal blood glucose levels. *Environment International* **2020,** *134*, 105295.
32. H. Frank, D. R., A. Klein, H. Scholl, Trace analysis of airborne haloacetates. *J. High Resolut. Chromatogr.* **1995,** *18*, 83-88.
33. J. Wu, J. M., Z. Zhai, K. Lu, L. Li, X. Fang, H. Jin, J. Hu, J. Zhang, Airborne trifluoroacetic acid and its fraction from the degradation of HFC-134a in Beijing, China. *Environ. Sci. Technol.* **2014,** *48* (7), 3675-3681.
34. Z. Zhai, J. W., X. Hu, L.i. Li, J. Guo, B. Zhang, J. Hu, J. Zhang, A 17-fold increase of trifluoroacetic acid in landscape waters of Beijing, China during the last decade. *Chemosphere* **2015,** *129*, 110-117.
35. M. Berg, S. R. M., J. Mühlemann, A. Wiedmer, R.P. Schwarzenbach, Concentrations and mass fluxes of chloroacetic acids and trifluoroacetic acid in rain and natural waters in Switzerland. *Environ. Sci. Technol.* **2000,** *34*, 2675-2683.
36. Scott, B. F.; Moody, C. A.; Spencer, C.; Small, J. M.; Muir, D. C. G.; Mabury, S. A., Analysis for Perfluorocarboxylic Acids/Anions in Surface Waters and Precipitation Using GC−MS and Analysis of PFOA from Large-Volume Samples. *Environmental Science & Technology* **2006,** *40* (20), 6405-6410.
37. S. Taniyasu, K. K., L.W. Yeung, K.Y. Kwok, P.K. Lam, N. Yamashita, Analysis of trifluoroacetic acid and other short-chain perfluorinated acids (C2-C4) in precipitation by liquid chromatography–tandem mass spectrometry: comparison to patterns of long-chain perfluorinated acids (C5-C18). *Anal. Chim. Acta* **2008,** *619*, 221-230.
38. L.W.Y. Yeung, C. S., S.A. Mabury, Simultaneous analysis of perfluoroalkyl and polyfluoroalkyl substances including ultrashort-chain C2 and C3 compounds in rain and river water samples by ultra performance convergence chromatography. *J. Chromatogr. A* **2017,** *1522*, 78.
39. Reemtsma, T.; Berger, U.; Arp, H. P. H.; Gallard, H.; Knepper, T. P.; Neumann, M.; Quintana, J. B.; Voogt, P. d., Mind the Gap: Persistent and Mobile Organic Compounds—Water

Contaminants That Slip Through. *Environmental Science & Technology* **2016,** *50* (19), 10308-10315.
40. Schulze, S.; Zahn, D.; Montes, R.; Rodil, R.; Quintana, J. B.; Knepper, T. P.; Reemtsma, T.; Berger, U., Occurrence of emerging persistent and mobile organic contaminants in European water samples. *Water Research* **2019,** *153*, 80-90.
41. Niu, X.-Z.; Abrell, L.; Sierra-Alvarez, R.; Field, J. A.; Chorover, J., Analysis of hydrophilic per- and polyfluorinated sulfonates including trifluoromethanesulfonate using solid phase extraction and mixed-mode liquid chromatography-tandem mass spectrometry. *Journal of Chromatography A* **2022,** *1664*, 462817.
42. Montes, R., Rodil, R., Placer, L., Wilms, J.M., Cela, R., Quintana, J.B., Applicability of mixed-mode chromatography for the simultaneous analysis of C1-C18 perfluoroalkylated substances. *Anal Bioanal Chem* **2020,** *412*, 4849-4856.
43. Maria K. Björnsdotter, L. W. Y. Y., Anna Kärrman, Ingrid Ericson Jogsten, Mass Balance of Perfluoroalkyl Acids, Including Trifluoroacetic Acid, in a Freshwater Lake. *Environmental Science & Technology* **2022,** *56* (1), 251-259.
44. Rodríguez-Gonzalo, E.; García-Gómez, D., Liquid Chromatography | Hydrophilic Interaction Chromatography. In *Encyclopedia of Analytical Science (Third Edition)*, Worsfold, P.; Poole, C.; Townshend, A.; Miró, M., Eds. Academic Press: Oxford, 2019; pp 100-107.
45. Cavazzini, A.; Catani, M.; Felinger, A., Chapter 6 - Hydrophilic interaction liquid chromatography. In *Liquid Chromatography (Second Edition)*, Fanali, S.; Haddad, P. R.; Poole, C. F.; Riekkola, M.-L., Eds. Elsevier: 2017; pp 147-169.
46. Guo, Y.; Gaiki, S., Retention behavior of small polar compounds on polar stationary phases in hydrophilic interaction chromatography. *Journal of Chromatography A* **2005,** *1074* (1), 71-80.
47. Vo Duy, S.; Munoz, G.; Dinh, Q. T.; Zhang, Y.; Simon, D. F.; Sauvé, S., Fast screening of saxitoxin, neosaxitoxin, and decarbamoyl analogues in fresh and brackish surface waters by on-line enrichment coupled to HILIC-HRMS. *Talanta* **2022,** *241*, 123267.
48. Treadway, J. W.; Philibert, G. S.; Olesik, S. V., Enhanced fluidity liquid chromatography for hydrophilic interaction separation of nucleosides. *Journal of Chromatography A* **2011,** *1218* (35), 5897-5902.
49. Churms, S. C., Recent progress in carbohydrate separation by high-performance liquid chromatography based on hydrophilic interaction. *Journal of Chromatography A* **1996,** *720* (1), 75-91.
50. Linden, J. C.; Lawhead, C. L., Liquid chromatography of saccharides. *Journal of Chromatography A* **1975,** *105* (1), 125-133.
51. Langrock, T.; Czihal, P.; Hoffmann, R., Amino acid analysis by hydrophilic interaction chromatography coupled on-line to electrospray ionization mass spectrometry. *Amino Acids* **2006,** *30* (3), 291-297.
52. Yoshida, T., Peptide separation by Hydrophilic-Interaction Chromatography: a review. *Journal of Biochemical and Biophysical Methods* **2004,** *60* (3), 265-280.
53. Kingsley, S. L.; Walker, D. I.; Calafat, A. M.; Chen, A. M.; Papandonatos, G. D.; Xu, Y. Y.; Jones, D. P.; Lanphear, B. P.; Pennell, K. D.; Braun, J. M., Metabolomics of childhood

exposure to perfluoroalkyl substances: a cross-sectional study. *Metabolomics* **2019,** *15* (7).
54. Chen, Z. H.; Yang, T. Y.; Walker, D. I.; Thomas, D. C.; Qiu, C. Y.; Chatzi, L.; Alderete, T. L.; Kim, J. S.; Conti, D. V.; Breton, C. V.; Liang, D. H.; Hauser, E. R.; Jones, D. P.; Gilliland, F. D., Dysregulated lipid and fatty acid metabolism link perfluoroalkyl substances exposure and impaired glucose metabolism in young adults. *Environment International* **2020,** *145*.
55. Zahn, D.; Frömel, T.; Knepper, T. P., Halogenated methanesulfonic acids: A new class of organic micropollutants in the water cycle. *Water Research* **2016,** *101*, 292-299.
56. Schwichtenberg, T.; Bogdan, D.; Carignan, C. C.; Reardon, P.; Rewerts, J.; Wanzek, T.; Field, J. A., PFAS and dissolved organic carbon enrichment in surface water foams on a northern U.S. freshwater lake. *Environmental Science & Technology* **2020,** *54* (22), 14455-14464.
57. Alsmeyer, Y. W., Childs, W.V., Flynn, R.M., Moore, G.G.I., Smeltzer, J.C., *Electrochemical fluorination and its applications.* New York, NY: Plenum: 1994.
58. Rayne, S., Forest, K., Friesen, K.J., Congener-specific numbering systems for the environmentally relevant C4 through C8 perfluorinated homologue groups of alkyl sulfonates, carboxylates, telomer alcohols, olefins, and acids, and their derivatives. *Journal of Environmental Science and Health A* **2008,** *43*, 1391-1401.
59. Riddell, N., Arsenault, G., Benskin, J.P., Chittim, B., Martin, J.W., McAlees, A., McCrindle, R. , Branched perfluorooctane sulfonate isomer quantification and characterization in blood serum samples by HPLC/ESI-MS(/MS). . *Environmental Science and Technology* **2009,** *43*, 7902-7908.
60. Glüge, J.; Scheringer, M.; Cousins, I. T.; DeWitt, J. C.; Goldenman, G.; Herzke, D.; Lohmann, R.; Ng, C. A.; Trier, X.; Wang, Z., An overview of the uses of per- and polyfluoroalkyl substances (PFAS). *Environmental Science: Processes & Impacts* **2020,** *22* (12), 2345-2373.
61. Harris, K. J.; Munoz, G.; Woo, V.; Sauvé, S.; Rand, A. A., Targeted and Suspect Screening of Per- and Polyfluoroalkyl Substances in Cosmetics and Personal Care Products. *Environmental Science & Technology* **2022,** *56* (20), 14594-14604.
62. Munoz, G.; Michaud, A. M.; Liu, M.; Vo Duy, S.; Montenach, D.; Resseguier, C.; Watteau, F.; Sappin-Didier, V.; Feder, F.; Morvan, T.; Houot, S.; Desrosiers, M.; Liu, J.; Sauvé, S., Target and Nontarget Screening of PFAS in Biosolids, Composts, and Other Organic Waste Products for Land Application in France. *Environmental Science & Technology* **2022,** *56* (10), 6056-6068.
63. Place, B. J.; Field, J. A., Identification of Novel Fluorochemicals in Aqueous Film-Forming Foams Used by the US Military. *Environmental Science & Technology* **2012,** *46* (13), 7120-7127.
64. Krafft, M. P.; Riess, J. G., Per- and polyfluorinated substances (PFASs): Environmental challenges. *Curr. Opin. Colloid Interface Sci.* **2015,** *20* (3), 192-212.
65. Lang, J. R.; Allred, B. M.; Field, J. A.; Levis, J. W.; Barlaz, M. A., National Estimate of Per- and Polyfluoroalkyl Substance (PFAS) Release to U.S. Municipal Landfill Leachate. *Environ. Sci. Technol.* **2017,** *51* (4), 2197-2205.
66. Kim, K. Y.; Ndabambi, M.; Choi, S.; Oh, J.-E., Legacy and novel perfluoroalkyl and polyfluoroalkyl substances in industrial wastewater and the receiving river water: Temporal

changes in relative abundances of regulated compounds and alternatives. *Water Research* **2021,** *191*, 116830.
67. Masoner, J. R.; Kolpin, D. W.; Cozzarelli, I. M.; Smalling, K. L.; Bolyard, S. C.; Field, J. A.; Furlong, E. T.; Gray, J. L.; Lozinski, D.; Reinhart, D.; Rodowa, A.; Bradley, P. M., Landfill leachate contributes per-/poly-fluoroalkyl substances (PFAS) and pharmaceuticals to municipal wastewater. *Environmental Science: Water Research & Technology* **2020,** *6* (5), 1300-1311.
68. McCord, J. P.; Strynar, M. J.; Washington, J. W.; Bergman, E. L.; Goodrow, S. M., Emerging Chlorinated Polyfluorinated Polyether Compounds Impacting the Waters of Southwestern New Jersey Identified by Use of Nontargeted Analysis. *Environmental Science & Technology Letters* **2020,** *7* (12), 903-908.
69. Holder, C.; DeLuca, N.; Luh, J.; Alexander, P.; Minucci, J. M.; Vallero, D. A.; Thomas, K.; Cohen Hubal, E. A., Systematic Evidence Mapping of Potential Exposure Pathways for Per- and Polyfluoroalkyl Substances Based on Measured Occurrence in Multiple Media. *Environmental Science & Technology* **2023,** *57* (13), 5107-5116.
70. Hu, X. C.; Andrews, D. Q.; Lindstrom, A. B.; Bruton, T. A.; Schaider, L. A.; Grandjean, P.; Lohmann, R.; Carignan, C. C.; Blum, A.; Balan, S. A.; Higgins, C. P.; Sunderland, E. M., Detection of Poly- and Perfluoroalkyl Substances (PFASs) in U.S. Drinking Water Linked to Industrial Sites, Military Fire Training Areas, and Wastewater Treatment Plants. *Environmental Science & Technology Letters* **2016,** *3* (10), 344-350.
71. Jian, J.-M.; Guo, Y.; Zeng, L.; Liang-Ying, L.; Lu, X.; Wang, F.; Zeng, E. Y., Global distribution of perfluorochemicals (PFCs) in potential human exposure source–A review. *Environment International* **2017,** *108*, 51-62.
72. VanNoy, B. N.; Lam, J.; Zota, A. R., Breastfeeding as a Predictor of Serum Concentrations of Per- and Polyfluorinated Alkyl Substances in Reproductive-Aged Women and Young Children: A Rapid Systematic Review. *Current Environmental Health Reports* **2018,** *5* (2), 213-224.
73. Zheng, G.; Boor, B. E.; Schreder, E.; Salamova, A., Indoor exposure to per- and polyfluoroalkyl substances (PFAS) in the childcare environment. *Environmental Pollution* **2020,** *258*, 113714.
74. Braun, J. M.; Chen, A.; Romano, M. E.; Calafat, A. M.; Webster, G. M.; Yolton, K.; Lanphear, B. P., Prenatal perfluoroalkyl substance exposure and child adiposity at 8 years of age: The HOME study. *Obesity* **2016,** *24*, 231-237.
75. Barry, V.; Winquist, A.; Steenland, K., Perfluorooctanoic acid (PFOA) exposures and incident cancers among adults living near a chemical plant. *Environ. Health Perspect* **2013,** *121* (11-12), 1313-1318.
76. Grandjean, P.; Andersen, E.; Budtz-Jørgensen, E.; Nielsen, F.; Mølbak, K.; Weihe, P.; Heilmann, C., Serum vaccine antibody concentrations in children exposed to perfluorinated compounds. *JAMA* **2012,** *307* (4), 391-397.
77. Cousins IT, N. C., Wang Z, Scheringer M., Why is high persistence alone a major cause of concern? *Environ Sci Process Impacts* **2019,** *21* (5), 781-792.
78. Bălan SA, M. V., Guo DF, Algazi AM., Regulating PFAS as a chemical class under the

California Safer Consumer Products Program. *Environ Health Perspect* **2021,** *129* (2), 25001.
79. Rossella, G.; Teofilo, V.; Sergio, M., Accumulation of perfluorinated alkyl substances (PFAS) in agricultural plants: A review. *Environ. Res.* **2019,** *169*, 326-341.
80. Lutz, A., Polyfluoroalkyl compounds in the aquatic environment: a review of their occurrence and fate. *J. Environ. Monit.* **2011,** *13* (1), 20-31.
81. Quinones, O.; Snyder, S. A., Occurrence of per- fluoroalkyl carboxylates and sulfonates in drinking water utilities and related waters from the United States. *Environmental Science & Technology* **2009,** *43* (24), 9089-9095.
82. Hu, X. D. C.; Andrews, D. Q.; Lindstrom, A. B.; Bruton, T. A.; Schaider, L. A.; Grandjean, P., Detection of poly- and perfluoroalkyl substances (PFASs) in US drinking water linked to industrial sites, military fire training areas, and wastewater treatment plants. *Environmental Science & Technology Letters* **2016,** *3* (10), 344-350.
83. Teymoorian, T.; Munoz, G.; Vo Duy, S.; Liu, J.; Sauvé, S., Tracking PFAS in Drinking Water: A Review of Analytical Methods and Worldwide Occurrence Trends in Tap Water and Bottled Water. *ACS ES&T Water* **2023,** *3* (2), 246-261.
84. Brennan, N. M.; Evans, A. T.; Fritz, M. K.; Peak, S. A.; von Holst, H. E., Trends in the Regulation of Per- and Polyfluoroalkyl Substances (PFAS): A Scoping Review. *International Journal of Environmental Research and Public Health* **2021,** *18* (20), 10900.
85. Ke, G.; Yu, C.; Qiao, X.; Jie, F.; Kehan, F.; Jianjie, F.; Aiqian, Z.; Zongwei, C.; Guibin, J., Trends and perspectives in per-and polyfluorinated alkyl substances (PFASs) determination: Faster and broader. *Trends in Analytical Chemistry* **2020,** *133*, 116114.
86. Barzen-Hanson, K. A.; Roberts, S. C.; Choyke, S.; Oetjen, K.; McAlees, A.; Riddell, N.; McCrindle, R.; Ferguson, P. L.; Higgins, C. P.; Field, J. A., Discovery of 40 Classes of Per- and Polyfluoroalkyl Substances in Historical Aqueous Film-Forming Foams (AFFFs) and AFFF-Impacted Groundwater. *Environmental Science & Technology* **2017,** *51* (4), 2047-2057.
87. Liu, Y.; D'Agostino, L. A.; Qu, G.; Jiang, G.; Martin, J. W., High-Resolution Mass Spectrometry (HRMS) Methods for Nontarget Discovery and Characterization of Poly- and per-Fluoroalkyl Substances (PFASs) in Environmental and Human Samples. *TrAC, Trends Anal. Chem.* **2019,** *121*, 115420.
88. Barzen-Hanson, K. A.; Roberts, S. C.; Choyke, S.; Oetjen, K.; McAlees, A.; Riddell, N., Discovery of 40 classes of per- and polyfluoroalkyl substances in historical aqueous film-forming foams (AFFFs) and AFFF-impacted groundwater. *Environmental Science & Technology* **2017,** *51* (4), 2047-2057.
89. B.J., P.; J.A., F., Identification of novel fluorochemicals in aqueous film- forming foams used by the US military. *Environmental Science & Technology* **2012,** *46*, 7120.
90. Y., L.; M., Q.; X., M.; L., Z.; J.W., M., Nontarget mass spectrometry reveals new perfluoroalkyl substances in fish from the Yangtze River and Tangxun Lake, China. *Environmental Science & Technology* **2018,** *52*, 5830-5840.
91. F., X.; S.A., G.; M.Y., G., Identification of novel non-ionic, cationic, zwitterionic, and anionic polyfluoroalkyl substances using UPLCeTOFeMSE high-resolution parent ion search. *Anal. Chim. Acta* **2017,** *988*, 41-49.

92. Liu, Y.; D'Agostino, L. A.; Qu, G.; Jiang, G.; Martin, J. W., High-resolution mass spectrometry (HRMS) methods for nontarget discovery and characterization of poly- and per-fluoroalkyl substances (PFASs) in environmental and human samples. *Trends in Analytical Chemistry* **2019,** *121*, 115420.
93. Shafique, U.; Schulze, S.; Slawik, C.; Kunz, S.; Paschke, A.; Schüürmann, G., Gas chromatographic determination of perfluorocarboxylic acids in aqueous samples – A tutorial review. *Analytica Chimica Acta* **2017,** *949*, 8-22.
94. Naile, J. E.; Garrison, A. W.; Avants, J. K.; Washington, J. W., Isomers/enantiomers of perfluorocarboxylic acids: Method development and detection in environmental samples. *Chemosphere* **2016,** *144*, 1722-1728.
95. Benskin, J. P.; Bataineh, M.; Martin, J. W., Simultaneous Characterization of Perfluoroalkyl Carboxylate, Sulfonate, and Sulfonamide Isomers by Liquid Chromatography−Tandem Mass Spectrometry. *Analytical Chemistry* **2007,** *79* (17), 6455-6464.
96. Benskin, J. P.; Ikonomou, M. G.; Woudneh, M. B.; Cosgrove, J. R., Rapid characterization of perfluoralkyl carboxylate, sulfonate, and sulfonamide isomers by high-performance liquid chromatography-tandem mass spectrometry. *Journal of Chromatography A* **2012,** *1247*, 165-170.
97. Benskin, J. P.; De Silva, A. O.; Martin, J. W., Isomer Proflling of Perfluorinated Substances as a Tool for Source Tracking: A Review of Early Findings and Future Applications. *In Reviews of Environmental Contamination and Toxicology* **2010,** *208*, 111-160.
98. Benskin, J. P.; De Silva, A. O.; Martin, J. W., *Reviews of Environmental Contamination and Toxicology Volume: Perfluorinated Alkylated Substances.* Springer New York: New York, NY, 2010; Vol. 208.
99. Kempisty, D. M.; Xing, Y.; Racz, L., *Perfluoroalkyl Substances in the Environment: Theory, Practice, and Innovation (1st ed.)*. CRC Press: New York, 2018.
100. Zhu, J.; Harada, K. H.; Zou, X. L.; Sun, C. J., Investigating isomers/enantiomers of perfluorooctanoic acid in river water by gas chromatography-mass spectrometry with chiral derivatization. *Chemosphere* **2020,** *238*, 124617.
101. Bidleman, T. F.; Falconer, R. L., Using enantiomers to trace pesticide emissions. *Environ. Sci.Technol.* **1999,** *33*, 206A-209A.
102. Liu, Y. N.; Pereira, A. S.; Beesoon, S.; Vestergren, R.; Berger, U.; Olsen, G. W.; Glynn, A.; Martin, J. W., Temporal trends of perfluorooctanesulfonate isomer and enantiomer patterns in archived Swedish and American serum samples. *Environ. Int.* **2015,** *75*, 215-222.
103. Wang, Y.; Arsenault, G.; Riddell, N.; McCrindle, R.; McAlees, A.; Martin, J. W., Perfluorooctane Sulfonate (PFOS) Precursors Can Be Metabolized Enantioselectively: Principle for a New PFOS Source Tracking Tool. *Environmental Science & Technology* **2009,** *43* (21), 8283-8289.
104. Asher, B. J.; Wang, Y.; De Silva, A. O.; Backus, S.; Muir, D. C. G.; Wong, C. S.; Martin, J. W., Enantiospecific Perfluorooctane Sulfonate (PFOS) Analysis Reveals Evidence for the Source Contribution of PFOS-Precursors to the Lake Ontario Foodweb. *Environmental Science & Technology* **2012,** *46* (14), 7653-7660.
105. Wang, Y.; Beesoon, S.; Benskin, J. P.; De Silva, A. O.; Genuis, S. J.; Martin, J. W.,

Enantiomer Fractions of Chiral Perfluorooctanesulfonate (PFOS) in Human Sera. *Environmental Science & Technology* **2011,** *45* (20), 8907-8914.
106. Zhao, L.; Chen, F. F.; Guo, F. J.; Liu, W. P.; Liu, K., Enantioseparation of chiral perfluorooctane sulfonate (PFOS) by supercritical fluid chromatography (SFC): Effects of the chromatographic conditions and separation mechanism. *Chirality* **2019,** *31* (10), 870-878.
107. Zhao, L.; Chen, F. F.; Yin, S. S.; Xie, J. Q.; Aamir, M.; Liu, S. R.; Liu, W. P., Enantioselectivity in transplacental transfer of perfluoro-1-methylheptanesulfonate (1m-PFOS): Human biomonitoring and in silico study. *Environmental Pollution* **2020,** *261*.
108. D., R. S.; Y., K. S., Water Analysis: Emerging Contaminants and Current Issues. *Anal. Chem.* **2020,** *92*, 473-505.
109. Willach, S.; Brauch, H.-J.; Lange, F. T., Contribution of Selected Perfluoroalkyl and Polyfluoroalkyl Substances to the Adsorbable Organically Bound Fluorine in German Rivers and in a Highly Contaminated Groundwater. *Chemosphere* **2016,** *145*, 342-350.
110. Yuling, H.; Pulikkal Vivek Francis; Mei, S., Comprehensive Validation of the Adsorbable Organic Fluorine Analysis and Performance Comparison of Current Methods for Total Per- and Polyfluoroalkyl Substances in Water Samples. *ACS EST Water* **2021,** *XXX*, XXX-XXX.
111. Abercron, E. V.; S. Falk; T. Stahl; S. Georgii; G. Hamscher; H. Brunn; Schmitz., F., Determination of adsorbable organically bound fluorine (AOF) and adsorbable organically bound halogens as sum parameters in aqueous environmental samples using combustion ion chromatography (CIC). *Science of the Total Environment* **2019,** *673*, 384-391.
112. A., M. C.; L., G. J.; P., H. C., Measuring total PFASs in water: The tradeoff between selectivity and inclusivity. *Curr. Opin. Environ. Sci. Health* **2019,** *7*, 13-18.
113. Martin, D.; Munoz, G.; Mejia-Avendaño, S.; Duy, S. V.; Yao, Y.; Volchek, K.; Brown, C. E.; Liu, J.; Sauvé, S., Zwitterionic, cationic, and anionic perfluoroalkyl and polyfluoroalkyl substances integrated into total oxidizable precursor assay of contaminated groundwater. *Talanta* **2019,** *195*, 533-542.
114. Ruyle, B. J.; Thackray, C. P.; McCord, J. P.; Strynar, M. J.; Mauge-Lewis, K. A.; Fenton, S. E.; Sunderland, E. M., Reconstructing the Composition of Per- and Polyfluoroalkyl Substances in Contemporary Aqueous Film-Forming Foams. *Environmental Science & Technology Letters* **2021,** *8* (1), 59-65.
115. E., R. A.; Kristin, M.; Margaret, D.; David, L.; Craig, B.; Graham, P.; M., S. H.; A., F. J., Closing the Mass Balance on Fluorine on Papers and Textiles. *Environmental Science & Technology* **2017,** *51* (16), 9022-9032.
116. Zhang, C.; Hopkins, Z. R.; McCord, J.; Strynar, M. J.; Knappe, D. R., Fate of Per- and Polyfluoroalkyl Ether Acids in the Total Oxidizable Precursor Assay and Implications for the Analysis of Impacted Water. *Environmental Science & Technology Letters* **2019,** *6* (11), 662-668.
117. UNEP, Stockholm Convention on Persistent Organic Pollutants. **2014**.
118. Sun, M.; Arevalo, E.; Strynar, M.; Lindstrom, A.; Richardson, M.; Kearns, B.; Pickett, A.; Smith, C.; Knappe, D. R. U., Legacy and Emerging Perfluoroalkyl Substances Are Important Drinking Water Contaminants in the Cape Fear River Watershed of North Carolina. *Environmental Science & Technology Letters* **2016,** *3* (12), 415-419.

119.Kaboré, H. A.; Vo Duy, S.; Munoz, G.; Méité, L.; Desrosiers, M.; Liu, J.; Sory, T. K.; Sauvé, S., Worldwide drinking water occurrence and levels of newly-identified perfluoroalkyl and polyfluoroalkyl substances. *Science of The Total Environment* **2018,** *616-617*, 1089-1100.
120. Barzen-Hanson, K. A.; Davis, S. E.; Kleber, M.; Field, J. A., Sorption of Fluorotelomer Sulfonates, Fluorotelomer Sulfonamido Betaines, and a Fluorotelomer Sulfonamido Amine in National Foam Aqueous Film-Forming Foam to Soil. *Environmental Science & Technology* **2017,** *51* (21), 12394-12404.
121. Lindstrom, A. B.; Strynar, M. J.; Libelo, E. L., Polyfluorinated Compounds: Past, Present, and Future. *Environmental Science & Technology* **2011,** *45* (19), 7954-7961.
122. Hurley, M. D.; Sulbaek Andersen, M. P.; Wallington, T. J.; Ellis, D. A.; Martin, J. W.; Mabury, S. A., Atmospheric Chemistry of Perfluorinated Carboxylic Acids: Reaction with OH Radicals and Atmospheric Lifetimes. *The Journal of Physical Chemistry A* **2004,** *108* (4), 615-620.
123. Lee, H.; D'eon, J.; Mabury, S. A., Biodegradation of Polyfluoroalkyl Phosphates as a Source of Perfluorinated Acids to the Environment. *Environmental Science & Technology* **2010,** *44* (9), 3305-3310.
124. Liou, J. S. C.; Szostek, B.; DeRito, C. M.; Madsen, E. L., Investigating the biodegradability of perfluorooctanoic acid. *Chemosphere* **2010,** *80* (2), 176-183.
125. Butt, C. M.; Muir, D. C. G.; Mabury, S. A., Biotransformation pathways of fluorotelomer-based polyfluoroalkyl substances: A review. *Environmental Toxicology and Chemistry* **2014,** *33* (2), 243-267.
126. Arp, H. P. H.; Niederer, C.; Goss, K.-U., Predicting the Partitioning Behavior of Various Highly Fluorinated Compounds. *Environmental Science & Technology* **2006,** *40* (23), 7298-7304.
127. Li, F.; Fang, X.; Zhou, Z.; Liao, X.; Zou, J.; Yuan, B.; Sun, W., Adsorption of perfluorinated acids onto soils: Kinetics, isotherms, and influences of soil properties. *Science of The Total Environment* **2019,** *649*, 504-514.
128. Neumann, M.; Schliebner, I., Protecting the sources of our drinking water: the criteria for identifying persistent, mobile and toxic (PMT) substances and very persistent and very mobile (vPvM) substances under EU Regulation REACH (EC) No 1907/2006. *German Environment Agency (UBA Texte 127/2019). Dessau-Rosslau (87 pages, ISSN 1862-4804)* **2019**.
129. Gagliano, E.; Sgroi, M.; Falciglia, P. P.; Vagliasindi, F. G.; Roccaro, P., Removal of poly-and perfluoroalkyl substances (PFAS) from water by adsorption: Role of PFAS chain length, effect of organic matter and challenges in adsorbent regeneration. *Water research* **2020,** *171*, 115381.
130. Coggan, T. L.; Moodie, D.; Kolobaric, A.; Szabo, D.; Shimeta, J.; Crosbie, N. D.; Lee, E.; Fernandes, M.; Clarke, B. O., An investigation into per-and polyfluoroalkyl substances (PFAS) in nineteen Australian wastewater treatment plants (WWTPs). *Heliyon* **2019,** *5* (8), e02316.
131. Gallen, C.; Eaglesham, G.; Drage, D.; Nguyen, T. H.; Mueller, J., A mass estimate of perfluoroalkyl substance (PFAS) release from Australian wastewater treatment plants. *Chemosphere* **2018,** *208*, 975-983.
132. Lenka, S. P.; Kah, M.; Padhye, L. P., A review of the occurrence, transformation, and

removal of poly-and perfluoroalkyl substances (PFAS) in wastewater treatment plants. *Water research* **2021,** *199*, 117187.
133. Belisle, J.; Hagen, D. F., Method for the determination of the total fluorine content of whole blood, serum/plasma, and other biological samples. *Analytical Biochemistry* **1978,** *87* (2), 545-555.
134. Scott, B. F.; Spencer, C.; Mabury, S. A.; Muir, D. C., Poly and perfluorinated carboxylates in North American precipitation. *Environmental science & technology* **2006,** *40* (23), 7167-7174.
135. Belisle, J.; Hagen, D., A method for the determination of perfluorooctanoic acid in blood and other biological samples. *Analytical biochemistry* **1980,** *101* (2), 369-376.
136. Henderson, W. M.; Weber, E. J.; Duirk, S. E.; Washington, J. W.; Smith, M. A., Quantification of fluorotelomer-based chemicals in mammalian matrices by monitoring perfluoroalkyl chain fragments with GC/MS. *Journal of Chromatography B* **2007,** *846* (1-2), 155-161.
137. Moody, C. A.; Field, J. A., Determination of perfluorocarboxylates in groundwater impacted by fire-fighting activity. *Environmental science & technology* **1999,** *33* (16), 2800-2806.
138. Alzaga, R.; Salgado-Petinal, C.; Jover, E.; Bayona, J., Development of a procedure for the determination of perfluorocarboxylic acids in sediments by pressurised fluid extraction, headspace solid-phase microextraction followed by gas chromatographic–mass spectrometric determination. *Journal of Chromatography A* **2005,** *1083* (1-2), 1-6.
139. Fujii, Y.; Yan, J.; Harada, K. H.; Hitomi, T.; Yang, H.; Wang, P.; Koizumi, A., Levels and profiles of long-chain perfluorinated carboxylic acids in human breast milk and infant formulas in East Asia. *Chemosphere* **2012,** *86* (3), 315-321.
140. Shafique, U.; Schulze, S.; Slawik, C.; Kunz, S.; Paschke, A.; Schüürmann, G., Gas chromatographic determination of perfluorocarboxylic acids in aqueous samples–A tutorial review. *Analytica Chimica Acta* **2017,** *949*, 8-22.
141. Kaufmann, A.; Widmer, M.; Maden, K.; Butcher, P.; Walker, S., Analysis of a variety of inorganic and organic additives in food products by ion-pairing liquid chromatography coupled to high-resolution mass spectrometry. *Analytical and bioanalytical chemistry* **2018,** *410*, 5629-5640.
142. Candelaria, L.; Frolova, L. V.; Kowalski, B. M.; Artyushkova, K.; Serov, A.; Kalugin, N. G., Surface-modified three-dimensional graphene nanosheets as a stationary phase for chromatographic separation of chiral drugs. *Scientific reports* **2018,** *8* (1), 14747.
143. Roussis, S. G.; Koch, C.; Capaldi, D.; Rentel, C., Rapid oligonucleotide drug impurity determination by direct spectral comparison of ion-pair reversed-phase high-performance liquid chromatography electrospray ionization mass spectrometry data. *Rapid Communications in Mass Spectrometry* **2018,** *32* (14), 1099-1106.
144. Piovesana, S.; Montone, C. M.; Cavaliere, C.; Crescenzi, C.; La Barbera, G.; Laganà, A.; Capriotti, A. L., Sensitive untargeted identification of short hydrophilic peptides by high performance liquid chromatography on porous graphitic carbon coupled to high resolution mass spectrometry. *Journal of Chromatography A* **2019,** *1590*, 73-79.

145. Pereira, L., Porous graphitic carbon as a stationary phase in HPLC: theory and applications. *Journal of Liquid Chromatography & Related Technologies®* **2008,** *31* (11-12), 1687-1731.
146. Vaudreuil, M.-A.; Vo Duy, S.; Munoz, G.; Furtos, A.; Sauvé, S., A framework for the analysis of polar anticancer drugs in wastewater: On-line extraction coupled to HILIC or reverse phase LC-MS/MS. *Talanta* **2020,** *220*, 121407.
147. Jandera, P., Stationary and mobile phases in hydrophilic interaction chromatography: a review. *Analytica chimica acta* **2011,** *692* (1-2), 1-25.
148. Van Nuijs, A. L.; Tarcomnicu, I.; Covaci, A., Application of hydrophilic interaction chromatography for the analysis of polar contaminants in food and environmental samples. *Journal of Chromatography A* **2011,** *1218* (35), 5964-5974.
149. Buszewski, B.; Noga, S., Hydrophilic interaction liquid chromatography (HILIC)—a powerful separation technique. *Analytical and Bioanalytical Chemistry* **2012,** *402* (1), 231-247.
150. Guo, H.; Gao, Y.; Guo, D.; Liu, W.; Wang, J.; Zheng, J.; Zhong, J.; Zhao, Q., Sensitive, rapid and non-derivatized determination of glyphosate, glufosinate, bialaphos and metabolites in surface water by LC–MS/MS. *SN Applied Sciences* **2019,** *1*, 1-8.
151. Seitz, W.; Schulz, W.; Winzenbacher, R., Advantage of liquid chromatography with high-resolution mass spectrometry for the detection of the small and polar molecules trifluoroacetic acid and sulfamic acid. *Journal of separation science* **2018,** *41* (24), 4437-4448.
152. Kovalova, L.; McArdell, C. S.; Hollender, J., Challenge of high polarity and low concentrations in analysis of cytostatics and metabolites in wastewater by hydrophilic interaction chromatography/tandem mass spectrometry. *Journal of Chromatography A* **2009,** *1216* (7), 1100-1108.
153. Fontanals, N.; Marcé, R. M.; Borrull, F., On-line solid-phase extraction coupled to hydrophilic interaction chromatography–mass spectrometry for the determination of polar drugs. *Journal of Chromatography A* **2011,** *1218* (35), 5975-5980.
154. Zarębska, M.; Bajkacz, S., Poly– and perfluoroalkyl substances (PFAS) - recent advances in the aquatic environment analysis. *TrAC Trends in Analytical Chemistry* **2023,** *163*, 117062.
155. Deng, Z.-H.; Cheng, C.-G.; Wang, X.-L.; Shi, S.-H.; Wang, M.-L.; Zhao, R.-S., Preconcentration and Determination of Perfluoroalkyl Substances (PFASs) in Water Samples by Bamboo Charcoal-Based Solid-Phase Extraction Prior to Liquid Chromatography–Tandem Mass Spectrometry. *Molecules* **2018,** *23* (4), 902.
156. Lin, Y.; Liu, R.; Hu, F.; Liu, R.; Ruan, T.; Jiang, G., Simultaneous qualitative and quantitative analysis of fluoroalkyl sulfonates in riverine water by liquid chromatography coupled with Orbitrap high resolution mass spectrometry. *Journal of Chromatography A* **2016,** *1435*, 66-74.
157. Zacs, D.; Bartkevics, V., Trace determination of perfluorooctane sulfonate and perfluorooctanoic acid in environmental samples (surface water, wastewater, biota, sediments, and sewage sludge) using liquid chromatography – Orbitrap mass spectrometry. *Journal of Chromatography A* **2016,** *1473*, 109-121.
158. Luque, N.; Ballesteros-Gómez, A.; van Leeuwen, S.; Rubio, S., Analysis of

perfluorinated compounds in biota by microextraction with tetrahydrofuran and liquid chromatography/ion isolation-based ion-trap mass spectrometry. *Journal of Chromatography A* **2010,** *1217* (24), 3774-3782.
159. Huang, Y.; Li, H.; Bai, M.; Huang, X., Efficient extraction of perfluorocarboxylic acids in complex samples with a monolithic adsorbent combining fluorophilic and anion-exchange interactions. *Analytica Chimica Acta* **2018,** *1011*, 50-58.
160. D'Agostino, L. A.; Mabury, S. A., Identification of Novel Fluorinated Surfactants in Aqueous Film Forming Foams and Commercial Surfactant Concentrates. *Environmental Science & Technology* **2014,** *48* (1), 121-129.
161. Song, X.; Vestergren, R.; Shi, Y.; Huang, J.; Cai, Y., Emissions, Transport, and Fate of Emerging Per- and Polyfluoroalkyl Substances from One of the Major Fluoropolymer Manufacturing Facilities in China. *Environmental Science & Technology* **2018,** *52* (17), 9694-9703.
162. Xu, L.; Shi, Y.; Li, C.; Song, X.; Qin, Z.; Cao, D.; Cai, Y., Discovery of a Novel Polyfluoroalkyl Benzenesulfonic Acid around Oilfields in Northern China. *Environmental Science & Technology* **2017,** *51* (24), 14173-14181.
163. Hansen, K. J.; Clemen, L. A.; Ellefson, M. E.; Johnson, H. O., Compound-Specific, Quantitative Characterization of Organic Fluorochemicals in Biological Matrices. *Environmental Science & Technology* **2001,** *35* (4), 766-770.
164. Munoz, G.; Ray, P.; Mejia-Avendaño, S.; Vo Duy, S.; Tien Do, D.; Liu, J.; Sauvé, S., Optimization of extraction methods for comprehensive profiling of perfluoroalkyl and polyfluoroalkyl substances in firefighting foam impacted soils. *Analytica Chimica Acta* **2018,** *1034*, 74-84.
165. Wang, Y.; Yu, N.; Zhu, X.; Guo, H.; Jiang, J.; Wang, X.; Shi, W.; Wu, J.; Yu, H.; Wei, S., Suspect and Nontarget Screening of Per- and Polyfluoroalkyl Substances in Wastewater from a Fluorochemical Manufacturing Park. *Environmental Science & Technology* **2018,** *52* (19), 11007-11016.
166. Castiglioni, S.; Valsecchi, S.; Polesello, S.; Rusconi, M.; Melis, M.; Palmiotto, M.; Manenti, A.; Davoli, E.; Zuccato, E., Sources and fate of perfluorinated compounds in the aqueous environment and in drinking water of a highly urbanized and industrialized area in Italy. *Journal of Hazardous Materials* **2015,** *282*, 51-60.
167. Ciofi, L.; Renai, L.; Rossini, D.; Ancillotti, C.; Falai, A.; Fibbi, D.; Bruzzoniti, M. C.; Santana-Rodriguez, J. J.; Orlandini, S.; Del Bubba, M., Applicability of the direct injection liquid chromatographic tandem mass spectrometric analytical approach to the sub-ngL−1 determination of perfluoro-alkyl acids in waste, surface, ground and drinking water samples. *Talanta* **2018,** *176*, 412-421.
168. Mottaleb, M. A.; Ding, Q. X.; Pennell, K. G.; Haynes, E. N.; Morris, A. J., Direct injection analysis of per and polyfluoroalkyl substances in surface and drinking water by sample filtration and liquid chromatography-tandem mass spectrometry. *Journal of Chromatography A* **2021,** *1653*, 462426.
169. Mejia-Avendaño, S.; Munoz, G.; Sauvé, S.; Liu, J., Assessment of the Influence of Soil Characteristics and Hydrocarbon Fuel Cocontamination on the Solvent Extraction of

Perfluoroalkyl and Polyfluoroalkyl Substances. *Analytical Chemistry* **2017,** *89* (4), 2539-2546.
170. Srivastava, P.; Williams, M.; Du, J.; Navarro, D.; Kookana, R.; Douglas, G.; Bastow, T.; Davis, G.; Kirby, J. K., Method for extraction and analysis of per- and poly-fluoroalkyl substances in contaminated asphalt. *Analytical Methods* **2022,** *14* (17), 1678-1689.
171. Baduel, C.; Mueller, J. F.; Rotander, A.; Corfield, J.; Gomez-Ramos, M.-J., Discovery of novel per- and polyfluoroalkyl substances (PFASs) at a fire fighting training ground and preliminary investigation of their fate and mobility. *Chemosphere* **2017,** *185*, 1030-1038.
172. Liu, M.; Munoz, G.; Vo Duy, S.; Sauvé, S.; Liu, J., Per- and Polyfluoroalkyl Substances in Contaminated Soil and Groundwater at Airports: A Canadian Case Study. *Environmental Science & Technology* **2022,** *56* (2), 885-895.
173. Munoz, G.; Vo Duy, S.; Roy-Lachapelle, A.; Husk, B.; Sauvé, S., Analysis of individual and total microcystins in surface water by on-line preconcentration and desalting coupled to liquid chromatography tandem mass spectrometry. *Journal of Chromatography A* **2017,** *1516*, 9-20.
174. Janda, J.; Nödler, K.; Brauch, H.-J.; Zwiener, C.; Lange, F. T., Robust trace analysis of polar (C2-C8) perfluorinated carboxylic acids by liquid chromatography-tandem mass spectrometry: method development and application to surface water, groundwater and drinking water. *Environmental Science and Pollution Research* **2019,** *26* (8), 7326-7336.
175. Jacob, P.; Helbling, D. E., Rapid and Simultaneous Quantification of Short- and Ultrashort-Chain Perfluoroalkyl Substances in Water and Wastewater. *ACS ES&T Water* **2022**.
176. Willenberg, I.; Meschede, A. K.; Schebb, N. H., Determining cyclooxygenase-2 activity in three different test systems utilizing online-solid phase extraction-liquid chromatography-mass spectrometry for parallel quantification of prostaglandin E2, D2 and thromboxane B2. *Journal of Chromatography A* **2015,** *1391*, 40-48.
177. Kadar, H.; Veyrand, B.; Barbarossa, A.; Pagliuca, G.; Legrand, A.; Bosher, C.; Boquien, C.-Y.; Durand, S.; Monteau, F.; Antignac, J.-P.; Le Bizec, B., Development of an analytical strategy based on liquid chromatography–high resolution mass spectrometry for measuring perfluorinated compounds in human breast milk: Application to the generation of preliminary data regarding perinatal exposure in France. *Chemosphere* **2011,** *85* (3), 473-480.
178. Dinh, Q. T.; Munoz, G.; Simon, D. F.; Vo Duy, S.; Husk, B.; Sauvé, S., Stability issues of microcystins, anabaenopeptins, anatoxins, and cylindrospermopsin during short-term and long-term storage of surface water and drinking water samples. *Harmful Algae* **2021,** *101*, 101955.
179. Sörengård, M.; Franke, V.; Tröger, R.; Ahrens, L., Losses of poly- and perfluoroalkyl substances to syringe filter materials. *Journal of Chromatography A* **2020,** *1609*, 460430.
180. Agency, U. S. E. P., Method 8327: PFAS Using External Standard Calibration and MRM LC/MS/MS. Agency, U. S. E. P., Ed. 2021.
181. Cahill, T. M., Increases in Trifluoroacetate Concentrations in Surface Waters over Two Decades. *Environmental Science & Technology* **2022**.
182. Shaw, D. M. J.; Munoz, G.; Bottos, E. M.; Duy, S. V.; Sauvé, S.; Liu, J.; Van Hamme, J. D., Degradation and defluorination of 6:2 fluorotelomer sulfonamidoalkyl betaine and 6:2 fluorotelomer sulfonate by Gordonia sp. strain NB4-1Y under sulfur-limiting conditions.

Science of The Total Environment **2019,** *647*, 690-698.
183. Wang, N.; Buck, R. C.; Szostek, B.; Sulecki, L. M.; Wolstenholme, B. W., 5:3 Polyfluorinated acid aerobic biotransformation in activated sludge via novel "one-carbon removal pathways". *Chemosphere* **2012,** *87* (5), 527-534.
184. Harding-Marjanovic, K. C.; Houtz, E. F.; Yi, S.; Field, J. A.; Sedlak, D. L.; Alvarez-Cohen, L., Aerobic Biotransformation of Fluorotelomer Thioether Amido Sulfonate (Lodyne) in AFFF-Amended Microcosms. *Environmental Science & Technology* **2015,** *49* (13), 7666-7674.
185. D'Agostino, L. A.; Mabury, S. A., Aerobic biodegradation of 2 fluorotelomer sulfonamide–based aqueous film–forming foam components produces perfluoroalkyl carboxylates. *Environmental Toxicology and Chemistry* **2017,** *36* (8), 2012-2021.
186. Ahmadireskety, A.; Da Silva, B. F.; Townsend, T. G.; Yost, R. A.; Solo-Gabriele, H. M.; Bowden, J. A., Evaluation of extraction workflows for quantitative analysis of per- and polyfluoroalkyl substances: A case study using soil adjacent to a landfill. *Science of The Total Environment* **2021,** *760*, 143944.
187. Nickerson, A.; Maizel, A. C.; Kulkarni, P. R.; Adamson, D. T.; Kornuc, J. J.; Higgins, C. P., Enhanced Extraction of AFFF-Associated PFASs from Source Zone Soils. *Environmental Science & Technology* **2020,** *54* (8), 4952-4962.
188. Lorenzo, M.; Campo, J.; Picó, Y., Optimization and comparison of several extraction methods for determining perfluoroalkyl substances in abiotic environmental solid matrices using liquid chromatography-mass spectrometry. *Analytical and Bioanalytical Chemistry* **2015,** *407* (19), 5767-5781.
189. Munoz, G.; Duy, S. V.; Labadie, P.; Botta, F.; Budzinski, H.; Lestremau, F.; Liu, J.; Sauvé, S., Analysis of zwitterionic, cationic, and anionic poly- and perfluoroalkyl surfactants in sediments by liquid chromatography polarity-switching electrospray ionization coupled to high resolution mass spectrometry. *Talanta* **2016,** *152*, 447-456.
190. Baduel, C.; Paxman, C. J.; Mueller, J. F., Perfluoroalkyl substances in a firefighting training ground (FTG), distribution and potential future release. *Journal of Hazardous Materials* **2015,** *296*, 46-53.
191. Thai, P. K.; McDonough, J. T.; Key, T. A.; Thompson, J.; Prasad, P.; Porman, S.; Mueller, J. F., Release of perfluoroalkyl substances from AFFF-impacted concrete in a firefighting training ground (FTG) under repeated rainfall simulations. *Journal of Hazardous Materials Letters* **2022,** *3*, 100050.
192. Jason R. McDonald, B. Persistence and Mitigation of PFAS within Concrete Stormwater Drainage Infrastructure. Air Force Institute of Technology, 2021.
193. B. F. Scott, R. W. M., K. Kannan, A. Fisk, A. Witter, N. Yamashita, L. Durham, C. Spencer, D. C. G. Muir, Trifluoroacetate Profiles in the Arctic, Atlantic, and Pacific Oceans. *Environmental Science & Technology* **2005,** *39* (17), 6555-6560.
194. M. Scheurer, K. N., F. Freeling, J. Janda, O. Happel, M. Riegel, H. J. Brauch, Small, mobile, persistent: Trifluoroacetate in the water cycle - Overlooked sources, pathways, and consequences for drinking water supply. *Water Research* **2017,** *126*, 460-471.

195. Scheurer, M.; Nödler, K., Ultrashort-chain perfluoroalkyl substance trifluoroacetate (TFA) in beer and tea - An unintended aqueous extraction. *Food Chem.* **2021,** *351*, 129304.
196. M. Sun, J. C., J. Guo, Z. Zhai, P. Zuo, J. Zhang, Fluorochemicals biodegradation as a potential source of trifluoroacetic acid (TFA) to the environment. *Chemosphere* **2020,** *254*, 126894.
197. Y. Duan, H. S., Y. Yao, Y. Meng, Y. Li, Distribution of novel and legacy per-/polyfluoroalkyl substances in serum and its associations with two glycemic biomarkers among chinese adult men and women with normal blood glucose levels. *Environ. Int.* **2020,** *134*, 105295.
198. Ochoa-Herrera, V.; Field, J. A.; Luna-Velasco, A.; Sierra-Alvarez, R., Microbial toxicity and biodegradability of perfluorooctane sulfonate (PFOS) and shorter chain perfluoroalkyl and polyfluoroalkyl substances (PFASs). *Environmental Science: Processes & Impacts* **2016,** *18* (9), 1236-1246.
199. Montes, R.; Aguirre, J.; Vidal, X.; Rodil, R.; Cela, R.; Quintana, J. B., Screening for Polar Chemicals in Water by Trifunctional Mixed-Mode Liquid Chromatography–High Resolution Mass Spectrometry. *Environmental Science & Technology* **2017,** *51* (11), 6250-6259.
200. Tian, Y.; Yao, Y.; Chang, S.; Zhao, Z.; Zhao, Y.; Yuan, X.; Wu, F.; Sun, H., Occurrence and Phase Distribution of Neutral and Ionizable Per- and Polyfluoroalkyl Substances (PFASs) in the Atmosphere and Plant Leaves around Landfills: A Case Study in Tianjin, China. *Environmental Science & Technology* **2018,** *52* (3), 1301-1310.
201. Liang, S.-H., Chang, Mike,. , Integrating the Analysis of Ultrashort-Chain PFAS: Method Development for Simultaneous Analysis of Ultrashort-Chain, Alternative, and Legacy PFAS. *www.restek.com* **2019**.
202. Scott, B. F.; Spencer, C.; Marvin, C. H.; MacTavish, D. C.; Muir, D. C. G., Distribution of Haloacetic Acids in the Water Columns of the Laurentian Great Lakes and Lake Malawi. *Environmental Science & Technology* **2002,** *36* (9), 1893-1898.
203. Neuwald, I. J.; Hübner, D.; Wiegand, H. L.; Valkov, V.; Borchers, U.; Nödler, K.; Scheurer, M.; Hale, S. E.; Arp, H. P. H.; Zahn, D., Ultra-Short-Chain PFASs in the Sources of German Drinking Water: Prevalent, Overlooked, Difficult to Remove, and Unregulated. *Environmental Science & Technology* **2022,** *56* (10), 6380-6390.
204. Mak, Y. L.; Taniyasu, S.; Yeung, L. W. Y.; Lu, G.; Jin, L.; Yang, Y.; Lam, P. K. S.; Kannan, K.; Yamashita, N., Perfluorinated Compounds in Tap Water from China and Several Other Countries. *Environmental Science & Technology* **2009,** *43* (13), 4824-4829.
205. Zhang, W.; Zhang, Y.; Taniyasu, S.; Yeung, L. W. Y.; Lam, P. K. S.; Wang, J.; Li, X.; Yamashita, N.; Dai, J., Distribution and fate of perfluoroalkyl substances in municipal wastewater treatment plants in economically developed areas of China. *Environmental Pollution* **2013,** *176*, 10-17.
206. Wan, Y.; Wang, S.; Cao, X.; Cao, Y.; Zhang, L.; Wang, H.; Liu, J., Perfluoroalkyl acids (PFAAs) in water and sediment from the coastal regions of Shandong peninsula, China. *Environmental Monitoring and Assessment* **2017,** *189* (3), 100.
207. Takemine, S.; Matsumura, C.; Yamamoto, K.; Suzuki, M.; Tsurukawa, M.; Imaishi, H.; Nakano, T.; Kondo, A., Discharge of perfluorinated compounds from rivers and their influence on the coastal seas of Hyogo prefecture, Japan. *Environmental Pollution* **2014,** *184*, 397-

404.
208. Backe, W. J.; Day, T. C.; Field, J. A., Zwitterionic, Cationic, and Anionic Fluorinated Chemicals in Aqueous Film Forming Foam Formulations and Groundwater from U.S. Military Bases by Nonaqueous Large-Volume Injection HPLC-MS/MS. *Environmental Science & Technology* **2013,** *47* (10), 5226-5234.
209. Xiao, X.; Ulrich, B. A.; Chen, B.; Higgins, C. P., Sorption of Poly- and Perfluoroalkyl Substances (PFASs) Relevant to Aqueous Film-Forming Foam (AFFF)-Impacted Groundwater by Biochars and Activated Carbon. *Environmental Science & Technology* **2017,** *51* (11), 6342-6351.
210. Exner, M.; Färber, H., Perfluorinated Surfactants in Surface and Drinking Waters (9 pp). *Environmental Science and Pollution Research* **2006,** *13* (5), 299-307.
211.Sharma, B. M.; Bharat, G. K.; Tayal, S.; Larssen, T.; Bečanová, J.; Karásková, P.; Whitehead, P. G.; Futter, M. N.; Butterfield, D.; Nizzetto, L., Perfluoroalkyl substances (PFAS) in river and ground/drinking water of the Ganges River basin: Emissions and implications for human exposure. *Environmental Pollution* **2016,** *208*, 704-713.
212. Ahrens, L.; Felizeter, S.; Sturm, R.; Xie, Z.; Ebinghaus, R., Polyfluorinated compounds in waste water treatment plant effluents and surface waters along the River Elbe, Germany. *Marine Pollution Bulletin* **2009,** *58* (9), 1326-1333.
213. Campo, J.; Pérez, F.; Masiá, A.; Picó, Y.; Farré, M. l.; Barceló, D., Perfluoroalkyl substance contamination of the Llobregat River ecosystem (Mediterranean area, NE Spain). *Science of The Total Environment* **2015,** *503-504*, 48-57.